

AD-A125 231

WAVE TRANSMISSION AND MOORING-FORCE CHARACTERISTICS OF  
PIPE-TIRE FLOATING BREAKWATERS(U) COASTAL ENGINEERING  
RESEARCH CENTER FORT BELVOIR VA V W HARMS ET AL

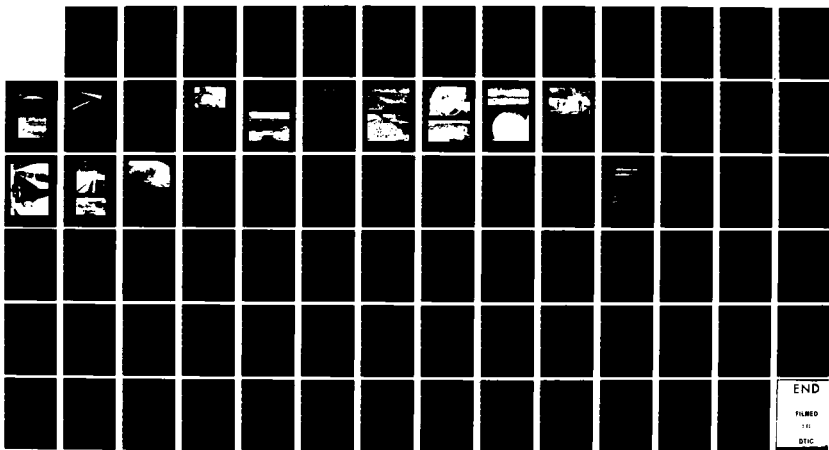
1/1

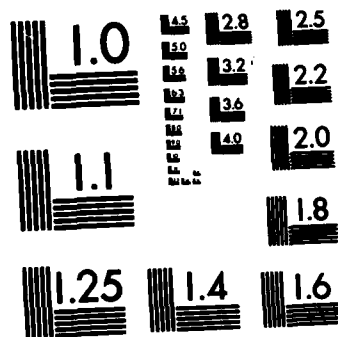
UNCLASSIFIED

OCT 82 CERC-TP-82-4

F/G 13/12

NL





MICROCOPY RESOLUTION TEST CHART  
NATIONAL BUREAU OF STANDARDS-1963-A

12

TP 82-4

AD A125231

# Wave Transmission and Mooring-Force Characteristics of Pipe-Tire Floating Breakwaters

by

Volker W. Harms, Joannes J. Westerink,  
Robert M. Sorensen, and James E. McTamany

TECHNICAL PAPER NO. 82-4

OCTOBER 1982



Approved for public release;  
distribution unlimited.

DTIC  
ELECTE  
MAR 03 1983  
S D E

U.S. ARMY, CORPS OF ENGINEERS  
COASTAL ENGINEERING  
RESEARCH CENTER

Kingman Building  
Fort Belvoir, Va. 22060

DTIC FILE COPY

83 03 02 024

Reprint or republication of any of this material shall give appropriate credit to the U.S. Army Coastal Engineering Research Center.

Limited free distribution within the United States of single copies of this publication has been made by this Center. Additional copies are available from:

*National Technical Information Service  
ATTN: Operations Division  
5285 Port Royal Road  
Springfield, Virginia 22161*

Contents of this report are not to be used for advertising, publication, or promotional purposes. Citation of trade names does not constitute an official endorsement or approval of the use of such commercial products.

The findings in this report are not to be construed as an official Department of the Army position unless so designated by other authorized documents.

UNCLASSIFIED

SECURITY CLASSIFICATION OF THIS PAGE (When Data Entered)

REPORT DOCUMENTATION PAGE		READ INSTRUCTIONS BEFORE COMPLETING FORM
1. REPORT NUMBER TP 82-4	2. GOVT ACCESSION NO. AD A125 231	3. RECIPIENT'S CATALOG NUMBER
4. TITLE (and Subtitle) WAVE TRANSMISSION AND MOORING-FORCE CHARACTERISTICS OF PIPE-TIRE FLOATING BREAKWATERS		5. TYPE OF REPORT & PERIOD COVERED Technical Paper
		6. PERFORMING ORG. REPORT NUMBER
7. AUTHOR(s) Volker W. Harms, Joannes J. Westerink, Robert M. Sorensen, and James E. McTamany		8. CONTRACT OR GRANT NUMBER(s)
9. PERFORMING ORGANIZATION NAME AND ADDRESS Department of the Army Coastal Engineering Research Center (CERRE-CS) Kingman Building, Fort Belvoir, VA 22060		10. PROGRAM ELEMENT, PROJECT, TASK AREA & WORK UNIT NUMBERS D31679
11. CONTROLLING OFFICE NAME AND ADDRESS Department of the Army Coastal Engineering Research Center Kingman Building, Fort Belvoir, VA 22060		12. REPORT DATE October 1982
		13. NUMBER OF PAGES 79
14. MONITORING AGENCY NAME & ADDRESS (if different from Controlling Office)		15. SECURITY CLASS. (of this report) UNCLASSIFIED
		15a. DECLASSIFICATION/DOWNGRADING SCHEDULE
16. DISTRIBUTION STATEMENT (of this Report)  Approved for public release; distribution unlimited.		
17. DISTRIBUTION STATEMENT (of the abstract entered in Block 20, if different from Report)		
18. SUPPLEMENTARY NOTES		
19. KEY WORDS (Continue on reverse side if necessary and identify by block number)  <div style="display: flex; justify-content: space-between;"> <div>           Floating breakwaters Laboratory tests Monochromatic waves         </div> <div>           Mooring loads Tires Wave transmission         </div> </div>		
20. ABSTRACT (Continue on reverse side if necessary and identify by block number)  Wave transmission and mooring-load features were tested for a floating breakwater created from massive cylindrical members (steel or concrete pipes, telephone poles, etc.) in a matrix of scrap truck or automobile tires. The Pipe-Tire Breakwater (PT-Breakwater) was tested at prototype scale using regular waves ranging in height from 0.15 to 1.78 meters and period from 2.6 to 8.1 seconds; water depths ranged from 2.0 to 4.6 meters. Two designs were <div style="text-align: right;">(continued)</div>		

DD FORM 1 JAN 73 1473

EDITION OF 1 NOV 65 IS OBSOLETE

UNCLASSIFIED

SECURITY CLASSIFICATION OF THIS PAGE (When Data Entered)

UNCLASSIFIED

SECURITY CLASSIFICATION OF THIS PAGE(When Data Entered)

tested--the PT-1 module, composed of steel-pipe buoyancy chambers and truck tires, and the PT-2 module, composed of telephone poles and car tires. Each design was 12.2 meters wide in the direction of wave propagation and was held together by conveyor-belt loops. Wave attenuation and mooring-force features were established based on data from 402 separate runs in which incident and transmitted wave heights were recorded, along with the tension in the seaward mooring line. Test results are compared with those of earlier experiments made on the Goodyear floating tire breakwater. The construction of these PT-Breakwater modules is outlined, along with the cost estimates for construction of components. A breakwater buoyancy test was made and the flotation requirements calculated. The influence of stiffness on the mooring system was experimentally investigated and conveyor-belt material tested to the point of failure. Design curves for determining the proper anchor requirements and breakwater size are given.

Apart from the incident wave height, the transmitted wave height and peak mooring force are shown to depend primarily on four dimensionless parameters: the relative wavelength, wave steepness, relative breakwater draft, and breakwater aspect ratio. The wave attenuation performance of PT-Breakwaters improves as either wavelength or water depth decreases, or the wave steepness increases. The shelter afforded by a particular PT-Breakwater is strongly dependent on the incident wavelength,  $L$ : substantial protection is provided from waves that are shorter than the width,  $B$ , of the breakwater but very little from waves longer than three times the width of the breakwater.

The wave attenuation performance of PT-1 was found to be superior to that of PT-2 and the Goodyear breakwater: for  $L/B = 1$  and deep water with  $H/L = 0.04$ ; for example, the wave height transmission ratios are approximately 0.6, 0.4, and 0.2 for the Goodyear, PT-2, and PT-1 breakwaters, respectively. For the conditions investigated, the peak mooring force increases approximately with the square of the wave height, more precisely:  $F \propto H^n$  where  $n = 1.5, 2$  and  $2$  for the PT-1, PT-2, and Goodyear breakwaters, respectively.

Accession For	
NTIS GRA&I	<input checked="" type="checkbox"/>
DTIC TAB	<input type="checkbox"/>
Unannounced	<input type="checkbox"/>
Justification	
By	
Distribution/	
Availability Codes	
Dist	Special
A	



## PREFACE

This report is published to provide coastal engineers the results of a series of prototype-scale tests of a floating breakwater that incorporates massive cylindrical members (steel or concrete pipes, telephone poles, etc.) in a matrix of scrap truck or automobile tires. The breakwater, which was developed by the senior author while serving on the faculty of the State University of New York at Buffalo (SUNY), is referred to as the Pipe-Tire Breakwater (PT-Breakwater). Tests were conducted in the large wave tank at the U.S. Army Coastal Engineering Research Center (CERC) in a joint effort by CERC and SUNY personnel. The work was carried out under CERC's Design of Floating Breakwaters work unit, Coastal Structure Evaluation and Design Program, Coastal Engineering Area of Civil Works Research and Development.

The report was prepared by Dr. Volker W. Harms, SUNY and University of California, Berkeley; Joannes J. Westerink, SUNY; Dr. Robert M. Sorensen, Chief, Coastal Processes and Structures Branch, CERC; and James E. McTamany, Coastal Oceanography Branch, CERC.


The authors gratefully acknowledge the assistance of SUNY technical specialist J. Sarvey and students T. Bender, P. Hughey, and P. Speranza, and the difficult crane operations and frequent wave generator stroke changes performed by CERC's research support personnel.

This research was sponsored in part by the New York Sea Grant Institute under a grant from the Office of Sea Grant, National Oceanic and Atmospheric Administration (NOAA), U.S. Department of Commerce, through SUNY. It was also supported by the U.S. Department of Energy under Contract W-7405-ENG-48 to the Marine Sciences Group, Lawrence Berkeley Laboratory, University of California.

Technical Director of CERC was Dr. Robert W. Whalin, P.E., upon publication of this report.

Comments on this publication are invited.

Approved for publication in accordance with Public Law 166, 79th Congress, approved 31 July 1945, as supplemented by Public Law 172, 88th Congress, approved 7 November 1963.

  
TED E. BISHOP  
Colonel, Corps of Engineers  
Commander and Director

# CONTENTS

	Page
CONVERSION FACTORS, U.S. CUSTOMARY TO METRIC (SI).....	7
SYMBOLS AND DEFINITIONS.....	8
I INTRODUCTION.....	9
II THE PIPE-TIRE BREAKWATER.....	10
1. Breakwater Modules and Components.....	12
2. Construction Procedures.....	16
3. Breakwater Buoyancy.....	20
4. Cost Estimates.....	23
III EXPERIMENTAL SETUP AND PROCEDURES.....	24
1. Test Facility and Instrumentation.....	24
2. Mooring System.....	28
3. Test Procedure and Conditions.....	31
IV DATA REDUCTION AND ANALYSIS.....	32
1. Dimensional Analysis.....	32
2. Data-Reduction Procedures.....	34
V EXPERIMENTAL RESULTS.....	37
1. Wave Transmission Data.....	37
2. Mooring-Force Data.....	45
VI SUMMARY AND CONCLUSIONS.....	50
LITERATURE CITED.....	53
APPENDIX	
A TABULATED TEST RESULTS.....	55
B FORCE MEASUREMENT CORRELATION (PT-1).....	65
C DETAILED WAVE TRANSMISSION DIAGRAM.....	74

## TABLES

1 Cost estimates of PT-Breakwater components.....	23
2 Compliance of mooring systems.....	29
3 Summary of test conditions.....	31
4 Summary of mooring-force data.....	46

## FIGURES

1 PT-Breakwater field installation.....	11
2 Typical PT-Breakwater module with tire-armored pipes.....	11



## CONTENTS

### FIGURES--Continued

	Page
3 Orientation of PT-Breakwater.....	12
4 Schematic of PT-1 breakwater module.....	13
5 Definition sketch for PT-Breakwater.....	13
6 Assembly of PT-1 and PT-2 modules.....	14
7 Tire retainer at end of pipe.....	14
8 Breakwater and mooring-system components.....	15
9 Tire mooring damper.....	16
10 First step in breakwater assembly--rolling tires into place.....	17
11 Tires are in position, ready to be tied.....	17
12 Guiding conveyor-belt strip through tire casings.....	18
13 Tensioning belt before completing belt-to-belt connection.....	18
14 Belts are overlapped and bolted together.....	19
15 Belt is anchored to sidewall of one tire.....	19
16 PT-1 module ready for lift into wave tank.....	20
17 Forces on pipe-tire unit.....	21
18 Large wave tank at CERC with breakwater and MS-1 mooring system.....	24
19 View toward wave generator.....	25
20 View toward beach.....	25
21 Inserting PT-1 breakwater.....	26
22 Turbulence associated with wave damping.....	26
23 Attachment of seaward mooring line.....	27
24 Strain-gage-cantilever force gage.....	27
25 Force-gage calibration record and curve.....	28
26 Mooring bridle used in field installation.....	29
27 Load elongation curves for mooring-line inserts.....	30

# CONTENTS

## FIGURES--Continued

	Page
28 Stress-strain diagram for belt connection.....	31
29 Wave and force record for long waves.....	34
30 Wave and force record for short waves.....	35
31 Wave and force record for steep waves.....	35
32 Wave and force record for shallow-water waves.....	36
33 Definition sketch for force analysis.....	37
34 Wave transmission data for PT-1 breakwater ( $d = 4.7$ m).....	38
35 Wave transmission data for PT-1 breakwater ( $d = 2.0$ m).....	39
36 Wave transmission design curves for PT-1 breakwater.....	39
37 Wave transmission data for PT-2 breakwater ( $d = 4.7$ m).....	40
38 Wave transmission data for PT-2 breakwater ( $d = 2.0$ m).....	41
39 Wave transmission design curves for PT-2 breakwater.....	41
40 Comparison of PT-1 and PT-2 wave attenuation.....	42
41 Comparison of Goodyear and PT-2 wave attenuation ( $d = 4.7$ m).....	43
42 Comparison of Goodyear and PT-2 wave attenuation ( $d = 2.0$ m).....	43
43 Influence of $D/d$ on Goodyear wave attenuation.....	44
44 Wave transmission design curves for Goodyear and PT-Breakwater.....	44
45 PT-1 peak mooring-force data (MS-1, $d = 2.0$ m).....	45
46 PT-1 peak mooring-force data (MS-1, $d = 4.7$ m).....	46
47 Effect of mooring-system compliance on $F$ .....	47
48 PT-1 peak mooring-force data (MS-3, $d = 4.7$ m).....	48
49 PT-2 peak mooring-force data (MS-3, $d = 4.7$ m).....	48
50 PT-2 peak mooring-force data (MS-3, $d = 2.0$ m).....	49
51 Goodyear peak mooring-force data (reference 3, $d = 2.0$ m).....	49
52 Goodyear peak mooring-force data (reference 3, $d = 4.0$ m).....	50

# CONVERSION FACTORS, U.S. CUSTOMARY TO METRIC (SI) UNITS OF MEASUREMENT

U.S. customary units of measurement used in this report can be converted to metric (SI) units as follows:

Multiply	by	To obtain
inches	25.4	millimeters
	2.54	centimeters
square inches	6.452	square centimeters
cubic inches	16.39	cubic centimeters
feet	30.48	centimeters
	0.3048	meters
square feet	0.0929	square meters
cubic feet	0.0283	cubic meters
yards	0.9144	meters
square yards	0.836	square meters
cubic yards	0.7646	cubic meters
miles	1.6093	kilometers
square miles	259.0	hectares
knots	1.852	kilometers per hour
acres	0.4047	hectares
foot-pounds	1.3558	newton meters
millibars	$1.0197 \times 10^{-3}$	kilograms per square centimeter
ounces	28.35	grams
pounds	453.6	grams
	0.4536	kilograms
ton, long	1.0160	metric tons
ton, short	0.9072	metric tons
degrees (angle)	0.01745	radians
Fahrenheit degrees	5/9	Celsius degrees or Kelvins <sup>1</sup>

<sup>1</sup>To obtain Celsius (C) temperature readings from Fahrenheit (F) readings, use formula:  $C = (5/9) (F - 32)$ .

To obtain Kelvin (K) readings, use formula:  $K = (5/9) (F - 32) + 273.15$ .

## SYMBOLS AND DEFINITIONS

B	width or beam of breakwater (dimension in direction of wave motion)
B/D	breakwater aspect ratio
$C_t$	wave height transmission ratio, $C_t = H_t/H$
D	tire diameter
D/d	relative draft
d	water depth
F	peak mooring force on seaward mooring line (per unit length of breakwater)
G	center-to-center distance between pipes of PT-Breakwater
g	gravitational acceleration
H	incident wave height
H/L	wave steepness
$H_t$	transmitted wave height
L	wavelength
L/B	relative wavelength
T	wave period
$\gamma$	specific weight of water
$\epsilon$	horizontal displacement of breakwater from equilibrium position
$\lambda$	length of breakwater (dimension at right angles to direction of wave motion)
$\nu$	kinematic viscosity of water

# WAVE TRANSMISSION AND MOORING-FORCE CHARACTERISTICS OF PIPE-TIRE FLOATING BREAKWATERS

by

*Volker W. Harms, Joannes J. Westerink,  
Robert M. Sorensen, and James E. McTamany*

## I. INTRODUCTION

This report presents methods for constructing a recently developed floating breakwater that consists largely of scrap pneumatic-tire casings, and also provides basic data for the design of such structures. The idea of constructing floating breakwaters almost entirely from scrap tires was originally conceived two decades ago by R.L. Stitt and resulted in a patent for the wave-maze floating tire breakwaters (Stitt, 1963; Kamel and Davidson, 1968). More recently, this concept was adapted in the development of the Goodyear floating tire breakwater (Kowalski, 1974; Candle, 1976). Both these breakwaters are flexible in all directions since there are no rigid structural members utilized. The Goodyear module differs from the Wave-Maze in the size of the tires used (automobile as opposed to truck tires), geometric arrangement of the tires (single-layer upright versus triple-layer "sandwich"), and binding materials and techniques used (typically conveyor-belt loops as opposed to bolted-tire connections). A number of floating breakwaters of both types have been installed on the Great Lakes, the east and west coasts of the United States, and overseas, with various levels of success.

Although the installation of floating breakwaters is frequently favored over bottom-resting structures for a number of environmentally related reasons (e.g., impact on water circulation, fish migrations), the principal reason for considering floating breakwaters made of tires is their relatively low cost. For small marinas of less than 100 boat slips, floating breakwaters are frequently the only wave protection system that is economically feasible with costs ranging from \$10 to \$100 per horizontal square meter of breakwater. At the same time, it must be recognized that floating tire breakwaters provide less wave protection, are less rugged, and have lower extreme event survival capabilities than conventional bottom-resting structures, such as rubble-mound and sheet-pile breakwaters. A comparison of knowledge acquired from field installations and prototype-scale laboratory tests suggests that the Goodyear and Wave-Maze floating tire breakwaters should be limited to semiprotected sites, or short fetch applications (e.g., 10 kilometers or less), with significant wave heights below 0.9 to 1.2 meters. At locations with severer wave climates (larger wave height and period), several limitations have been encountered with regards to:

(a) Structural Integrity. The response behavior of wave-induced mooring loads increases approximately with the square of the wave height. While under severe wave action the following problems have been encountered: (1) modules connected to the seaward mooring lines separate because of excessive loads, (2) anchors fail or "walk" because of the large mooring forces, (3) flotation material is lost from individual tires because of the excessive stretching and twisting, and (4) tire connection and binding materials reach their failure limit.

(b) Breakwater Size. As with all breakwaters, the size of a floating tire breakwater is site specific. The dimension of the breakwater in the direction of wave propagation (width or beam) must generally be at least as large as the locally predominant wavelength (design wave). This implies that a very large breakwater will be required at sites with long period waves, which not only increases the breakwater's cost but also may not be feasible because of space limitation.

(c) Buoyancy. Portions of the breakwater configuration may begin to sink if individual tires lose their flotation material (e.g., caused by stretching and twisting while under high loads) or if the structure gains too much weight with time (caused by deposition of suspended sediments in the tire casings or excessive marine growth).

In an attempt to improve on the design characteristics of the floating breakwaters discussed above, another wave protection concept utilizing pneumatic tire casings as the major construction material has recently been developed by the senior author at the State University of New York at Buffalo (Harms and Bender, 1978; Harms, 1979a). It is referred to as the Pipe-Tire Breakwater (PT-Breakwater), or Harms Breakwater, and is basically a hybrid structure with massive, rigid, cylindrical members (e.g., steel or concrete pipes) embedded in a flexible matrix of scrap tires. Experiments performed with several small-scale PT-Breakwater models (Harms, 1979b) and one full-scale breakwater demonstrated that this design provides significantly more wave protection than the Goodyear or Wave-Maze breakwaters constructed of equal size. These early laboratory tests also suggested that a full-scale PT-Breakwater would have superior extreme event survival capabilities, while preliminary calculations indicated that costs would remain low enough for this wave protection system to be economically attractive.

Because of the PT-Breakwater's potential contribution to low-cost wave protection, prototype-scale experiments over a wide range of wave conditions were conducted in a joint test program between the State University of New York at Buffalo and the U.S. Army Coastal Engineering Research Center (CERC). Full-scale tests, which are the subject of this report, were conducted in the large wave tank at CERC. Investigations were aimed at defining the wave transmission and mooring-force characteristics of PT-Breakwaters; it was also intended that structural failure modes be analyzed, should it be possible to induce them within the range of wave conditions that could be generated in the tank.

Figures 1 and 2 provide a general impression of a floating PT-Breakwater. This field installation at Mamaroneck, New York, is based on the PT-1 module discussed in this report; it is constructed of truck tires with steel pipes serving as the structural members and flotation chambers. The orientation of the pipes with respect to the incident wave train is shown in Figure 3.

## II. THE PIPE-TIRE BREAKWATER

The PT-Breakwater is basically a mat composed of flexibly interconnected scrap tires, floating near the surface, into which massive cylindrical members are inserted to provide stiffness in the direction of wave motion and to serve as buoyancy chambers. Major structural features of the PT-Breakwater are



Figure 1. PT-Breakwater field installation (PT-1 modules; Mamaroneck, New York).

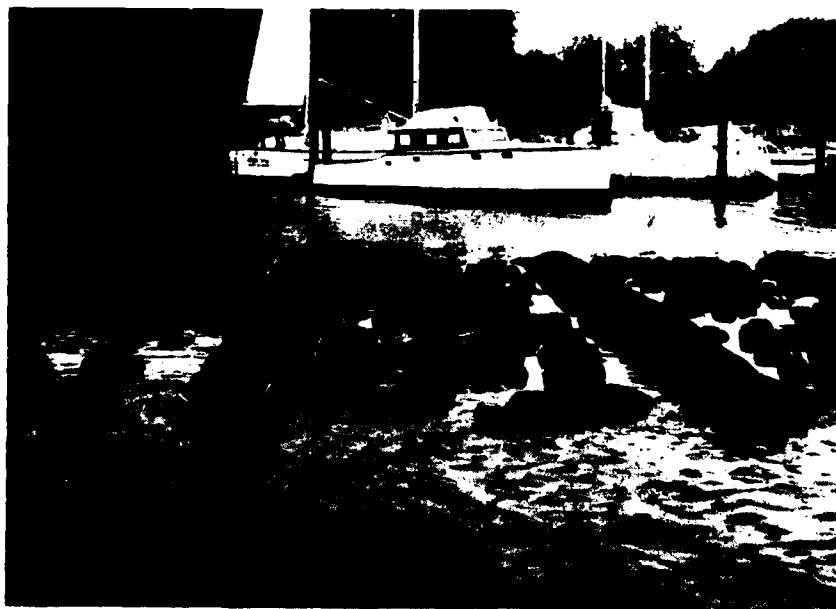


Figure 2. Typical PT-Breakwater module with tire-armored pipes (Mamaroneck, New York).

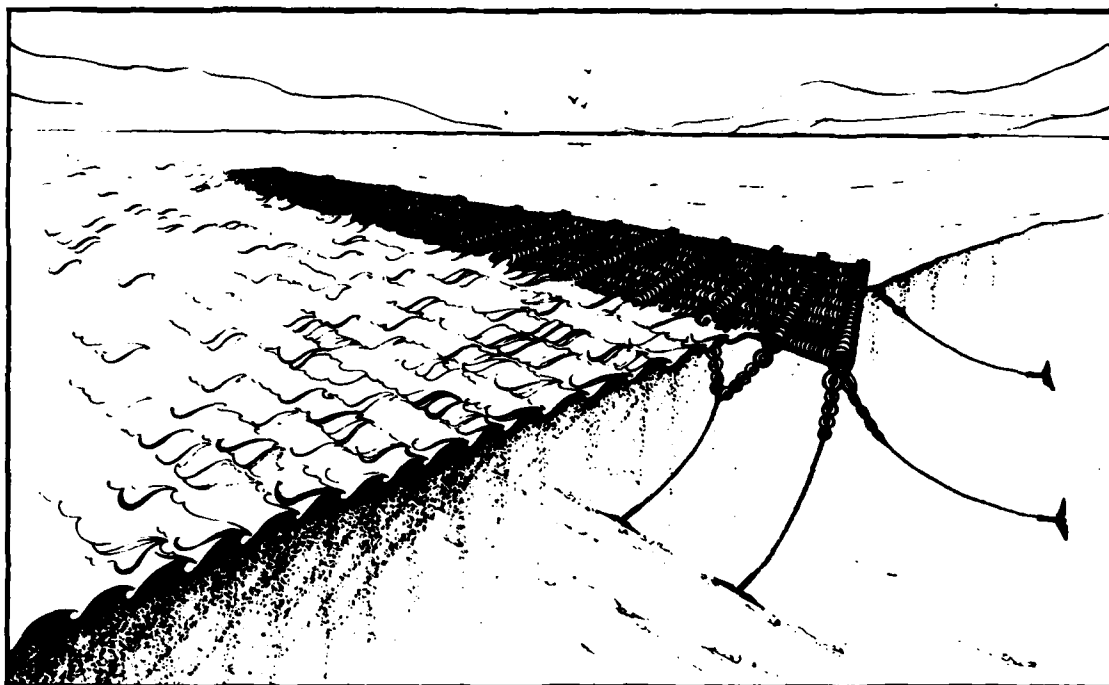


Figure 3. Orientation of PT-Breakwater.

(a) densely spaced tires, (b) tire-armored longitudinal stiffeners (frequently steel pipes), and (c) flexible connections and binding materials (no steel-to-rubber connections). The orientation of the pipes with respect to the incident wave train is shown in the drawing in Figure 3, with major structural features of the breakwater shown in the module schematic in Figure 4 and the definition sketch in Figure 5.

#### 1. Breakwater Modules and Components.

Two versions of the PT-Breakwater, designated as the PT-1 and PT-2 modules, were tested in the large wave tank at CERC (Fig. 6). The PT-1 module, which is the most massive of the two due to its composition of truck tires and steel pipes, is shown in the foreground. The PT-2 module is constructed from car tires and used telephone poles. From the detailed drawing of the PT-1 module (Fig. 4), several important structural features of the breakwater emerge:

(a) A series of parallel conveyor-belt loops receive all lateral loads (at right angles to the direction of wave motion), supports all tires that are not "riding" on the pipe, and couples one module to the next.

(b) Wave-induced hydrodynamic loads are ultimately transferred from tire strings to the tire-armored steel pipe. This takes place in stages. Wave action displaces tire strings and belt loops in the direction of the wave motion (along the pipe) causing the pipe tires to slide along the pipe and become compressed as they transfer their load to the tire retainer at the end of the pipe (Figs. 4 and 7).

(c) The pipe itself effectively floats in a dense matrix of flexibly connected tires.



**— 12' x 40' PT BREAKWATER MODULE —**

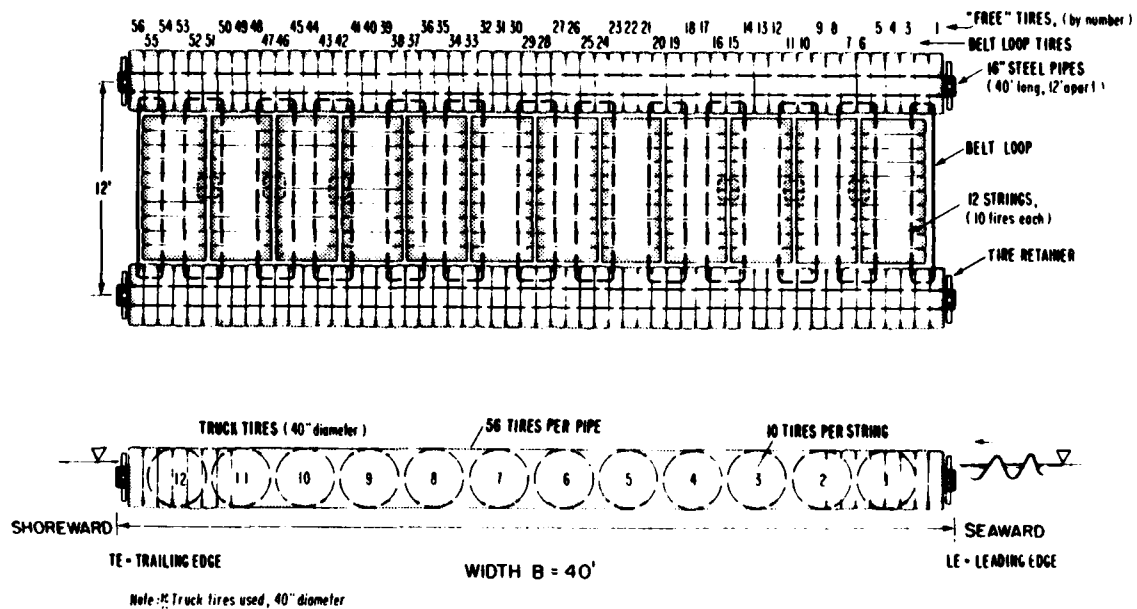


**Figure 4. Schematic of PT-1 breakwater module.**

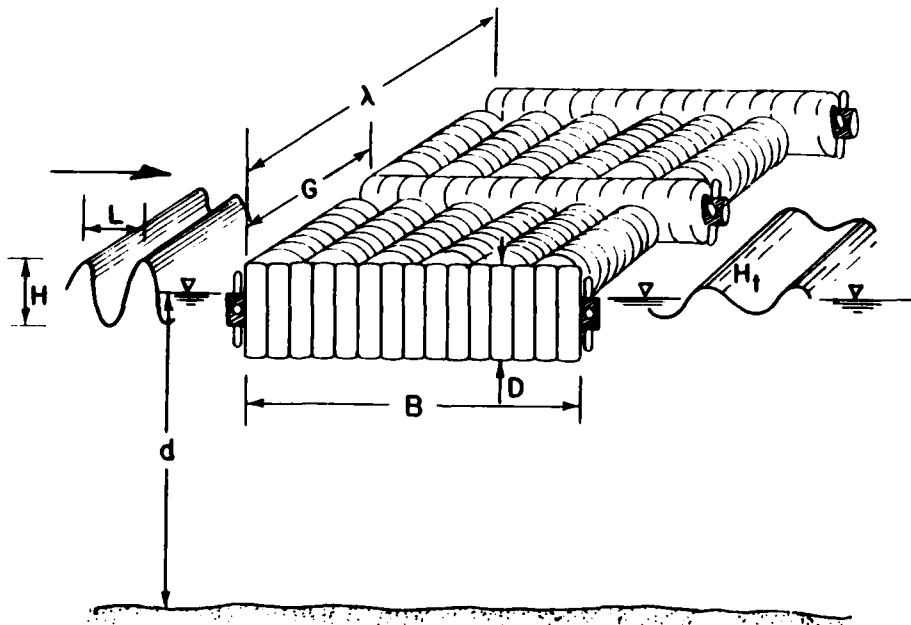


**Figure 5. Definition sketch for PT-Breakwater.**

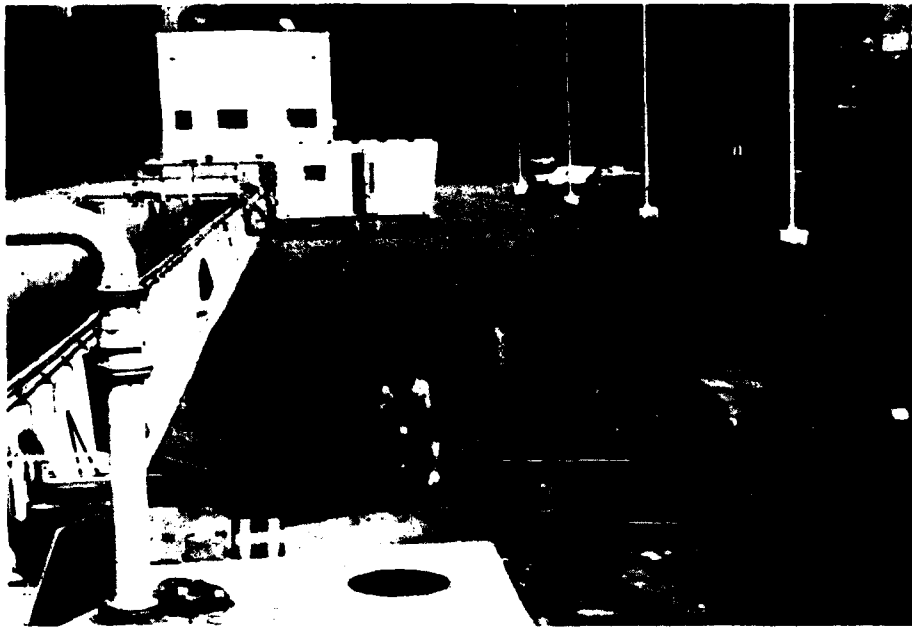


Figure 6. Assembly of PT-1 (foreground) and PT-2 modules.

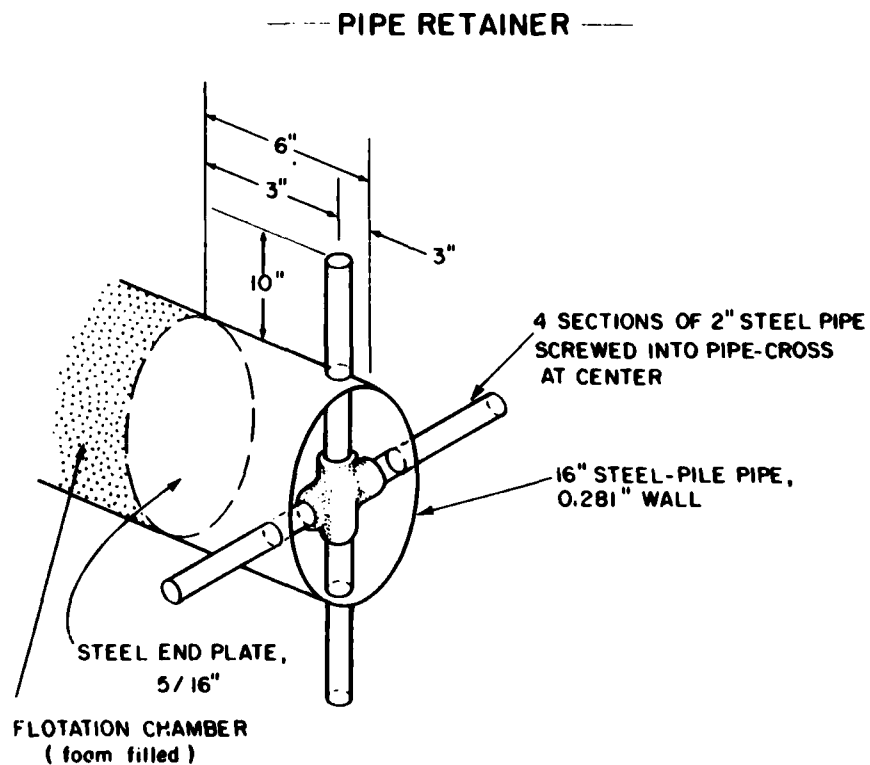


Figure 7. Tire retainer at end of pipe.

The tire retainer used in the PT-1 module is shown in Figures 4 and 7. In the case of the PT-2 module, the retainer was a tire casing that was held in place by a 1.9-centimeter threaded steel rod extending through the telephone pole and casing.

Standard marine steel-pile pipes were utilized as buoyancy chambers and stiffeners in the PT-1 module; they were 12.2 meters long and 41 centimeters in diameter, with a wall thickness of 0.71 centimeter. Scrap telephone poles were used for the PT-2 module; they were 12.2 meters long with a diameter of 33 centimeters at the butt end and 23 centimeters at the tip.

Truck tires ranging in size from 9.00-18 to 10.00-20, with an average diameter of 102 centimeters were used for PT-1. Car tires with rim sizes ranging from 32 to 38 centimeters were used for PT-2; the average diameter was about 65 centimeters.

A three-ply conveyor belt strip, 14 centimeters wide and 1.3 centimeters thick, was used as the binding material; this had a rated breaking strength of 7900 kilograms. A five-hole bolted connection (Figs. 8 and 9) was used to tie the belt into continuous loops.

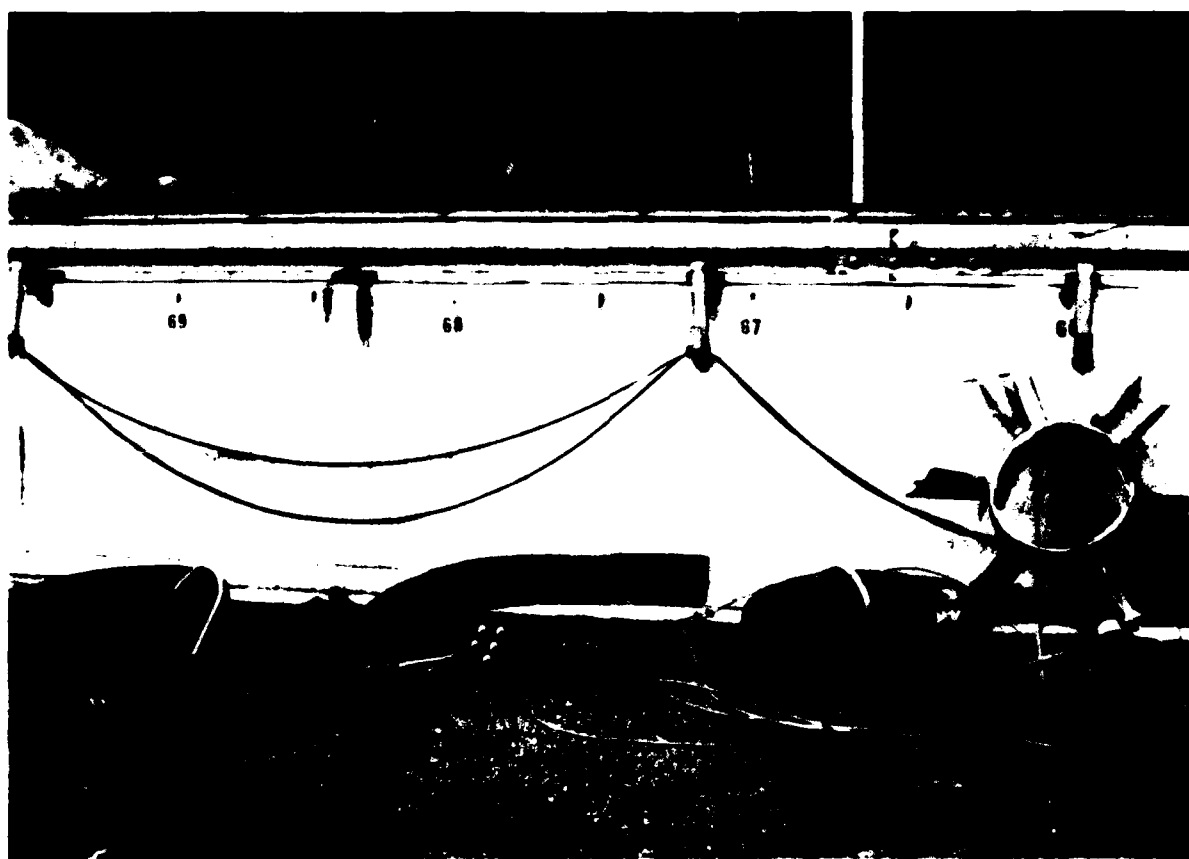


Figure 8. Breakwater and mooring-system components.

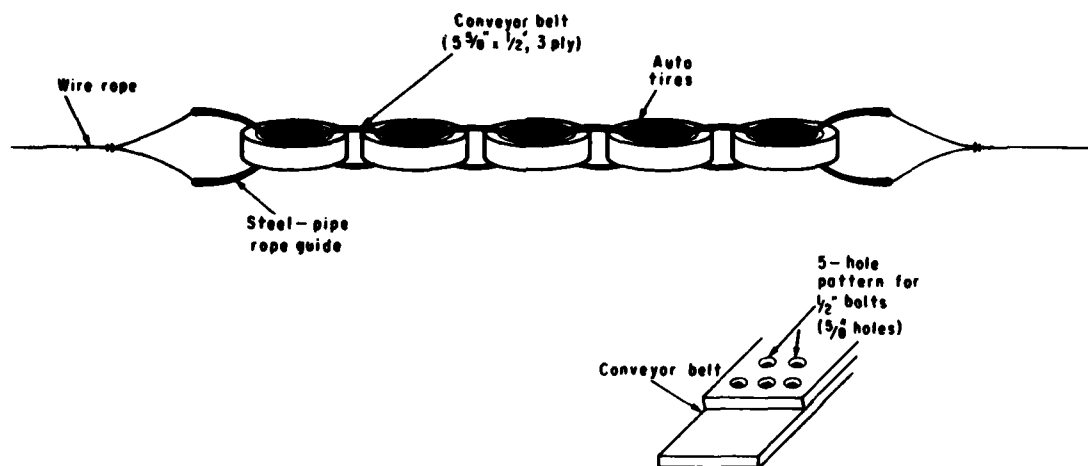


Figure 9. Tire mooring damper (six tires are used in the MS-1 mooring system discussed in Sec. III,2).

## 2. Construction Procedures.

The floating tire breakwater is a modular construction concept. The procedures followed in the actual construction of the PT-1 modules are described in this section. The procedures used for the PT-2 modules are very similar and therefore are not covered. When constructing these modules onsite and at field installations, it should be insured that a crane with sufficient lifting capacity is provided as the two-pipe PT-1 module weighs approximately 11 metric tons and the PT-2 module weighs about 4 metric tons.

Assembly of the breakwater is begun by arranging the tires according to the pattern shown in Figure 4 but leaving out those tires labeled *free tires* (i.e., all tires not connected in some way to a belt). This phase is depicted in Figure 10, where the last tire is just being rolled into place, and also in Figure 11, where the conveyor-belt strips are being prepared by cutting to length and punching the five-hole bolted pattern with a gasket or leather punch (also shown in Fig. 6).

Having assembled the tires, the belts are then guided through the tire casing according to the pattern shown in Figure 4. An illustration of this procedure is shown in Figures 12 and 13. The belt-to-belt connection is then completed by overlapping the belt ends and inserting the five bolts required for each connection (see Fig. 14). A single bolt is used to fix each belt loop to the sidewall of one belt-loop tire (see Figs. 15 and 4); this prevents the belt from rotating under wave action.

After all the belt loops have been bolted together and anchored, the remaining free tires are rolled into place. The unit is then ready for insertion of the pipe. One forklift is used to raise the pipe and position it for entry into the long tunnel created by the 56 aligned tires; a second forklift, or similar device, pushes and aligns the pipe as required. This having been accomplished, the module appears as shown in Figure 6. The tire retainer shown in Figure 7 (or the one depicted in Fig. 8) is then installed at each end of the pipe, and the PT-1 module is ready to be lifted into the water (see Fig. 16).

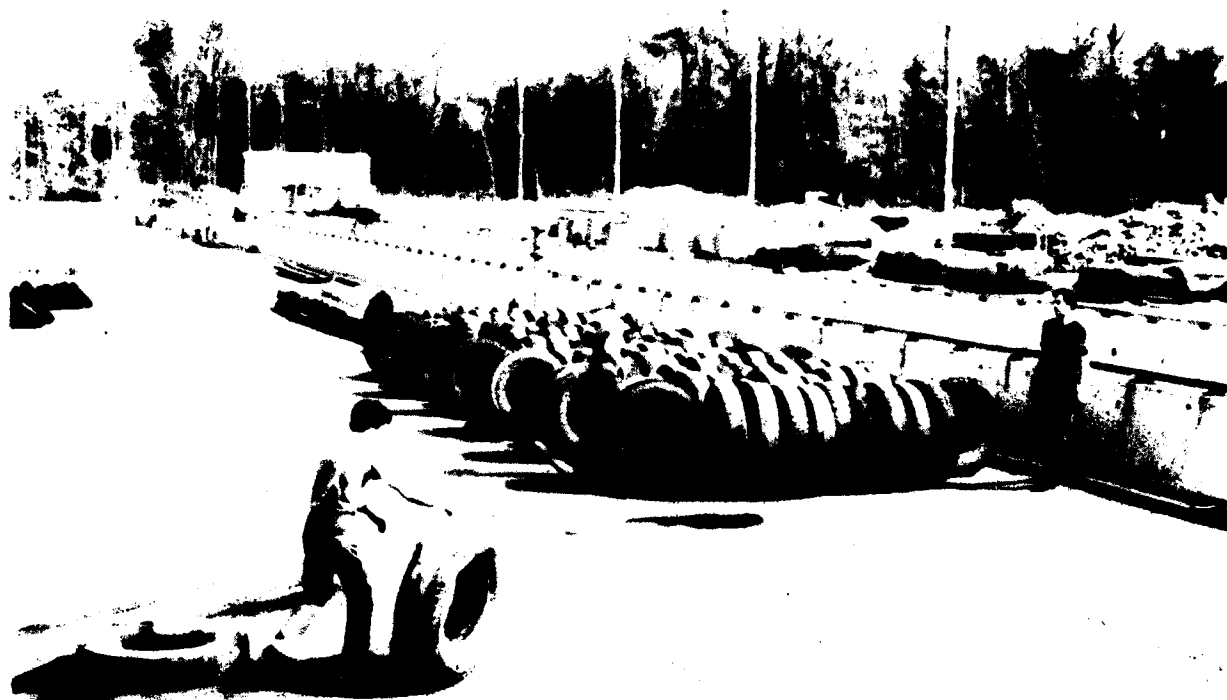


Figure 10. First step in breakwater assembly—rolling tires into place.



Figure 11. Tires are in position, ready to be tied.



Figure 12. Guiding conveyor-belt strip through tire casings.



Figure 13. Tensioning belt before completing belt-to-belt connection.



Figure 14. Belts are overlapped and bolted together.

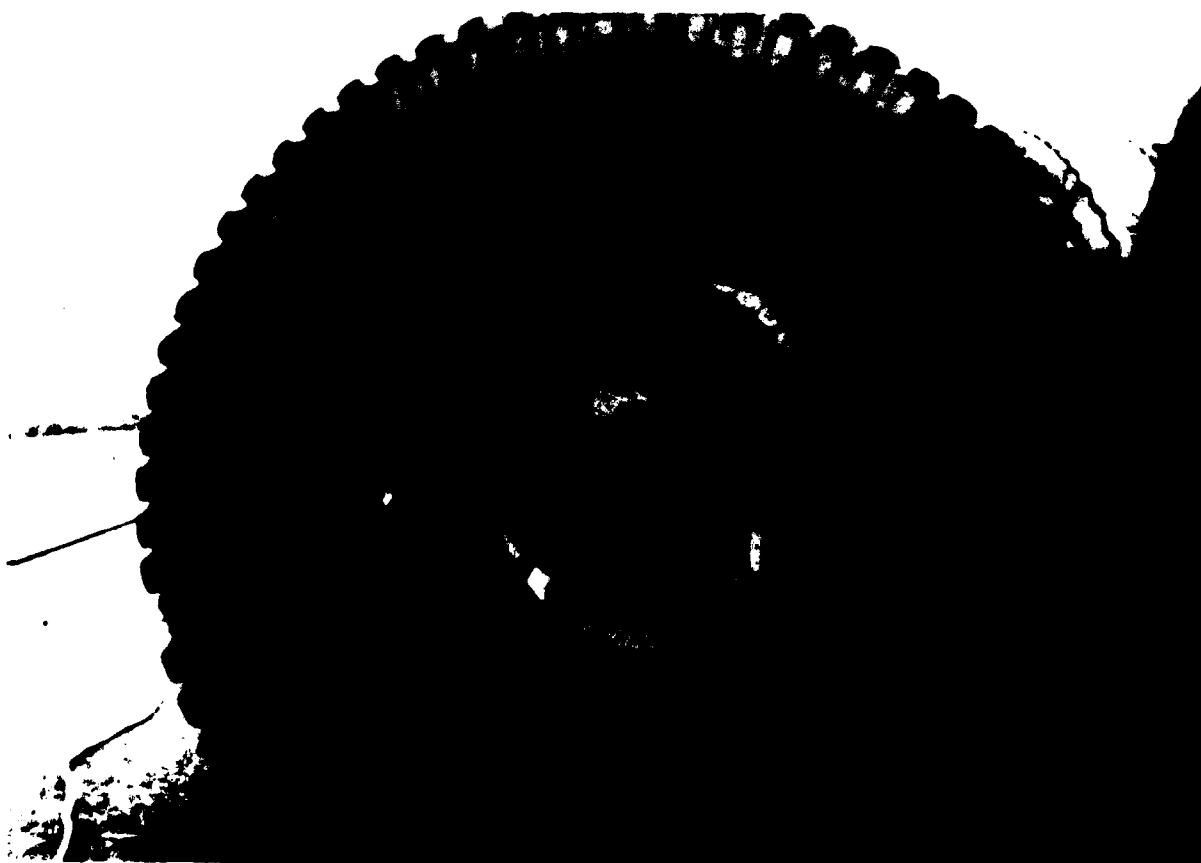


Figure 15. Belt is anchored to sidewall of one tire.

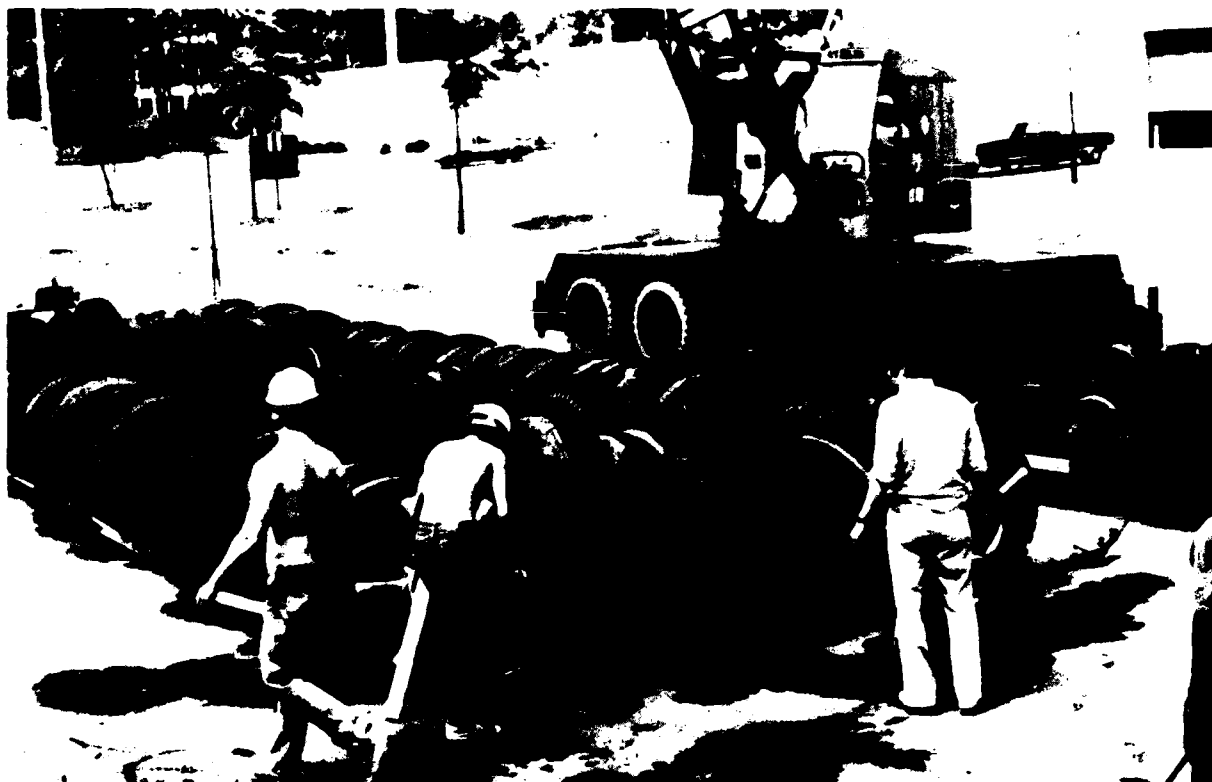


Figure 16. PT-1 module ready for lift into wave tank.

### 3. Breakwater Buoyancy.

a. Pipe Buoyancy Test. A simple buoyancy test was executed by resting steel I-beams on top of one of the tire-armored pipes of the PT-1 module until total submergence was attained (i.e., crown of tires just at the water surface, case B in Fig. 17). Starting from the static, no-load equilibrium position of the breakwater (i.e., crown of pipe at water level and interior of the tire vented to atmosphere, case A), two steel I-beams, each 10.7 meters long and weighing 98 kilograms per meter, were placed onto the tire-armored pipe. These beams provided the loading needed to attain total submergence of the pipe-tire unit. In each case, equilibrium demands that

$$F + n(W_{ta} + W_{tw}) + F_e = F_p + nF_a \quad (1)$$

where

- $F$  = added external load
- $F_e$  = extraneous loads (from mooring system, etc.)
- $F_a$  = buoyancy force per tire due to entrapped air
- $F_p$  = net buoyant force due to pipe (lift minus weight)
- $W_{tw}$  = weight of tire segment submerged in water
- $W_{ta}$  = weight of tire segment in air
- $n$  = number of tires on pipe



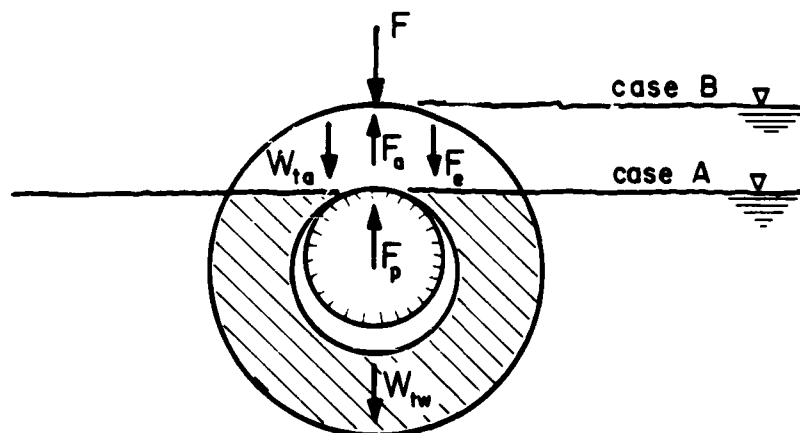


Figure 17. Forces on pipe-tire unit.

In this case the pipe is 12.2 meters long (41-centimeter outside diameter and 70.2-kilogram-per-meter weight in air), provides a net lift of 59.5 kilograms per meter when totally submerged, and supports 49 truck tires. Truck tires have a specific gravity of approximately 1.2 with a weight of  $W_{ta} = 41$  kilograms in air for the sizes predominantly used (i.e., 10.00-20 and 9.00-18 truck tires). Submerged in water this weight is reduced to approximately one-sixth of  $W_{ta}$ , or 6.8 kilograms if all air is expelled. Applying these values to case A (which corresponds to  $F = F_a = 0$  and approximately three-fourths of tire material submerged) and using equation (1), it follows that the extraneous load is a small lift force of 26 kilograms, (i.e.,  $F_e = -26$  kilograms). When the external load  $F$  is applied (case B), the buoyancy force resulting from air entrapped in each tire may be calculated from equation (1) to be:

$$10.7(196) + 49(0 + 6.8) + (-26) = 12.2(59.5) + 49F_a$$

$$F_a = 34.2 \text{ kilograms per tire}$$

On an average, this implies that 34 liters of air is trapped in the crown of each tire. It is not known at what rate this trapped air would escape under static conditions; during wave action the tire crown would be alternately vented and replenished with air. In determining the flotation requirements for the complete structure, the weight of suspended sediments that may accumulate in the tire casings as well as the influence of marine growth should be considered.

b. Equilibrium of Breakwater. The load-carrying capacity of the breakwater must be carefully considered, particularly in areas where the weight of the breakwater is likely to increase substantially with time due to deposition of suspended sediments within the tire casings, biofouling, etc. In extreme cases, all the tires may have to be foamed to provide adequate reserve buoyancy, whereas at other sites the lift provided by the steel-pipe flotation

chambers alone is sufficient. Equation (1) may be used to estimate the reserve buoyancy provided by a clean single-pipe PT-1 module if some terms are redefined:

$F_{sed}$  = sediment and biofouling load (per tire)

$F_e$  = extraneous load (from binding material, tire retainers, pipe end caps, shackles, etc.)

$F_a$  = buoyancy force due to entrapped air (for each tire not foamed)

$F_f$  = buoyancy force due to submersed foam (for each tire that is foamed)

$n$  = number of tires per module

$m$  = number of tires foamed (per module)

This leads to

$$nF_{sed} + nW_{tw} + F_e = F_p + (n - m) F_a + mF_f \quad (2)$$

$$F_{sed} = (F_a - W_{tw}) + \left(\frac{1}{n}\right)(F_p - F_e) + \left(\frac{m}{n}\right)(F_f - F_a)$$

Using the following approximate values and estimates for the PT-1 module:

$F_e$  = 220 kilograms

$F_p$  = (60 kilograms per meter) (12 meters) = 720 kilograms

$W_{tw}$  = 7 kilograms

$F_a$  = 17 kilograms (50 percent of value from buoyancy test)

$F_f$  = 34 kilograms (crown fully foamed, 34 liters)

$n$  = 176 tires

to obtain

$$F_{sed} = (17 - 7) + \left(\frac{1}{176}\right)(720 - 220) + \left(\frac{m}{n}\right)(34 - 17) \quad (3)$$

$$F_{sed} = 10 + 17\left(\frac{m}{n}\right)(\text{kilograms per tire})$$

The following examples demonstrate the increased load-carrying capacity when foam is added to the tires:

(a) Example 1. If none of the tires are foamed,  $m = 0$  and  $m/n = 0$  in equation (3) so that  $F_{sed} = 13$  kilograms per tire. Therefore, a weight increase of approximately 13 kilograms per tire can be accommodated before the breakwater starts to submerge.

(b) Example 2. If all the tires are foamed,  $m = n$  and  $m/n = 1$  above so that  $F_{sed} = 30$  kilograms per tire. In this case, each tire can carry approximately 30 kilograms of additional load for a total reserve buoyancy of about 5300 kilograms per single-pipe module.

#### 4. Cost Estimates.

Major construction components for the PT-1 module and their respective costs as of mid-1980 are listed in Table 1. It should be noted that the steel pipe accounts for nearly 60 percent of the total cost. Therefore, substantial savings are possible if used pipe can be purchased, which was done for the floating breakwater at the Mamaroneck site where used dredge pipe was obtained at a fraction of the cost indicated in Table 1. As a precautionary measure, steel pipe should be filled with foam before the end caps are welded into place. The total component cost amounts to \$19.60 per square meter of breakwater.

Table 1. Cost estimates of PT-Breakwater components.

Module dimensions: 3.7 by 12.2 m (B = 12.2 m)				
Materials:				
Truck tires (9.00-18 and 10.00-20)				
Steel pipe (41-cm-diameter steel-pile pipe)				
Conveyor-belt material (three-ply, 14 by 1.3 cm)				
Nylon bolts, washers, and nuts (13 mm)				
Item	Quantity	Unit cost	Total cost	Cost/m <sup>2</sup>
Steel pipe	12.2 m	\$43.00	\$524.60	\$11.60
Polyurethane foam (pipe plus 20 percent of tires)	2.4 m <sup>3</sup>	75.00	180.00	4.00
Tying material (conveyor belt)	94 m	1.15	108.10	2.40
Tires (transportation cost)	176	0.25	44.00	1.00
Nylon bolts, washers, and nuts	80	0.35	28.00	0.60
Cost of breakwater (excluding mooring system and assembly)				\$19.60

Assembly and launching procedures should be carefully considered and planned in advance so as to take full advantage of cost-saving site conditions. Since the anchoring system can be very costly, alternatives should be carefully investigated (e.g., the use of anchor piles may be less costly than concrete clump anchors or steel embedment anchors, depending on availability of pile-driving equipment and geotechnical conditions).

### III. EXPERIMENTAL SETUP AND PROCEDURES

#### 1. Test Facility and Instrumentation.

a. Wave Tank. Experiments were conducted in CERC's large wave tank which is 194 meters long, 4.6 meters wide, and 6.1 meters deep. The tank was operated at two water depths, 2.0 and 4.7 meters, using regular waves ranging in period from 2.6 to 8.1 seconds and height from 0.15 to 1.78 meters. A schematic of the wave tank operating with a piston-type wave generator at one end and a relatively ineffective rock revetment wave energy dissipator at the other end is shown in Figure 18. The breakwater at high and low water is shown in Figures 19 to 23.

b. Wave Gage. Two Marsh McBirney voltage-gradient water level gages (Model 100) were used to measure incident and transmitted waves. The waves were calibrated twice daily over a range of 2.0 meters by manually lowering and raising the wave staff. The output was recorded on a six-channel Brush oscillographic recorder.

c. Force Gage. Loads on the seaward mooring line were measured by a single force gage located above the tank near the wave generator. The force gage consisted of a cantilevered steel plate with strain gages mounted near its base, as shown in Figure 24. The strain gages formed two arms of a full Wheatstone bridge that was driven at carrier frequencies. The sensitivity of the force gage could be varied over a broad range, not only electronically but also mechanically, by varying the mooring-cable attachment point on the cantilever (Fig. 24). The force gage was generally calibrated before and after each test (one wave generator stroke setting) by applying a series of loads to the cantilever using a mechanical load tightener (*come-along*) and a 2270-kilogram dial force gage. The electrical output was displayed on the six-channel Brush oscillographic recorder; typical calibration curves are shown in Figure 25.

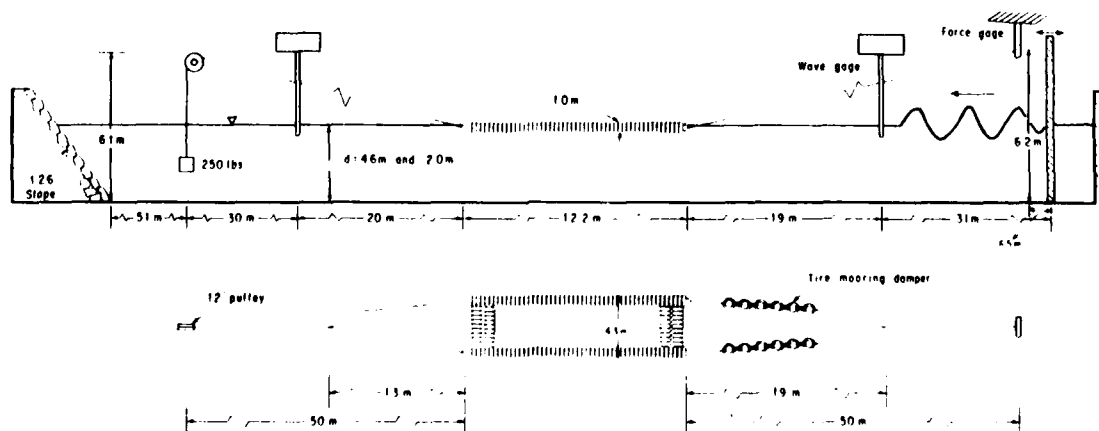


Figure 18. Large wave tank at CERC with breakwater and MS-1 mooring system.

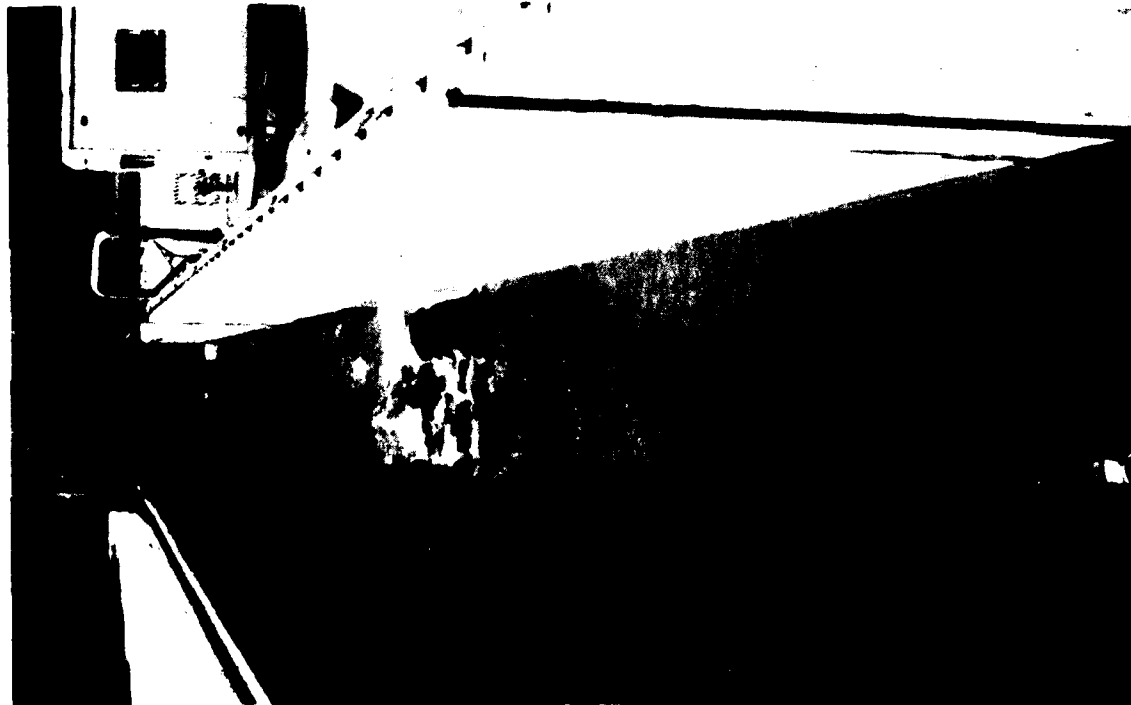


Figure 19. View toward wave generator (large wave tank, CERC).

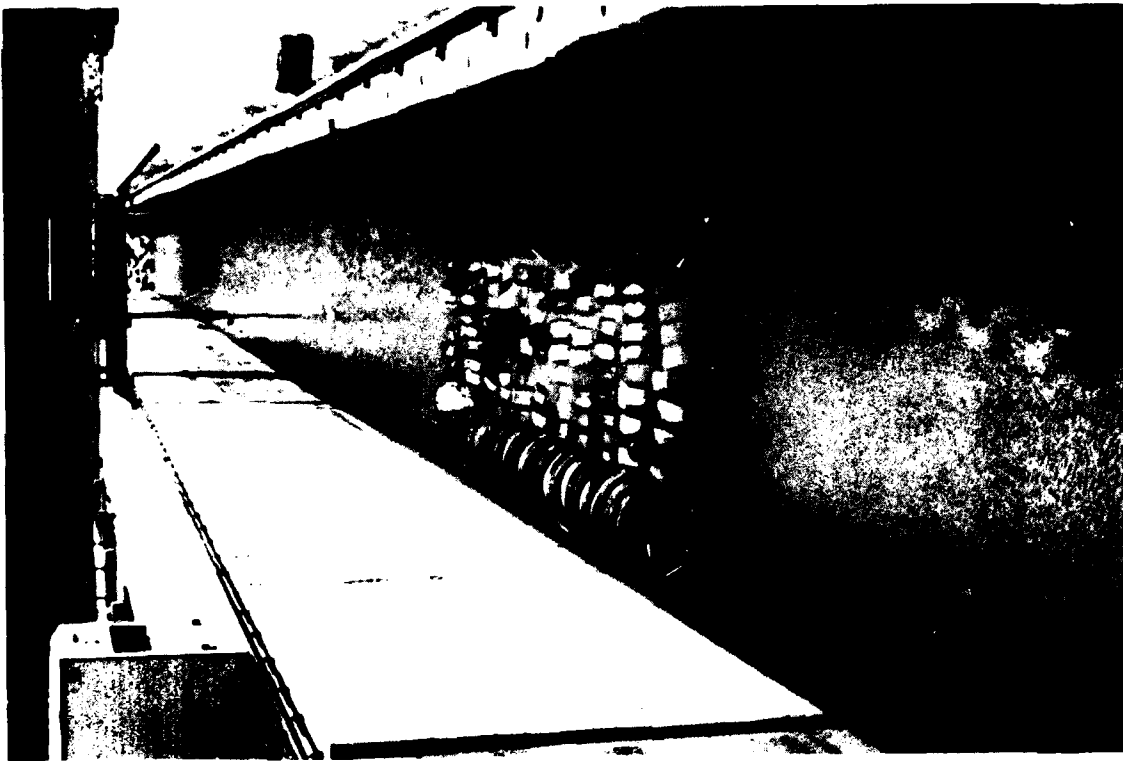


Figure 20. View toward beach (rock revetment).



Figure 21. Inserting PT-1 breakwater.



Figure 22. Turbulence associated with wave damping.



Figure 23. Attachment of seaward mooring line (MS-1 mooring system).

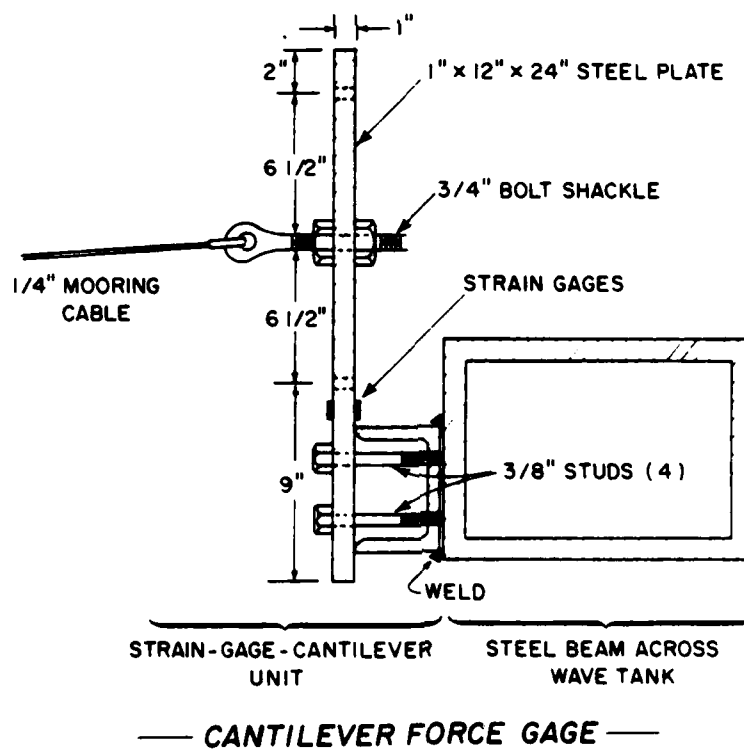


Figure 24. Strain-gage-cantilever force gage.

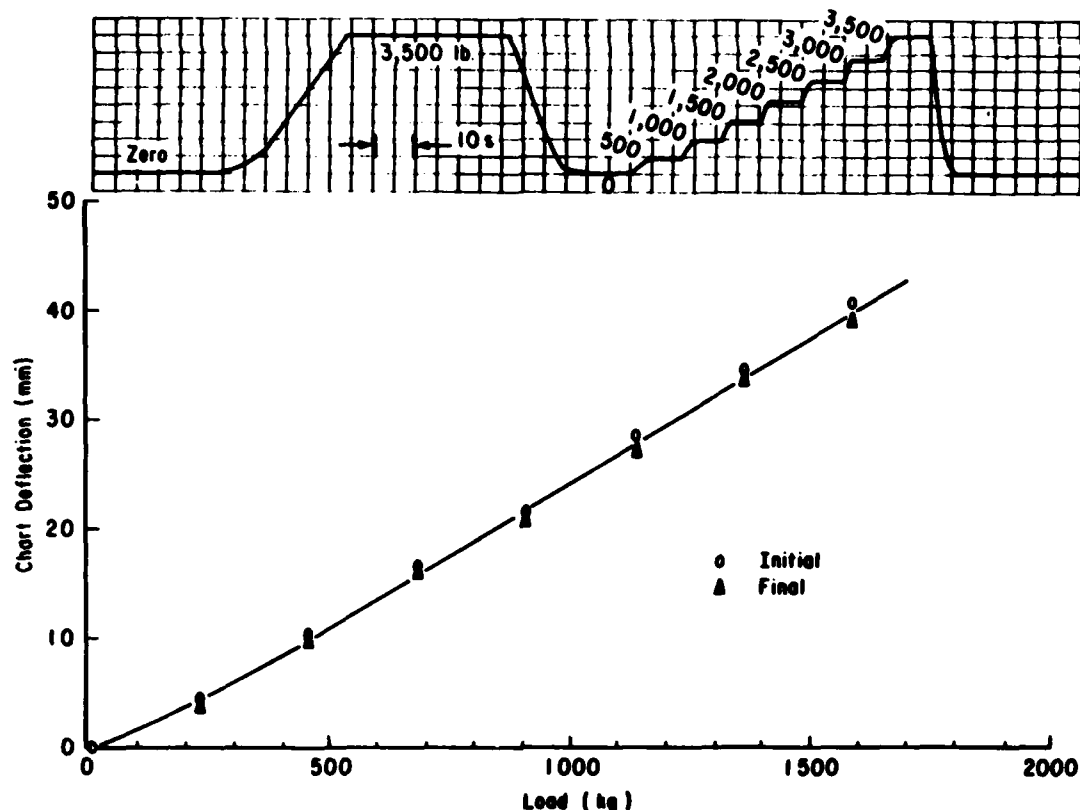


Figure 25. Force gage calibration record and curve.

## 2. Mooring System.

The basic mooring-line arrangement used throughout the test program is shown in Figure 18. The mooring lines were 6-millimeter-diameter wire rope, except for two removable segments 6 meters long that are labeled *tire mooring damper* as shown in Figure 18 and in more detail in Figure 9. These sections were installed in order to determine whether a pliant mooring-line insert such as the six-tire mooring damper could significantly reduce peak mooring forces. Should a relatively "soft" mooring system be desirable, it may be achieved by installing a tire mooring damper. The shoreward mooring bridle was always attached directly to the steel pipes; no mooring-line inserts were used on this side of the breakwater. On the seaward side the mooring bridle was most often attached to the steel pipe with cables connected to shackles extending through the pipe wall. An exception to this is the third mooring system tested in which the mooring bridle was attached to the breakwater via conveyor-belt loops that were laced through two tires armoring the pipe. In this case the mooring-line forces are first transmitted to those two tires, then transmitted to the pipe itself after the tires have shifted some distance along the pipe and encountered the compressive resistance of the other tires restrained by the retainer at the end of the pipe (Fig. 7).

The following mooring configurations were tested (major features are listed in Table 2):

- (1) Damper Pipe Connection (MS-1). In this module the tire mooring-force dampers are installed and the mooring bridle is connected directly to the pipes (soft line, hard connection) (see Figs. 18, 23, and 26).



Table 2. Compliance of mooring systems.

	Mooring system		
	MS-1	MS-2	MS-3
Type of mooring-line insert <sup>1</sup>	Tire (soft)	Belting (hard)	Belting (hard)
Type of breakwater connection	Pipe (hard)	Pipe (hard)	Tires on pipe (soft)
Mooring line stiffness (ranked)	3	1	2

<sup>1</sup> Inserts are 6 meters long; belting is in the form of a loop (used double strength) with elongation characteristics under load approximately equal to that of wire rope used.

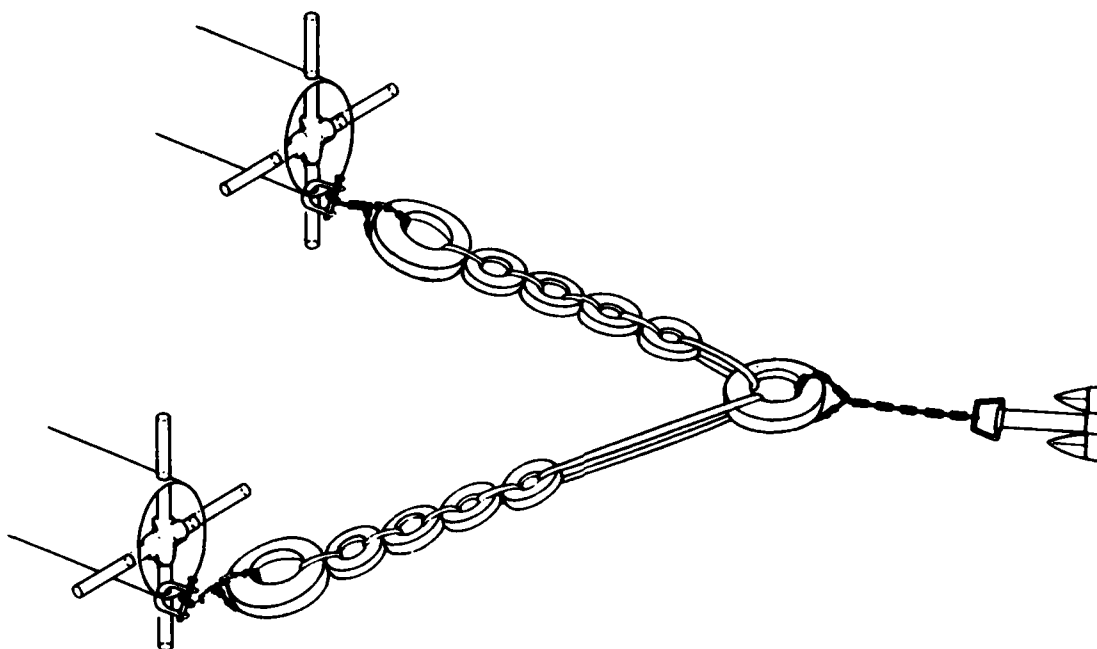


Figure 26. Mooring bridle used in field installation.

(2) No-Damper Pipe Connection (MS-2). In this module the mooring bridle remained attached to the pipes but the mooring-force damper was removed and replaced with a conveyor-belt loop of equal length. The load elongation characteristics of the conveyor-belt loop are similar to those of the wire rope used (hard line, hard connection) (Fig. 27).

(3) No-Damper Tire Connection (MS-3). In this module the conveyor-belt loop remained in place, but connection to the breakwater was made by guiding the belt around two tires located on each pipe. In the PT-1 module, tires numbered 9 and 10 were used for this purpose; in the PT-2 module, tires numbered 15 and 16 were used (hard line, soft connection).

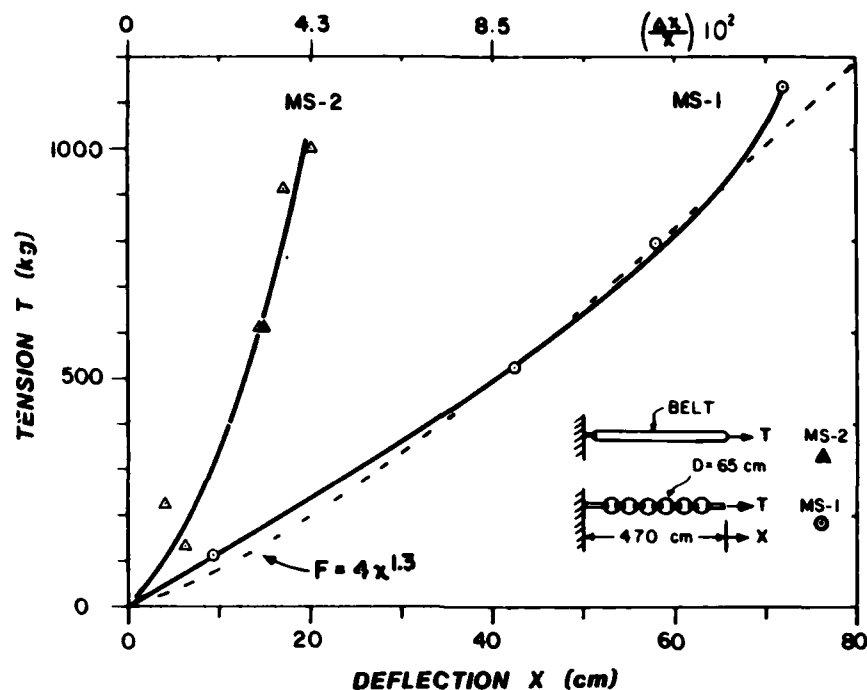


Figure 27. Load elongation curves for mooring-line inserts.

A stress-strain diagram for the conveyor belt with a five-hole bolted connection is shown in Figure 28. The strain values are influenced by the connection itself (i.e., elongation of the boltholes is being measured along with any stretching of the belt). The belt failed at a load of 2270 kilograms, not at the five-hole bolted connection but at the transition, where the belt had to be reduced in width from 14.3 to 8.9 centimeters in order to fit into the testing machine.

Force displacement relationships for MS-1 and MS-2 were obtained by tensioning the insert, using a large dump truck, and determining deflection and force, using a measuring tape and a dial force gage. The results are plotted in Figure 27. Corresponding relationships for MS-3 were not determined, but observations indicate that the elastic properties of MS-3 are between those of MS-2 and MS-1.

A mooring bridle utilizing both truck and automobile tires is shown in Figure 26. This unit was not tested at CERC; however, it has been used in field installations.

### 3. Test Procedure and Conditions.

This experimental program is limited to two designs, the PT-1 and PT-2 modules, and two water depths, 2.0 and 4.7 meters. The summary of the test conditions shown in Table 3 lists one other breakwater design—the PT-DB module; this design is simply a PT-1 breakwater that has been lengthened in the

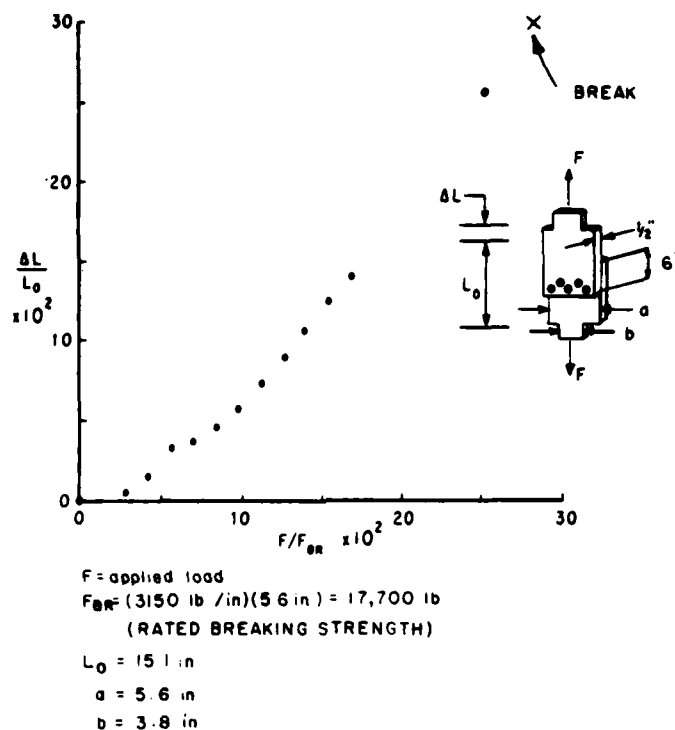


Figure 28. Stress-strain diagram for belt connection.

Table 3. Summary of test conditions.

Breakwater Type	Beam (m)	No. of runs	Water depth (m)	Mooring system	Generator stroke (cm)	Wave height (cm)	Wave period (s)
PT-1	12.2	101	2.0	MS-1	61 to 213	15 to 113	2.6 to 8.1
PT-1	12.2	92	4.7	MS-1	61 to 168	42 to 178	2.6 to 8.0
PT-1	12.2	62	4.7	MS-2	61 to 152	32 to 132	2.6 to 8.1
PT-1	12.2	37	4.7	MS-3	61 to 122	30 to 130	2.6 to 8.1
PT-2	12.2	40	2.0	MS-3	61 to 122	18 to 110	2.6 to 8.1
PT-2	12.2	36	4.7	MS-3	61 to 122	30 to 150	2.6 to 8.1
PT-DB	25.9	34	2.0	MS-3	61 to 122	28 to 132	2.6 to 8.1

shoreward direction by flexibly attaching the PT-2 module by use of conveyor-belt loops. Data for the PT-DB configuration are listed in Appendix A. The PT-1 module was tested with three different mooring systems and was, in general, emphasized in the experimental program. Out of 402 runs tested, 290 were devoted to the PT-1 breakwater. Wave heights ranged from 0.15 to 1.78 meters, with wave periods ranging from 2.6 to 8.1 seconds; the wave generator stroke varied from 0.61 to 2.13 meters.

With the breakwater floating in the wave tank and attached to the mooring system, test preparations were generally initiated each day by adjusting the water level, calibrating the wave and force gages, and checking the stroke

setting of the wave generator. The generator was adjusted to the desired frequency, started, and waves generated for about 5 minutes; this constituted a run. After shutdown of the wave generator, a necessary waiting period followed in order to regain quiescent conditions in the wave tank. When these conditions were attained, waves of another frequency were generated and this process was repeated until all the desired wave periods for that stroke setting were obtained; this process constituted a test. One, and sometimes two, tests were completed per day, and the generator stroke was changed in the afternoon so that a new test could be started the following morning. Wave and force gages were calibrated both at the beginning and end of each day's testing (and sometimes more frequently).

#### IV. DATA REDUCTION AND ANALYSIS

##### 1. Dimensional Analysis.

For a particular breakwater and mooring system, the transmitted wave height,  $H_t$ , may be expressed as a function of the following variables:

$$H_t = f(H, L, B, D, G, \lambda, m, k, \epsilon, d, \gamma, \nu, g)$$

where

$\epsilon$  = horizontal excursion of the breakwater from its equilibrium position

$k$  = measure of mooring-system stiffness (equivalent spring constant per unit length,  $\lambda$ )

$m$  = mass of breakwater (per unit length,  $\lambda$ )

$\gamma$  = specific weight of water

$\nu$  = kinematic viscosity of water

$g$  = gravitational acceleration

The remaining terms are defined in the definition sketch (Fig. 5). Since this expression contains three dimensionally independent physical variables (length, mass, time), this relationship involving 14 physical variables may be replaced, according to Buckingham's  $\pi$ -Theorem, by one involving 11 dimensionless groups:

$$\frac{H_t}{H} = \text{wave transmission ratio, } C_t$$

$$\frac{B}{D}, \frac{G}{D}, \frac{\lambda}{D}, \frac{k\epsilon}{mg} = \text{structure parameters}$$

$$\frac{H}{L} = \text{wave steepness}$$

$\frac{L}{B}, \frac{\epsilon}{H}$  = wave structure parameters

$\frac{D}{d}, \frac{\gamma BD}{mg}$  = fluid structure parameters

$\left(\frac{H}{L}\right)\left(\frac{D\sqrt{gL}}{v}\right)$  = Reynold's number

Delete the following parameters for the stated reasons:

$\frac{\lambda}{D}$  Only quasi-two-dimensional experiments will be considered (i.e., diffraction effects are absent when the breakwater extends across the full width of the tank).

$\frac{kc}{mg}$  This is the ratio of mooring-system static restoring force to structure weight and is not changed during the experiment.

$\frac{\epsilon}{H}$  Assumed to be a weak parameter that is of little importance for small values of  $\epsilon/H$  (i.e., for horizontal motions of the structure that are small compared to the wave height).

$\frac{\gamma BD}{mg}$  This parameter relates the mass of fluid displaced by the breakwater to the mass of the breakwater itself. It would remain constant for geometrically similar breakwaters constructed from the same materials.

$\left(\frac{H}{L}\right)\left(\frac{D\sqrt{gL}}{v}\right)$  This Reynold's number is based on the tire diameter and a velocity that is related to the maximum wave-induced water particle velocity; it will be assumed large enough to insure Reynold's number independence.

By eliminating the above dimensionless groups, the following is obtained

$$C_t = f\left(\frac{L}{B}, \frac{H}{L}, \frac{D}{d}, \frac{B}{D}\right) \quad (4)$$

This is the relationship on which the experimental program was based.

Similarly, consider the mooring-force relationship to be

$$F = f(H, H_c, L, B, D, G, \lambda, m, k, \epsilon, d, \gamma, \nu, g)$$

and, by similar reasoning, obtain

$$\frac{F}{\gamma H^2} = f\left(\frac{L}{B}, \frac{H}{L}, \frac{D}{d}, \frac{B}{D}\right) \quad (5)$$

## 2. Data-Reduction Procedures.

Analog signals from the wave gages and force transducer were recorded on three channels of a six-channel Brush oscillographic recorder. Typical records of the seaward mooring-line force and the incident and transmitted waves are reproduced in Figures 29 to 32.

Wave reflections from the steep, rock-armored beach at the end of the wave tank (Fig. 18) were an annoyance, particularly for the longer waves generated. The incident and transmitted wave heights were therefore generally obtained from the first 5 to 10 waves in the run (i.e., before wave reflections could substantially influence wave height measurements. Beach reflections were particularly bothersome when generating waves of low steepness and of periods larger than about 5 seconds.

From the force gage records it can be seen that the seaward mooring load fluctuates with the passage of each wave between a maximum value, which varies

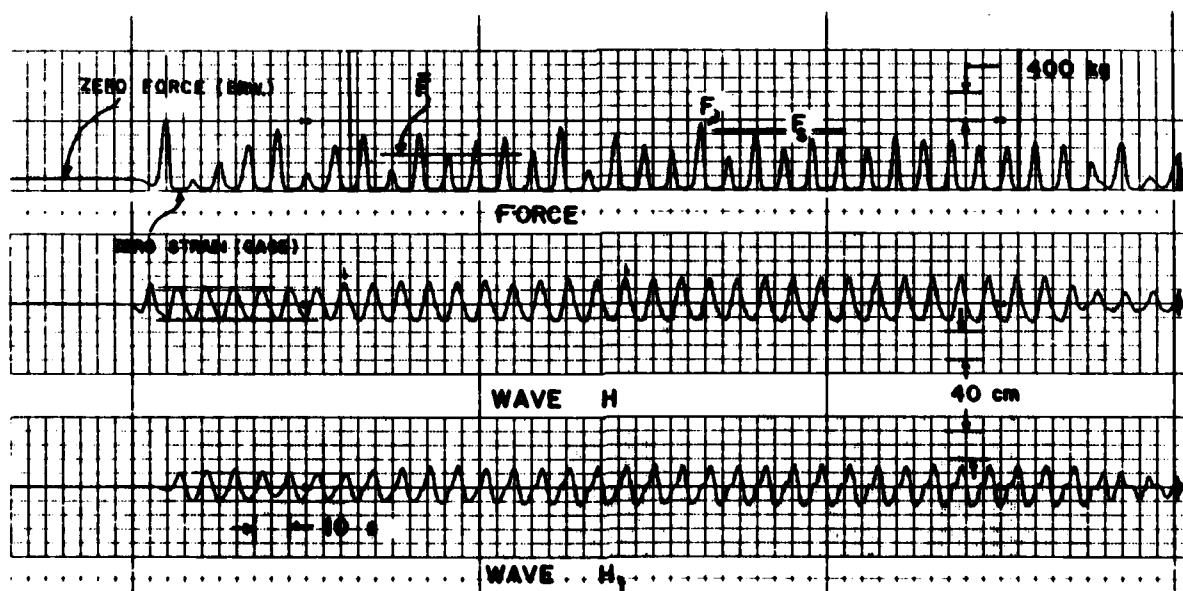


Figure 29. Wave and force record for long waves ( $d = 4.7$  m,  $T = 8.0$  s).

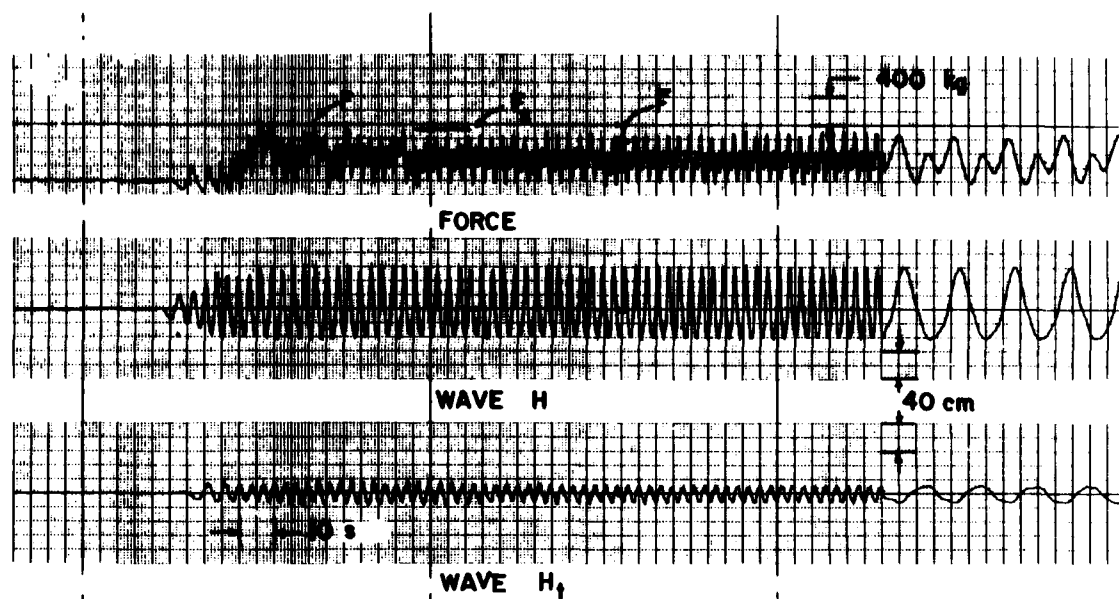


Figure 30. Wave and force record for short waves ( $d = 4.7$  m,  $T = 3.2$  s).

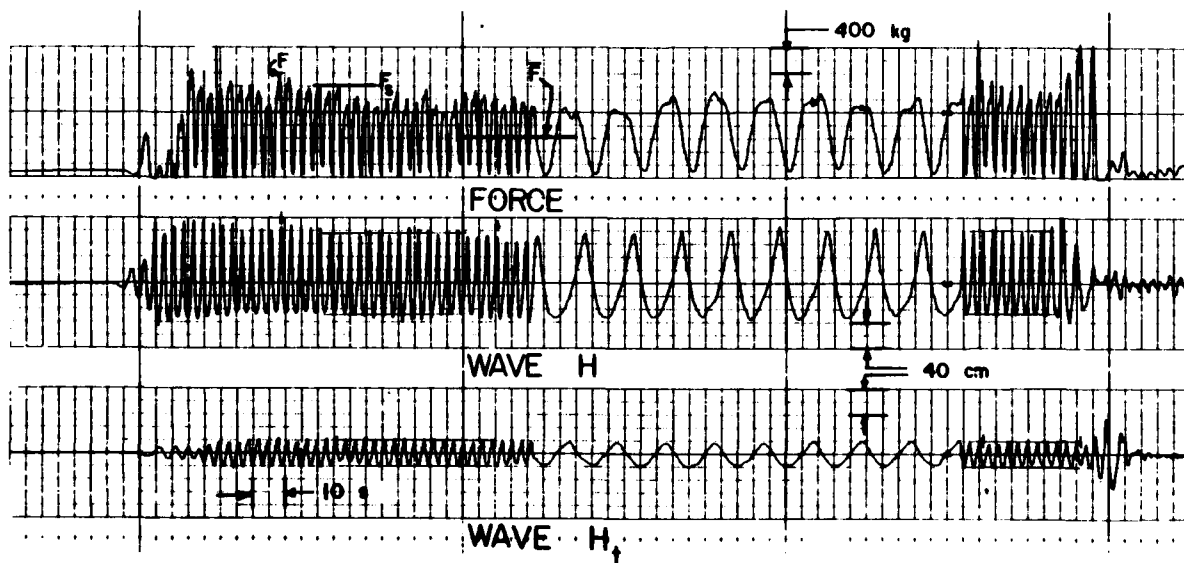


Figure 31. Wave and force record for steep waves ( $d = 4.7$  m,  $T = 3.0$  s).

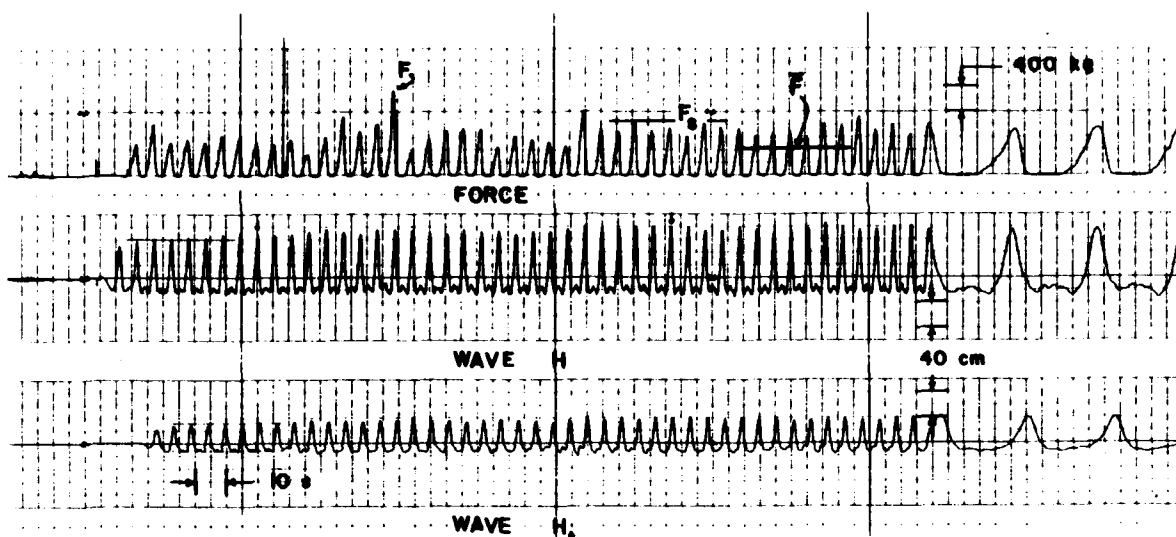


Figure 32. Wave and force record for shallow-water waves ( $d = 2.0$  m,  $T = 5.5$  s).

throughout the run, and a minimum value, which remains essentially constant. The individual force peaks occur as the breakwater surges shoreward during the passage of each wave crest, but is prevented from moving too far in this direction by the mooring-line restraint. On the other hand, the seaward movement of the breakwater is not similarly opposed, since no force cantilever was installed on the leeward side of the breakwater. Instead, only a constant negative restoring force or preload of approximately 113 kilograms was exerted on the breakwater via the shoreward mooring line and pulley-weight arrangement shown in Figure 18. The zero-force reference recorded at the beginning of each run always corresponds to this static preloaded condition of the cantilever force gage. Negative force values up to the magnitude of this preload can consequently be obtained as the breakwater surges seaward; these constitute the stable lower limit of the force records.

A time-series analysis of the force data was not performed because the experiments were limited to regular waves and because the level of effort required did not make it feasible. For practical purposes, each force record is therefore characterized by a single force value that is considered most useful for design purposes—the peak force,  $F$ , occurring during the length of record (excluding wave generator start-and-stop transients, which have no counterpart in nature). Typically, this implies that the first 5 to 10 waves were not included in the analysis, nor were those last waves propagating down the tank after shutdown of the wave generator. Each run consists of at least 50 waves. In addition to the peak mooring force,  $F$ , an approximation to the drift force,  $\bar{F}$ , is also obtained, as is the significant peak force,  $F_g$ . The drift force  $\bar{F}$  is the net, time-averaged force acting on the seaward mooring line; it was determined "by eye" as shown in Figure 33 and is therefore subject to larger errors. The significant force,  $F_g$ , represents the average of the largest one-third of the force peaks, again excluding stop-and-start transients; it is obtained manually, directly from the data trace.

If stop-and-start transients are included in the determination of the peak mooring force, as has been done by other investigators (Giles and Sorensen,



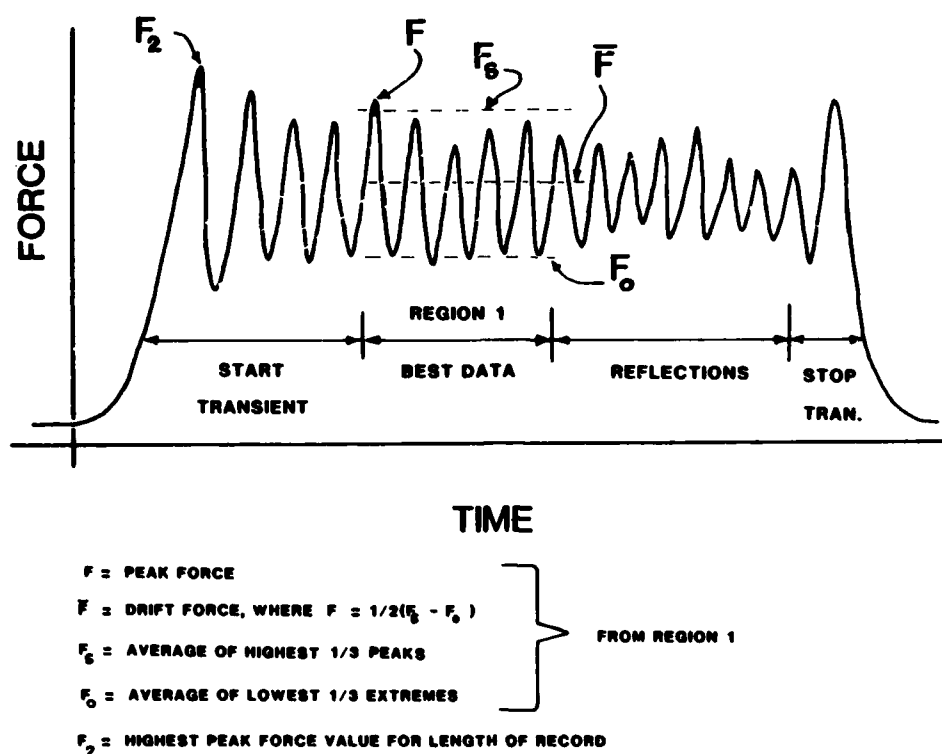


Figure 33. Definition sketch for force analysis.

1978), the difference between  $F$  and this peak force is frequently small, but on the other hand can be quite large as shown in Appendix B. In that appendix the peak mooring force,  $F$ , is also compared to the significant peak force,  $F_g$ , for a large number of the tests.

The cantilever force gage is calibrated at least once at the beginning and ending of each day's testing; if zero drifts are observed, it is calibrated more frequently. Calibration is accomplished manually via a separate cable with mechanical load tightener and 2270-kilogram dial force gage in series, attached close to the cantilever. A typical calibration record is shown in Figure 25. The force values are always referenced to the static no-load condition (i.e., with pulley preload but no waves).

## V. EXPERIMENTAL RESULTS

### 1. Wave Transmission Data.

For each breakwater configuration and water depth, the transmitted wave height depends primarily on the width of the structure and the incident wavelength (or period) and wave height. Dimensional analysis and physical insight were invoked in Section IV to arrive at dimensionless parameters that would describe the problem more succinctly and clearly and would also guide the experimental effort and analysis of the results. This evolved in the presentation of the data in the format shown in Figure 34. The wave height transmission ratio,  $C_t = H_t/H$ , is presented as a function of relative wavelength  $L/B$ , with different symbols designating ranges of wave steepness  $H/L$ . These are the primary parameters. The secondary parameters are listed in the insert of each figure. These parameters specify the water depth (relative depth,

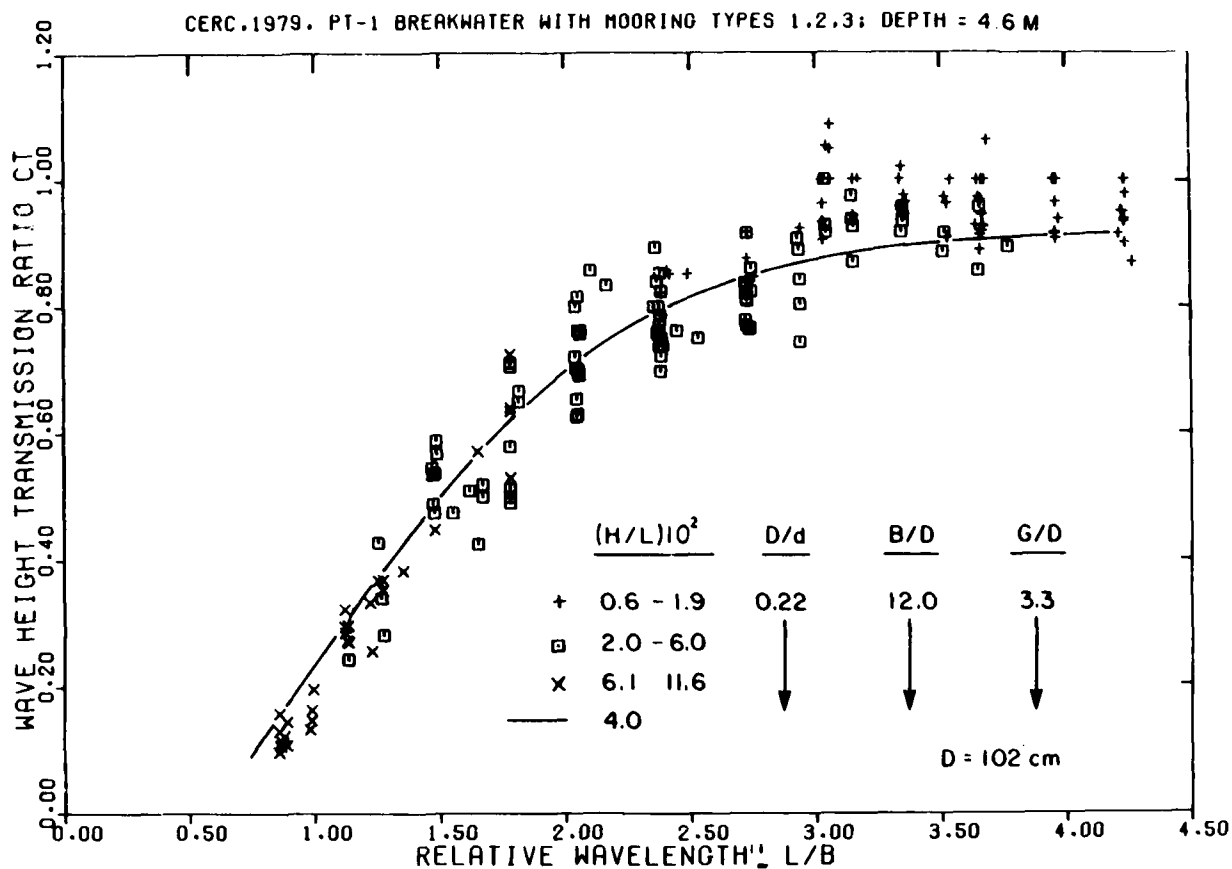


Figure 34. Wave transmission data for PT-1 breakwater ( $d = 4.7$  m).

$D/d$ ) and breakwater geometry (aspect ratio,  $B/D$ , and pipe spacing,  $G/D$ ). For design purposes, the transmission characteristics of each breakwater are summarized in the form of a single wave height transmission curve. This curve corresponds to a wave steepness of  $H/L = 0.04$  (a moderate value frequently encountered in practice) and different values of  $D/d$ . Although much data have been obtained at wave steepness other than 0.04, indicating that the transmission ratio,  $C_t$ , generally decreases with increasing wave steepness, the available data are not adequate for defining transmission curves for wave steepness other than 0.04. Nevertheless, the influence of wave steepness has been preserved to a large extent by grouping the data according to steepness categories; in Appendix C the value of  $H/L$  is actually listed next to each data point. Appendix C should be particularly useful for design cases with wave steepness near the extremes encountered in nature, either high or low (e.g.,  $H/L$  larger than 0.08 or less than 0.02), since deviations from the 4-percent design curve may then become significant. The wave transmission data in Appendix C have also been segregated with respect to the type of mooring system installed, but it was found that this had no discernible influence on wave transmission characteristics. It is therefore permissible to combine the data for all of the mooring systems as has been done in Figure 34.

a. PT-1 Breakwater. Wave transmission data for the PT-1 module (truck tires, steel pipe) are shown in Figures 34 and 35 for two water depths,  $D/d = 0.22$  and  $0.51$ . In both cases the transmission ratio,  $C_t$ , increases monotonically with relative wavelength  $L/B$ . The breakwater is very effective

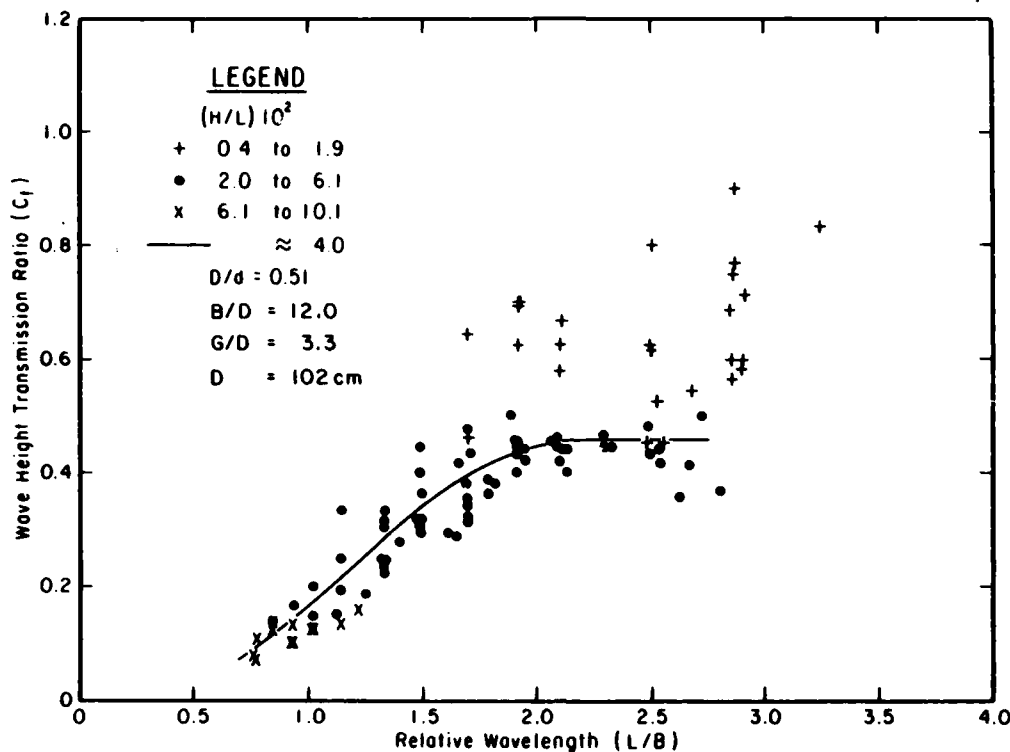


Figure 35. Wave transmission data for PT-1 breakwater ( $d = 2.0 \text{ m}$ ).

in filtering out waves that are shorter than the width of the structure, but becomes increasingly less effective as the wavelength increases. It is evident that the breakwater is significantly more effective at the lower depth, particularly for longer waves. The influence of water depth, or relative draft  $D/d$ , becomes particularly apparent in Figure 36 where the transmission curves are compared.

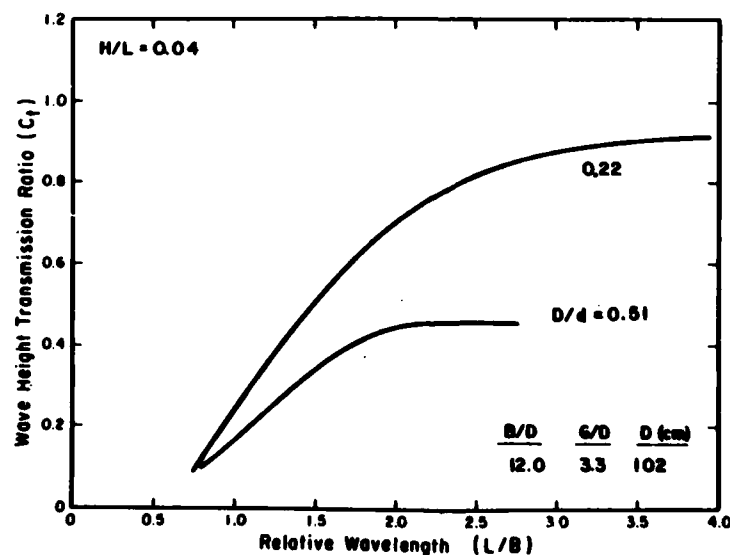


Figure 36. Wave transmission design curves for PT-1 breakwater.

The influence of wave steepness is most readily detectable for longer waves (e.g.,  $L/B$  larger than 2) and may be important at low water depths. For  $L/B = 2.9$  and  $D/d = 0.51$  (Fig. 35), the value of  $C_t$  decreases dramatically from 0.9 to 0.4 as  $H/L$  increases from 0.007 to 0.028 (refer also to Fig. C-7 in App. C). The data in Figures 34 and 36 apply to the PT-1 module, which has a pipe spacing of  $G/D = 3.3$ , aspect ratio of  $B/D = 12$ , and beam  $B = 12.2$  meters. These conditions may not be altered greatly without also influencing the wave transmission characteristics. For example, the design curves of Figure 36 may not apply to a structure with a much larger beam, e.g.,  $B = 24$  meters (i.e., or  $B/D = 24$ ). Until further data on the importance of  $B/D$  are obtained, it is suggested that the PT-1 wave transmission design curves of Figure 36 be limited to beam dimensions in the range from 9 to 15 meters. Such information has been recently provided in Harms, Bishop, and Westerink, 1981. Existing data from small-scale experiments (Harms, 1979) indicate that the transmission curve for  $D/d = 0.22$  does not change significantly as the water depth increases. For deepwater applications with  $D/d$  less than 0.2, it is therefore suggested that the  $D/d = 0.22$  curve be used for design purposes, at least until further data become available. In addition, curves should not be extrapolated beyond the range of data shown (i.e.,  $L/B > 4.5$  and 3.0).

b. PT-2 Breakwater. Wave transmission data for the PT-2 module (constructed of automobile tires and telephone poles) are shown in Figures 37 and 38, with design curves given in Figure 39. The behavior of the PT-2 module is very similar to that of the PT-1 module, although a decrease in wave attenuation performance is indicated, at least at the larger water depths considered in Figure 40. It was observed that the influence of wave steepness  $H/L$  is again particularly apparent at the lower water depth ( $D/d = 0.33$ , Fig. 38) and large values of  $L/B$ . The actual  $H/L$  values associated with each data point are given in the appendixes. Again, curves should not be extrapolated beyond the range of the data shown (i.e.,  $L/B > 4.5$  and 3.0).

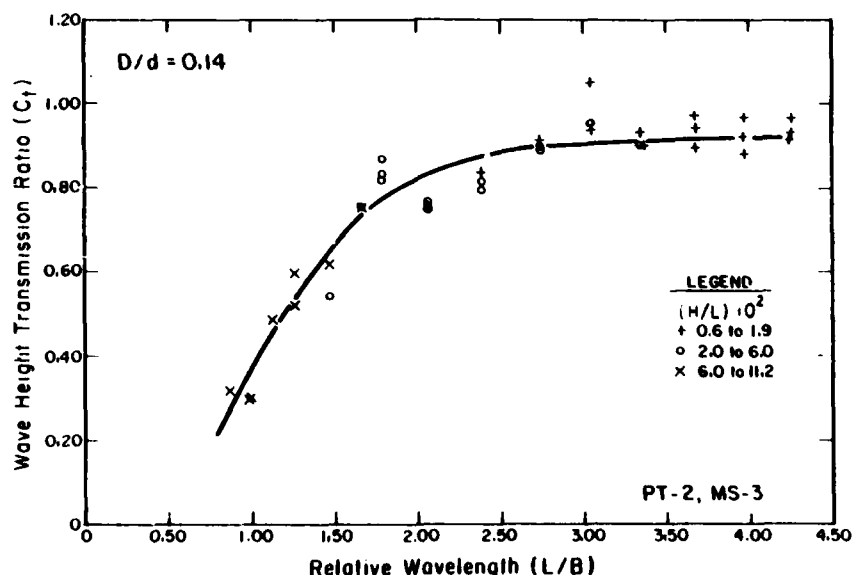


Figure 37. Wave transmission data for PT-2 breakwater ( $d = 4.7$  m).

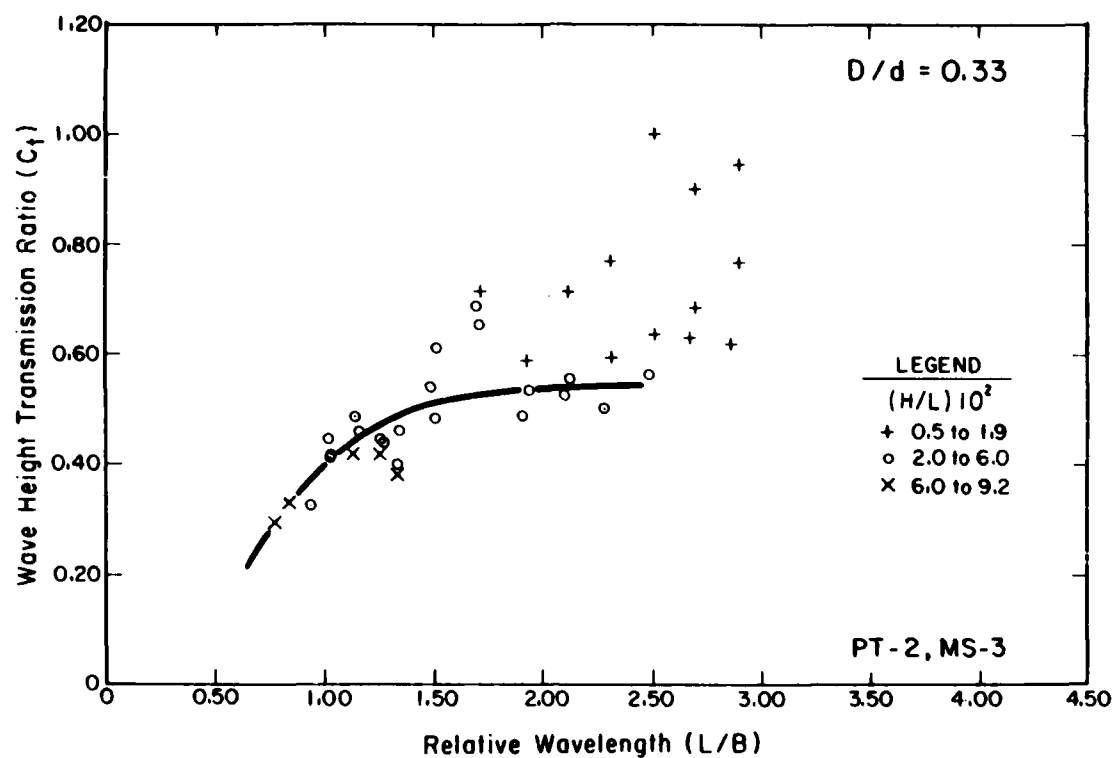


Figure 38. Wave transmission data for PT-2 breakwater ( $d = 2.0$  m).

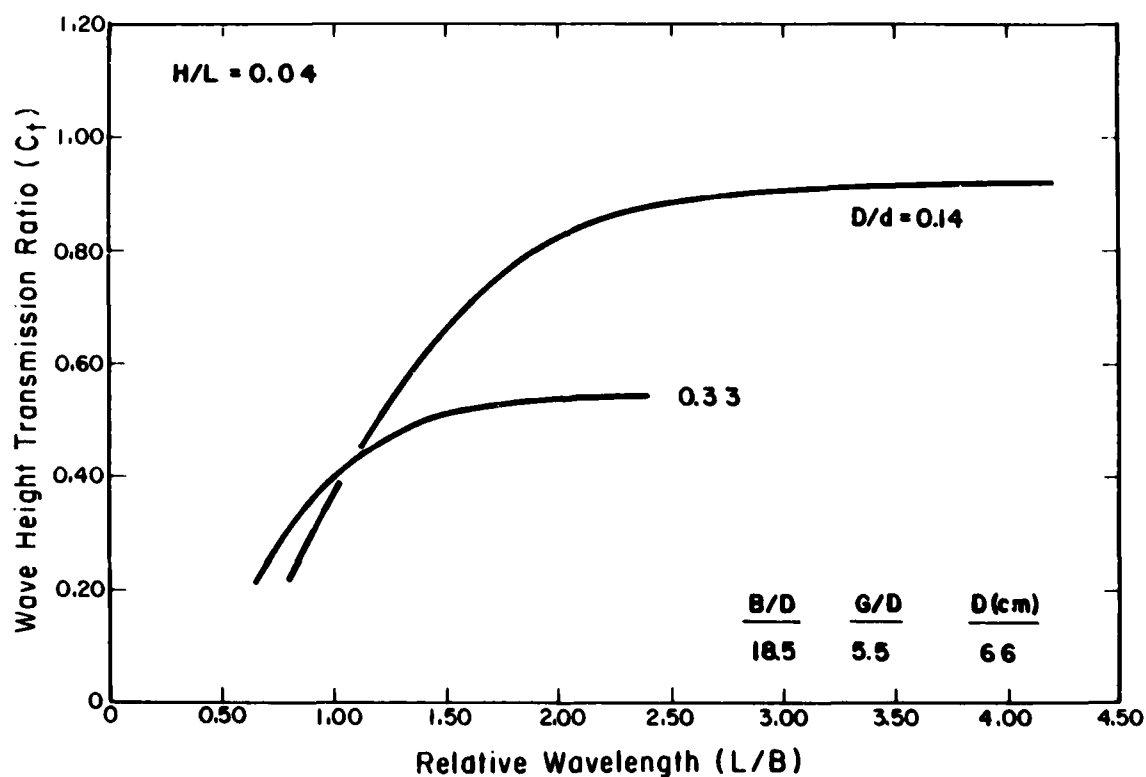


Figure 39. Wave transmission design curves for PT-2 breakwater.

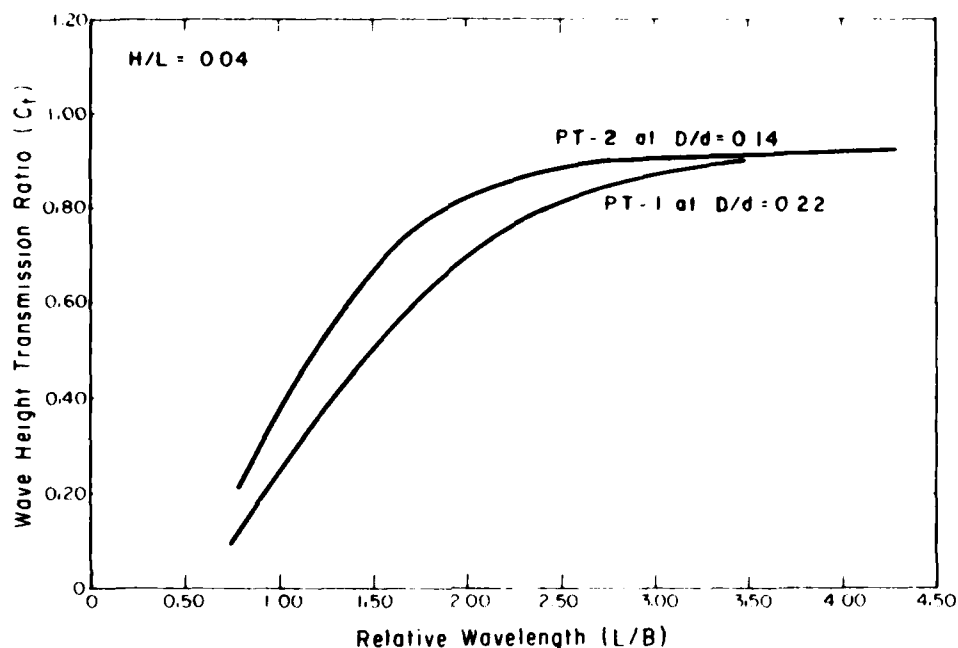


Figure 40. Comparison of PT-1 and PT-2 wave attenuation ( $d = 4.7$  m).

c. Goodyear Breakwater. Giles and Sorensen (1978) obtained prototype-scale wave transmission data for the Goodyear floating tire breakwater using the large wave tank at CERC. Data for the 6-module-wide Goodyear breakwater are plotted in Figures 41 and 42, along with the wave transmission curve for the PT-2 module. Both breakwaters are constructed from automobile tires and have a beam of 12.2 meters which is equivalent to  $B/D = 18.5$ . For the lower water depth case considered in Figure 42, it is evident that the PT-2 breakwater is substantially more effective than a Goodyear breakwater of equal size. At the larger water depth considered in Figure 41, the PT-2 breakwater is still superior but not as much so as at the lower water depth.

From extensive small-scale experiments by Harms (1979a, 1979b), the influence of water depth is found not to be of practical importance for the Goodyear breakwater, at least for values of  $D/d$  less than 0.4, although  $C_t$  clearly decreases as  $D/d$  increases. How significant the influence of  $D/d$  is for the full-scale Goodyear breakwater (Figs. 41 and 42) is shown in Figure 43 where the data for  $D/d = 0.16$  and 0.33 may be compared while keeping  $L/B$ ,  $H/L$ , and  $B/d$  constant; the difference in  $C_t$  is typically less than 0.1 (the  $C_t$  values near  $L/B = 2$  are probably false). Small-scale and prototype-scale data are therefore in agreement and the single Goodyear wave transmission curve of Figure 44 (Harms, 1979a) may be used for most practical applications as long as  $D/d$  does not exceed 0.4; near  $D/d = 0.4$  the design curve will be somewhat more conservative than at lower values of  $D/d$ .

The performance of the PT-1 module is compared to that of a Goodyear breakwater of equal size in Figure 44. It is apparent that the PT-Breakwater provides substantially more wave protection than the Goodyear breakwater. It

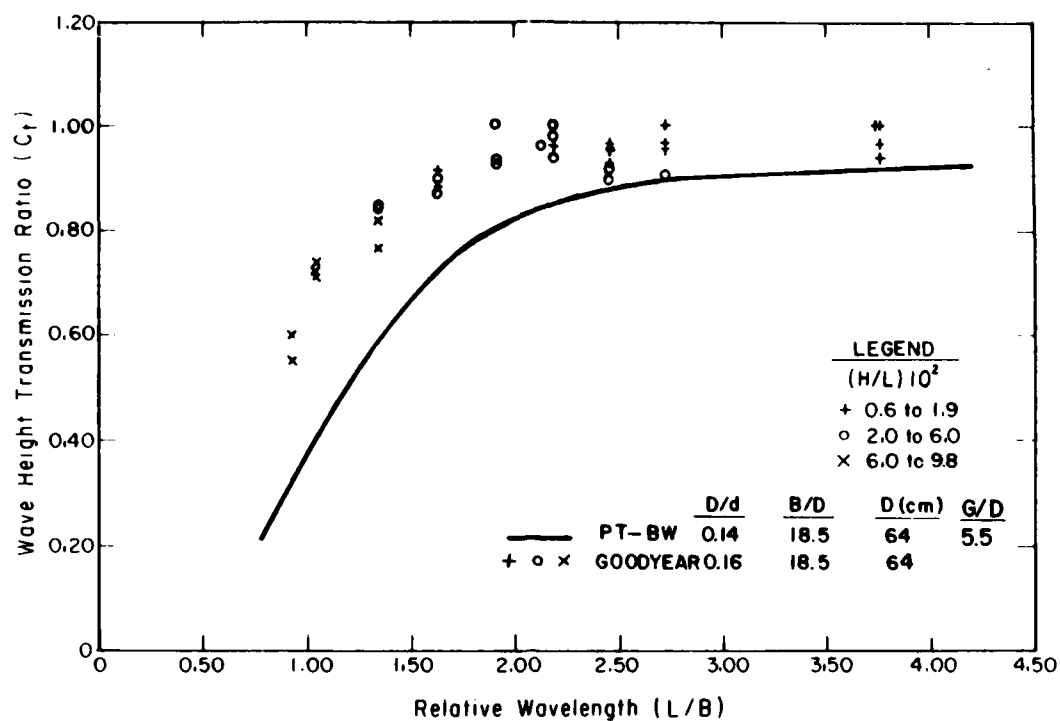


Figure 41. Comparison of Goodyear and PT-2 wave attenuation ( $d = 4.7$  m).

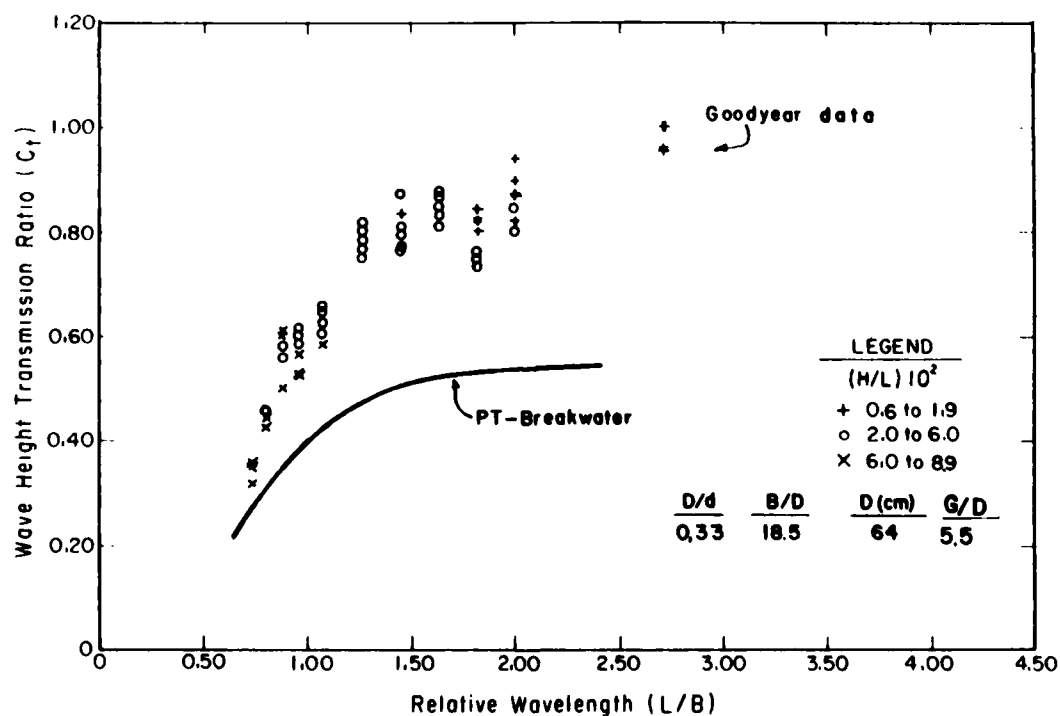


Figure 42. Comparison of Goodyear and PT-2 wave attenuation ( $d = 2.0$  m).

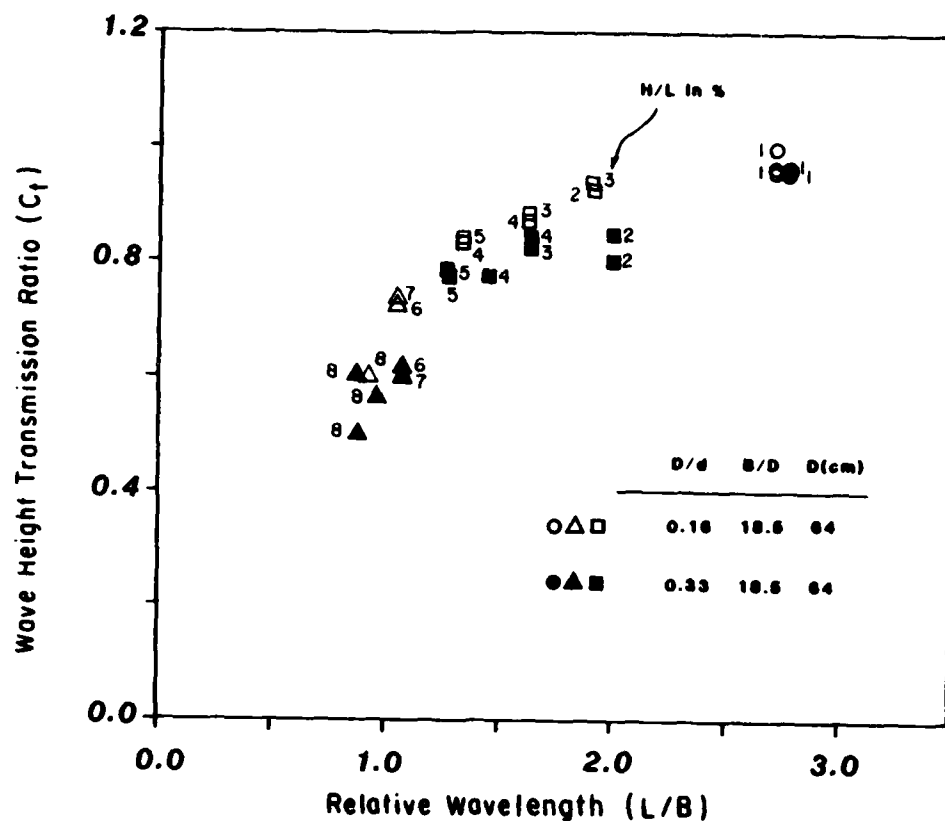


Figure 43. Influence of  $D/d$  on Goodyear wave attenuation.

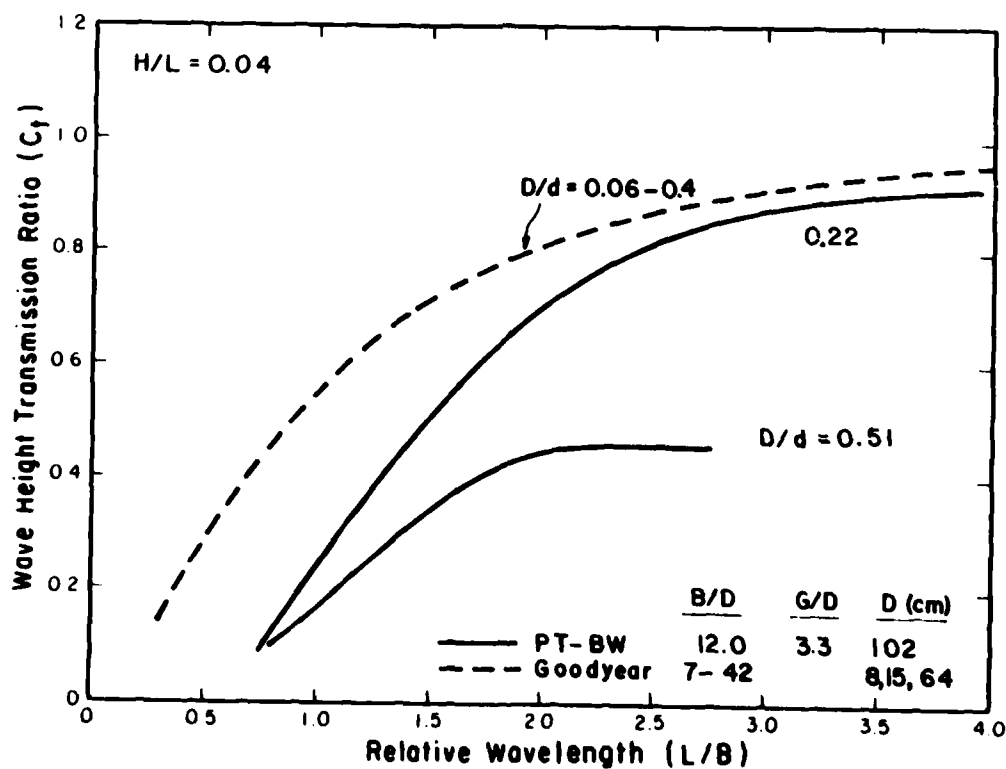


Figure 44. Wave transmission design curves for Goodyear and PT-Breakwater.



should be noted that the Goodyear design curve in Figure 44 is independent of B/D, having been tested over a broad range of B/D during experiments at the Canada Centre for Inland Waters (CCIW) (Harms, 1979a, 1979b). A similar series of experiments for the PT-Breakwater was scheduled at CCIW in September 1980 (see Harms, Bishop, and Westerink, 1981 for results).

## 2. Mooring-Force Data.

a. PT-1 Breakwater. This breakwater was tested most extensively in the MS-1 mooring configuration (i.e., with a six-tire mooring-force damper installed). It was also tested with the MS-2 and MS-3 mooring systems at the deepest water depth of 4.7 meters. As is explained in Section III, the MS-2 mooring configuration is the "stiffest" system tested and the MS-1 is the most elastic or "softest" system tested with the elastic properties of the MS-3 system lying somewhere between them.

The peak mooring force is plotted in Figures 45 and 46 as a function of wave height for the case of MS-1 and two water levels,  $D/d = 0.51$  and  $0.22$ . An exponential relationship between the mooring force and the wave height can be detected in the data, even though this information is masked at times by the relatively large scatter of data (even at fixed L/B) that is common in this type of measurement. The best "by eye" fit has been drawn and indicates that at both water levels  $F$  is proportional to  $H^{3/2}$ . For a given wave height and wavelength, the peak mooring forces are clearly higher at the lower water level. This is shown in Table 4 where the value of the force coefficient  $K$  is listed and defined. The influence of L/B is difficult to quantify from the data: an increase of  $F$  with L/B appears to be indicated, particularly at  $D/d = 0.51$ , but additional tests would have to be made to define this relationship.

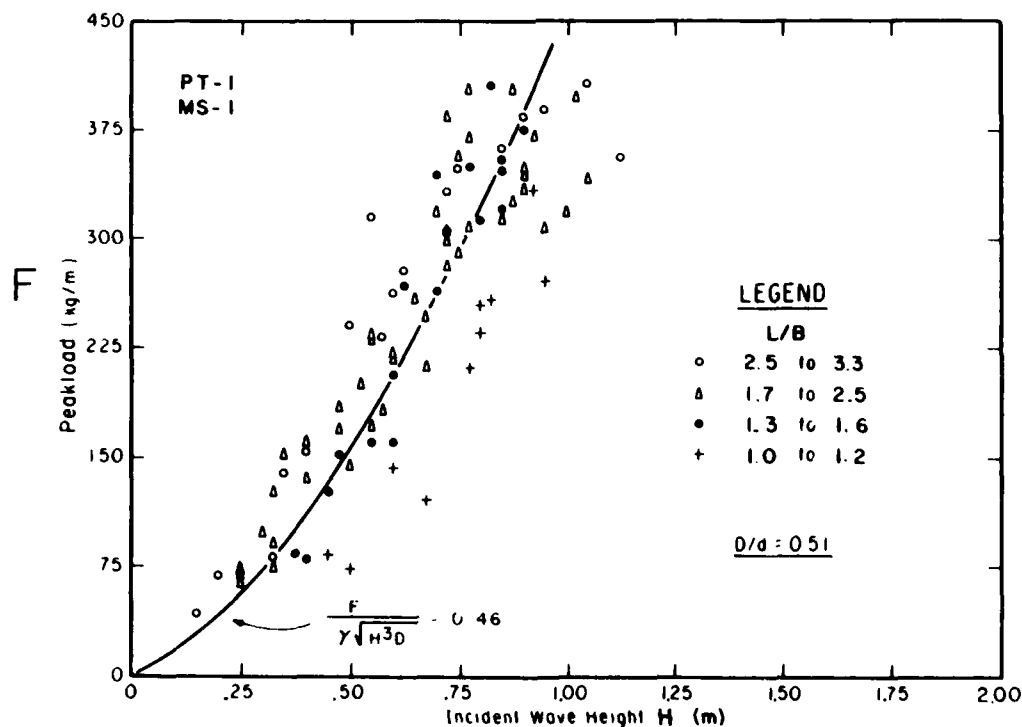


Figure 45. PT-1 peak mooring-force data (MS-1,  $d = 2.0$  m).

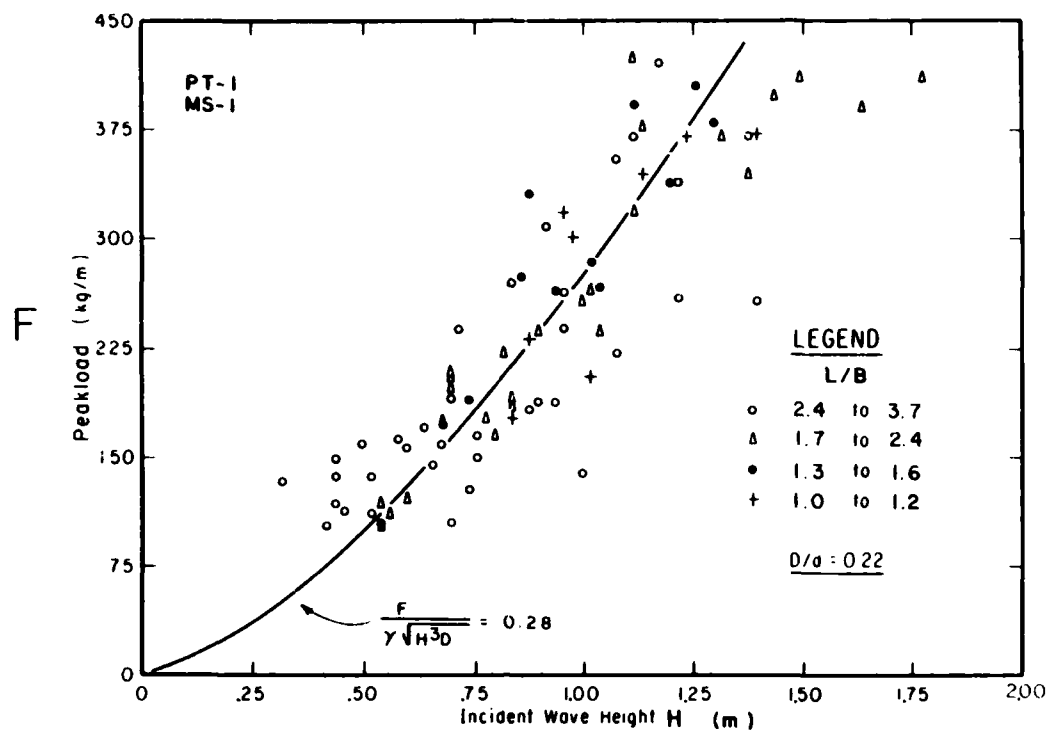


Figure 46. PT-1 peak mooring-force data (MS-1,  $d = 4.7$  m).

Table 4. Summary of mooring-force data.<sup>1</sup>

Mooring system	Force coefficient, K					
	PT-1		PT-2		Goodyear	
	$\frac{F}{\gamma \sqrt{H^3 D}} = K$		$\frac{F}{\gamma H^2} = K$		$\frac{F}{\gamma H^2} = K$	
	D/d		D/d		D/d	
	0.22	0.51	0.14	0.33	0.16	0.33
MS-1	0.28	0.46	0.20 <sup>2</sup>	0.33 <sup>2</sup>	----- <sup>3</sup>	-----
MS-2	0.50	-----	-----	-----	-----	-----
MS-3	0.37	-----	0.27	0.44	-----	-----
Goodyear	-----	-----	-----	-----	0.14	0.11

<sup>1</sup>For design purposes, suggest that  $F$  be increased by 100 kilograms per meter.

<sup>2</sup>Estimated values.

<sup>3</sup>Data not available.

How the mooring-system elasticity affects the peak mooring force is shown in Figures 46, 47, and 48. In each case the water level is fixed and only the mooring-line flexibility is changed. A substantial increase in  $F$  is noted when the six-tire mooring-force damper is removed and replaced with a relatively inflexible section of conveyor belt (i.e., switching from the MS-1 to the MS-2 system). This is apparent in Figure 47 where the MS-2 data are shown with relation to the MS-1 curve from Figure 46; all the data are above the MS-1 curve with much of the data far above it. The MS-3 data and curve-through data are shown in Figure 48. This system results in forces that are somewhat higher than those for the MS-1 system but lower than those for the MS-2 system. The corresponding values of  $K$  are provided in Table 4.

b. PT-2 Breakwater. The PT-2 module was tested only in the MS-3 mooring configuration; test results are shown in Figures 49 and 50. Again as for PT-1, the force is proportional to  $H^n$ , but for PT-2 the appropriate exponent is 2, not  $3/2$  as it is for PT-1. The curves for  $n = 2$ , fitted by eye, are shown in Figures 49 and 50; the corresponding values of  $K$  are listed in Table 4. Although PT-2 was tested with the MS-3, and not the preferred MS-1 mooring system, the effect of a change from MS-3 to MS-1 may be estimated by assuming that the ratio of the respective forces is the same as for the PT-1 module (for which such data exist and are conveniently summarized in Table 4). For PT-1 it is noted

$$\frac{K(\text{MS-1})}{K(\text{MS-3})} = \frac{280}{370} = 0.76$$

Assuming that this ratio holds for the PT-2 module as well, the estimated MS-1 values, shown in Table 4, are obtained. Although the peak mooring forces for the PT-1 module are higher than those for the PT-2 module for the same wave height and water depth, it should be noted that the transmitted wave is also smaller in the case of the PT-1 module.

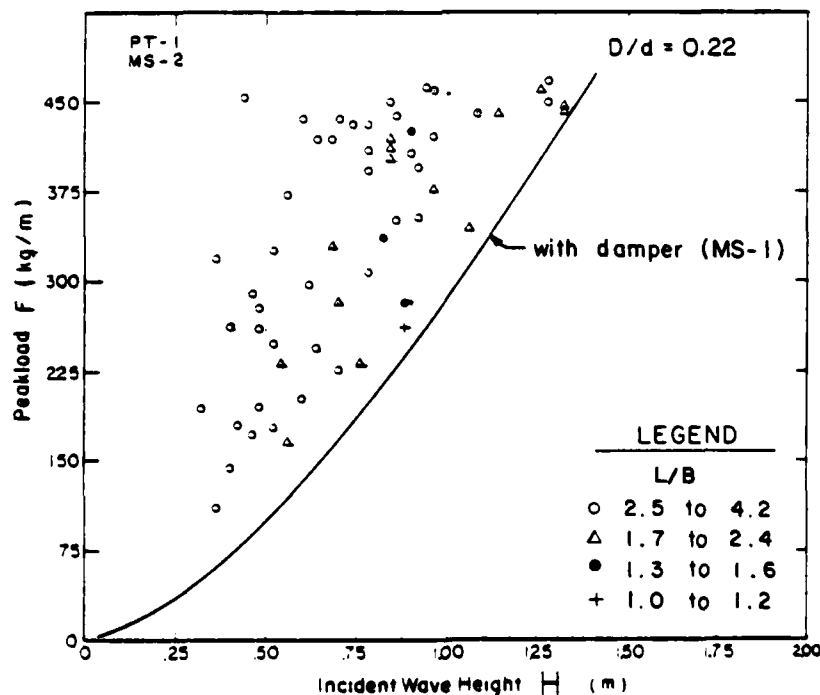


Figure 47. Effect of mooring-system compliance on  $F$  (MS-1 and MS-2,  $d = 4.7$  m).

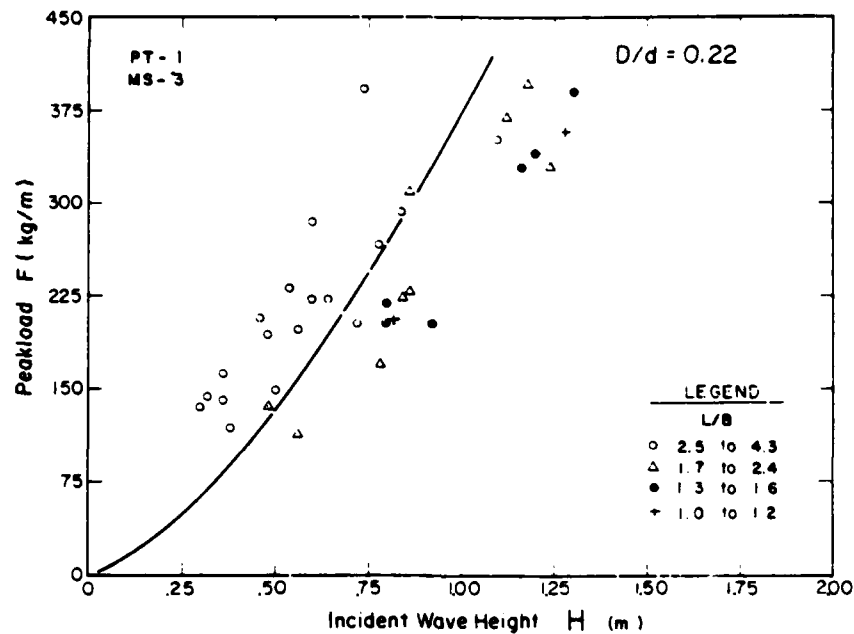


Figure 48. PT-1 peak mooring-force data (MS-3,  $d = 4.7$  m).

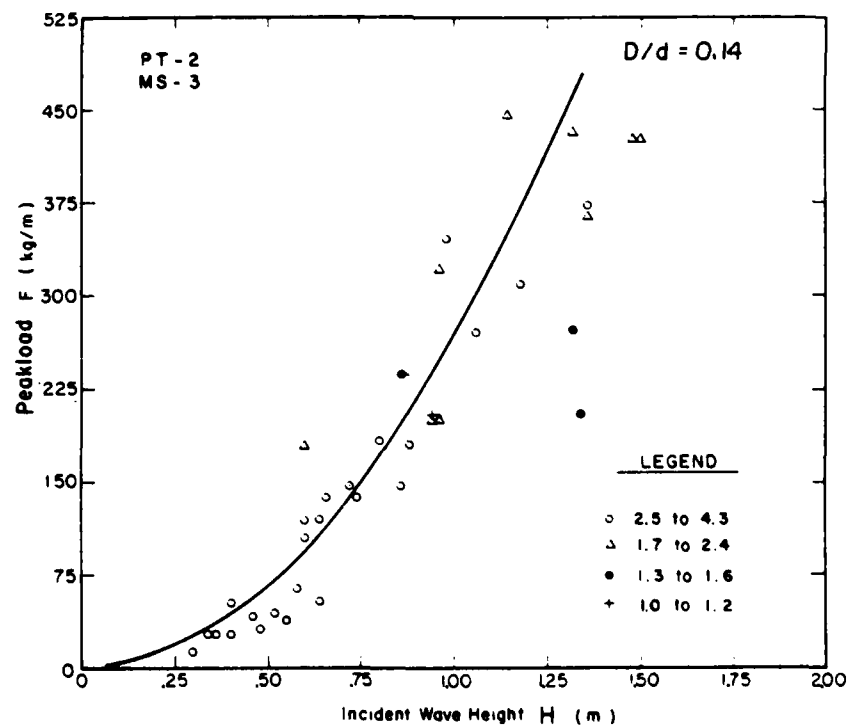


Figure 49. PT-2 peak mooring-force data (MS-3,  $d = 4.7$  m).

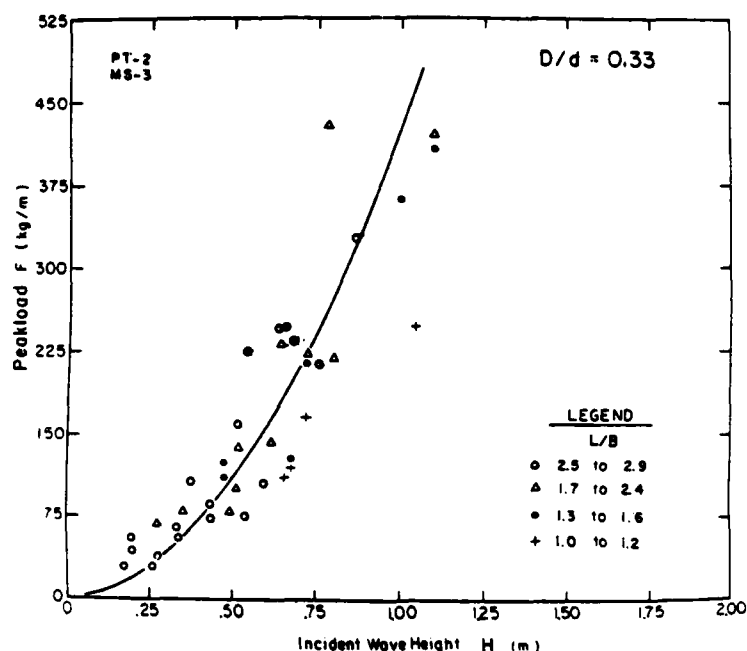


Figure 50. PT-2 peak mooring-force data (MS-3,  $d = 2.0$  m).

c. Goodyear Breakwater. The Goodyear module tests by Giles and Sorensen (1978) also included an evaluation of the breakwater mooring loads. Data from those experiments are plotted in Figures 51 and 52 for the case corresponding most nearly to the conditions in the present study (i.e., for the six-module-beam Goodyear breakwater that is also 12.2 meters wide). The curves shown in Figures 51 and 52 indicate that  $F$  is proportional to  $H^2$ ; the corresponding force coefficient  $K$  is listed in Table 4. The hyperbolic relationship between  $F$  and  $H$  adequately describes the data.

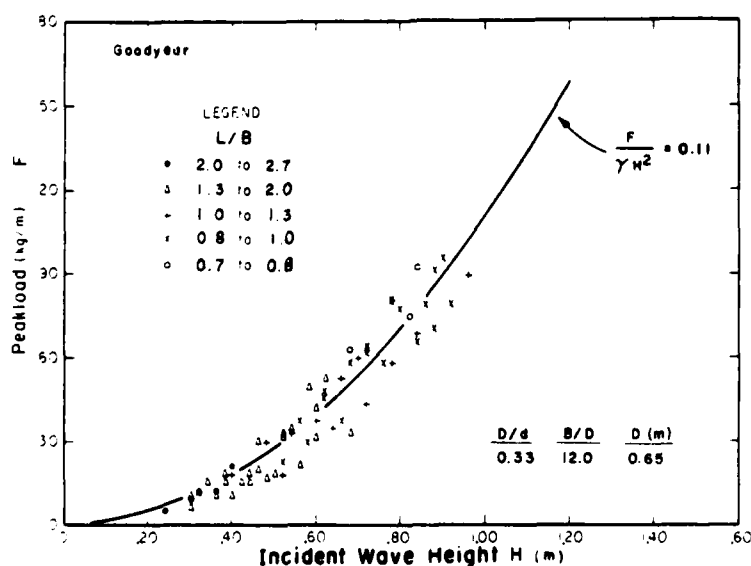


Figure 51. Goodyear peak mooring-force data (Giles and Sorensen, 1978;  $d = 2.0$  m).

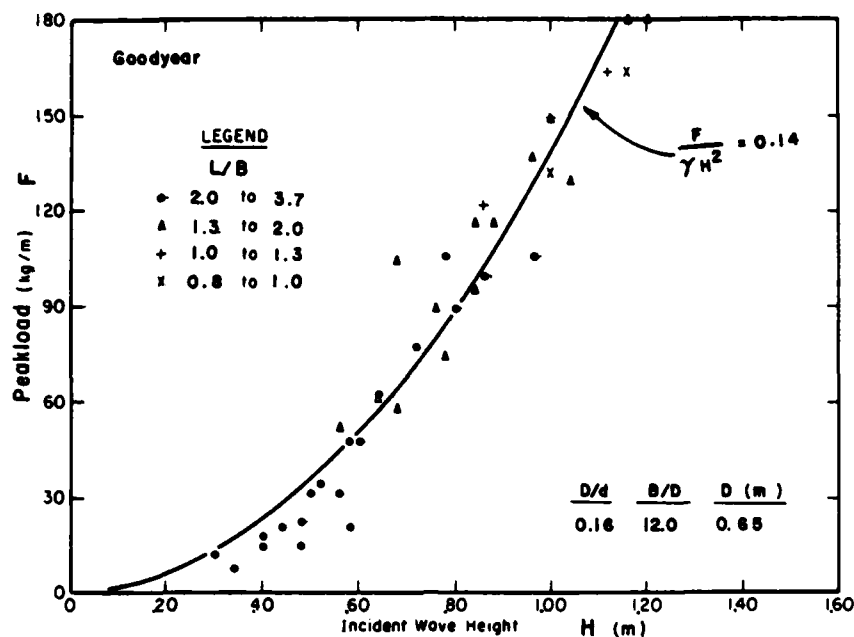


Figure 52. Goodyear peak mooring-force data  
(Giles and Sorensen, 1978; d = 4.0 m).

For a given wave height and length, the mooring forces on the Goodyear breakwater are clearly much lower than those for a PT-Breakwater of equal size. This finding is attributed principally to three factors, the relative importance of which cannot be quantified at this time:

(1) The transmitted wave for the PT-Breakwater is smaller than that for the Goodyear breakwater; i.e., different levels of energy dissipation occur on each structure (wave breaking and impact, etc.).

(2) Different mooring systems were utilized. The importance of this has already been demonstrated with regard to the PT-1 breakwater (see Table 4).

(3) The Goodyear breakwater design stretches extensively under load, being very pliable throughout. This influences or perhaps even dominates the mooring dynamics and load transmission characteristics.

## VI. SUMMARY AND CONCLUSIONS

Two prototype-scale PT-Breakwaters were tested in CERC's large wave tank using regular waves: the PT-1 module, constructed of truck tires and steel pipes in waves up to 1.8 meters high, and the smaller PT-2 module, constructed from automobile tires and telephone poles in waves up to 1.5 meters high. Wave transmission and mooring-load characteristics were established based on data from 402 separate runs in which incident and transmitted wave heights were recorded, along with tension in the seaward mooring line.

In the course of the investigation, it became increasingly evident (during construction, crane operations, and early experiments) that the PT-1 breakwater was more rugged and could potentially function and survive under more

severe wave conditions than those normally considered acceptable for floating tire breakwaters. For this reason, the PT-1 module was emphasized in the test program. Although structural failures were not experienced on either the PT-1 or the PT-2 breakwaters throughout the many weeks of testing, and posttest inspections did not reveal areas of imminent failure or excessive wear, it became clear that the PT-2 module was inherently more pliable than the PT-1 module because it was composed of automobile tires, not truck tires. Consequently, as waves broke over the structure, greater compression and displacement of leading-edge tires occurred on the PT-2 module than was true for the PT-1 module under the same conditions. Although PT-Breakwaters were designed to be pliable, with relative motion between individual components, under severe wave-induced loads, the observed compression of leading-edge tires on the PT-2 module is felt to be excessive for continuous operation. It is therefore suggested that the PT-2 breakwater be limited to sites with significant wave heights of less than 0.9 meter; this condition is considered to be equally appropriate for Goodyear or Wave-Maze floating tire breakwaters that are composed of automobile tires as well. The value of 0.9 meter was chosen by the researchers as representing the best, though inherently somewhat subjective, estimate for the maximum acceptable significant wave height; it is based on extensive laboratory observations and experience with a variety of field installations. The above rule is considered to be of practical importance because it reminds the designer that the environment is hostile and that PT-Breakwaters constructed from automobile tires are inherently less rugged than those composed of truck tires; both have survival limitations.

The wave attenuation performance of PT-Breakwaters improves as either wavelength or water depth decreases, or the wave steepness increases (i.e.,  $C_t$  increases with  $L/B$  and decreases with  $D/d$  or  $H/L$ ). The shelter afforded by a particular PT-Breakwater is strongly dependent on the incident wavelength: substantial protection is provided from waves that are shorter than the width of the breakwater (i.e.,  $L < B$ ), but very little from waves longer than three  $B$ . As the water depth decreases, the wave attenuation performance improves; a breakwater that provides inadequate shelter at high tide may therefore be satisfactory at low tide. Wave attenuation generally improves with increasing wave steepness, especially for relatively long waves in shallow water (e.g.,  $L > 3B$  and  $d < 3D$ ). This behavior is attributed principally to the inherent instability of waves, which increases with wave steepness and, for waves near the breaking limit, is so great that only a small perturbation is required to "trigger" the breaking process. For steep waves, breaking was observed to start just seaward of the breakwater with large amounts of energy being dissipated as the wave rolled and surged over the breakwater. The wave attenuation performance of the PT-1 module was found to be superior to that of the PT-2 module and the Goodyear breakwater. For  $L/B = 1$  (and deep water with  $d > 3D$  and  $H/L = 0.04$ ), for example, the wave height transmission ratio was approximately  $C_t = 0.6$ ,  $0.4$  and  $0.2$  for the Goodyear, PT-2, and PT-1 breakwaters, respectively. Wave transmission curves given in this report should not be used to design breakwaters that are less than 9 meters wide or more than 15 meters wide (see Harms, Bishop, and Westerink, 1981 for further data).

For a given breakwater, the peak mooring force,  $F$  (on the seaward mooring line, per unit length of breakwater) was found to depend primarily on the wave height,  $H$ , and water depth,  $d$ , with wavelength,  $L$ , apparently only of secondary importance. For the conditions investigated,  $F$  increases

approximately with the square of the wave height; more specifically,  $F \propto H^n$  where  $n = 1.5, 2$  and  $2$  for the PT-1, PT-2, and Goodyear breakwaters, respectively. For design purposes, and until the results from ongoing experiments become available, it is suggested that the following formula be used to calculate anchor requirements for breakwaters that range in width from 9 to 15 meters:

$$F = 100(1 + 10 KH^n) \quad (6)$$

where

$H$  = wave height (meters)

$F$  = restraining force (kilograms per meter) to be provided by the anchor system for each meter of breakwater length

$n$  =  $3/2$  for the PT-1 breakwater or  $2$  for the PT-2 and Goodyear breakwaters

$K$  = force coefficient from Table 4.

The available small-scale and prototype-scale data have recently been synthesized into detailed design curves (Harms, Bishop, and Westerink, 1981). In order to be conservative, mooring loads should be determined from these design curves as well as equation (6), and the larger value chosen for design purposes.



## LITERATURE CITED

- CANDLE, R.D., "Scrap Tire Shore Protection Structures," Engineering Research Department, Goodyear Tire and Rubber Company, Akron, Ohio, 1976.
- DAVIS, A.P., Jr., "Evaluation of Tying Materials for Floating Tire Breakwaters," Marine Technical Report No. 54, University of Rhode Island, Kingston, R.I., Apr. 1977.
- GILES, M.L., and SORENSEN, R.M., "Prototype Scale Mooring Load and Transmission Tests for a Floating Tire Breakwater," TP 78-3, U.S. Army, Corps of Engineers, Coastal Engineering Research Center, Fort Belvoir, Va., Apr. 1978.
- HARMS, V.W., "Design Criteria for Floating Tire Breakwaters," *Journal of the Waterway, Port, Coastal and Ocean Division*, Vol. 105, No. WW2, pp. 149-170, Mar. 1979a.
- HARMS, V.W., "Data and Procedures for the Design of Floating Tire Breakwaters," Water Resources and Environmental Engineering Report No. 79-1, Department of Civil Engineering, State University of New York, Buffalo, N.Y., Mar. 1979b.
- HARMS, V.W., and BENDER, T.J., "Preliminary Report on the Application of Floating Tire Breakwater Design Data," Water Resources and Environmental Engineering Report No. 78-1, Department of Civil Engineering, State University of New York, Buffalo, N.Y., Apr. 1978.
- HARMS, V.W., BISHOP, C.T., and WESTERINK, J.J., "Floating Breakwater Design Criteria from Model and Prototype-Scale Experiments," *Proceedings of the Second Conference on Floating Breakwaters*, 1981.
- KAMEL, A.M., and DAVIDSON, D.D., "Hydraulic Characteristics of Mobile Breakwaters Composed of Tires or Spheres," Technical Report No. H-68-2, U.S. Army Engineer Waterways Experiment Station, Vicksburg, Miss., 1968.
- KOWALSKI, T., "Scrap Tire Floating Breakwaters," *Floating Breakwater Conference Papers*, Marine Technical Report Series No. 24, University of Rhode Island, Kingston, R.I., Apr. 1974, pp. 233-246.
- STITT, R.L., "Wave-Maze Floating Breakwater," Brochure No. 10732, Temple City, Calif., 1963 (revised 1977).

APPENDIX A

TABULATED TEST RESULTS

**Table A-1. PT-1 breakwater with MS-1 ( $d = 4.7$  m).**

Water depth	:D	=	4.650 (m)	S	(cm)	T	(s)	H	(cm)	P	(kg/m)	F	(kg/m)	F <sub>2</sub>	(kg/m)	F <sub>g</sub>	(kg/m)	L	(m)	W/L	L/B	CT	R/DT	F	(γ)(DT)/(DT)
Tire diameter	:DT	=	101.600 (cm)	51	11	2.65	1.65	88	14	212	5	85	5	212	5	118	5	17	14	4.56	8.5	50.5	7	2.22	2
Breakwater beam	:B	=	12.200 (m)	11	11	2.65	1.65	92	14	129	5	35	5	212	5	118	5	17	14	4.56	8.5	50.5	7	2.22	2
Log spacing	:BLOG	=	3.350 (m)	61	11	2.65	1.65	102	14	212	5	169	5	212	5	118	5	17	14	4.56	8.5	50.5	7	2.22	2
Relative draft	:DT/D	=	0.218	51	11	2.65	1.65	88	14	212	5	44	5	212	5	118	5	17	14	4.56	8.5	50.5	7	2.22	2
B/DT	:B/DT	=	12.008	61	11	2.65	1.65	102	14	212	5	169	5	212	5	118	5	17	14	4.56	8.5	50.5	7	2.22	2
BLOG/DT	:BLOG/DT	=	3.297	51	11	2.65	1.65	88	14	212	5	169	5	212	5	118	5	17	14	4.56	8.5	50.5	7	2.22	2

**Table A-1. PT-1 breakwater with MS-1 (d = 4.7 m). ---Continued**

[illegible]

**Table A-2. PT-1 breakwater with MS-1 ( $d = 2.0 \text{ m}$ ).**

[illegible]

Table A-2. PT-1 breakwater with MS-1 (d = 2.0 m).--Continued

Water depth	D	T	H	HT	F	F̄	F <sub>2</sub>	F <sub>0</sub>	L	M/L	L/B	CT	M/DT	$\frac{F}{(\gamma)(DT)(DT)}$
2.000 (m)	0.000	0.000	0.000	0.000	0.000	0.000	0.000	0.000	0.000	0.000	0.000	0.000	0.000	0.000
101.600 (cm)	0.000	0.000	0.000	0.000	0.000	0.000	0.000	0.000	0.000	0.000	0.000	0.000	0.000	0.000
12.200 (m)	0.000	0.000	0.000	0.000	0.000	0.000	0.000	0.000	0.000	0.000	0.000	0.000	0.000	0.000
3.350 (m)	0.000	0.000	0.000	0.000	0.000	0.000	0.000	0.000	0.000	0.000	0.000	0.000	0.000	0.000
0.508	0.000	0.000	0.000	0.000	0.000	0.000	0.000	0.000	0.000	0.000	0.000	0.000	0.000	0.000
12.008	0.000	0.000	0.000	0.000	0.000	0.000	0.000	0.000	0.000	0.000	0.000	0.000	0.000	0.000
3.297	0.000	0.000	0.000	0.000	0.000	0.000	0.000	0.000	0.000	0.000	0.000	0.000	0.000	0.000

Table A-3. PT-1 breakwater with MS-2 ( $d = 4.7$  m).

[illegible]

**Table A-4. PT-1 breakwater with MS-3 ( $d = 4.7$  m).**

[illegible]



**Table A-5. PT-2 breakwater with MS-3 ( $d = 4.7$  m).**

[illegible]

Water depth	:D	=	2.000 (m)
Tire diameter	:DT	=	66.000 (cm)
Breakwater beam	:B	=	12.200 (m)
Log spacing	:BLOG	=	3.660 (m)
Malative draft	:DT/D	=	0.330
B/DT	:B/DT	=	18.485
BLOG/DT	:BLOG/DT	=	5.545

[illegible]

Water depth	:D	=	4.650 (m)
Tire diameter	:DT	=	101.600 (cm)
Breakwater beam	:B	=	25.900 (m)
Log spacing	:BLOG	=	3.350 (m)
Malative draft	:DT/D	=	0.218
B/D	:B/DT	=	25.492
BLOG/DT	:BLOG/DT	=	3.297

[illegible]

**APPENDIX B**

**FORCE MEASUREMENT CORRELATION (PT-1)**

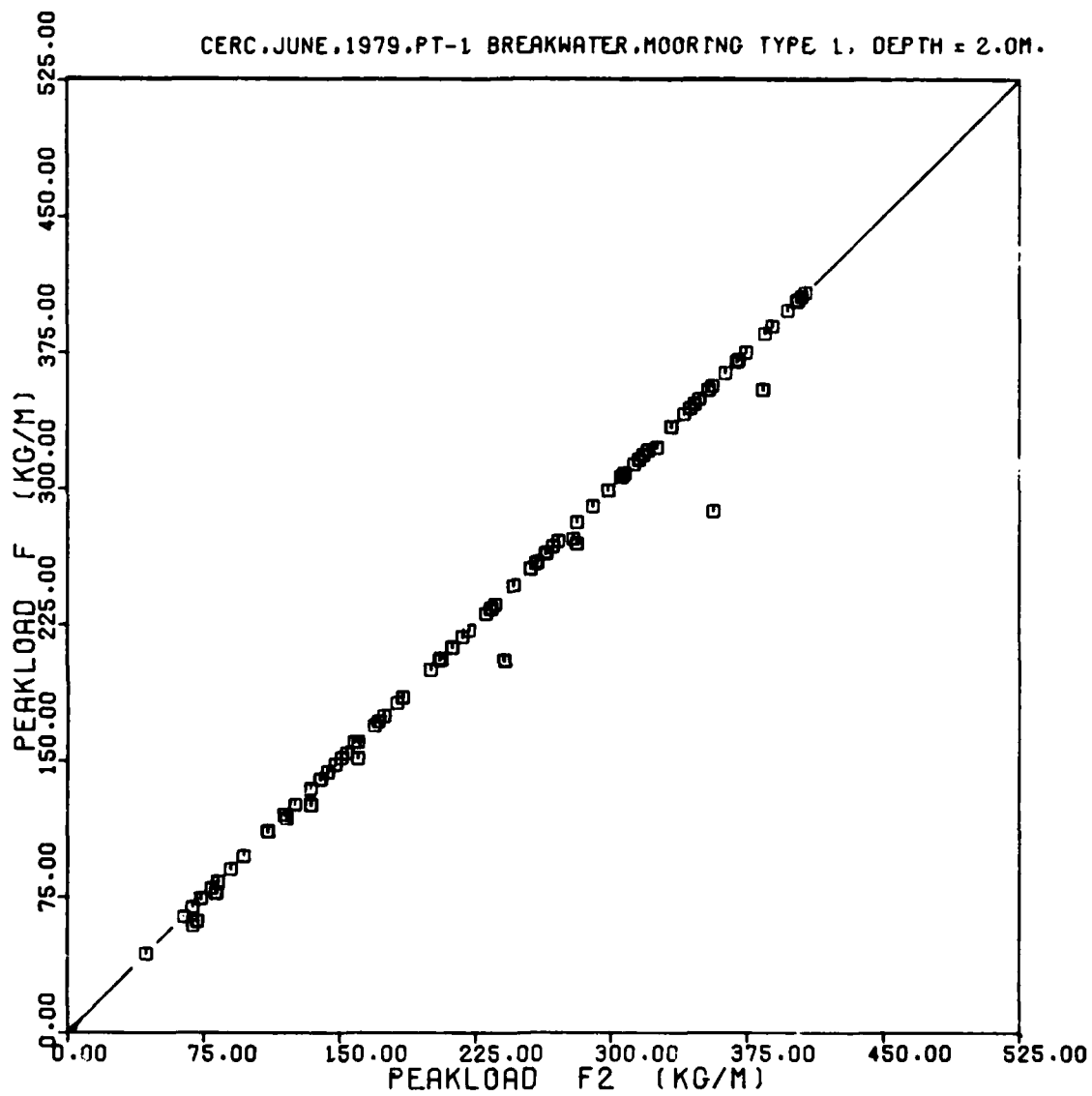


Figure B-1. Correlation of  $F$  and  $F_2$  (MS-1,  $d = 2.0$  m).

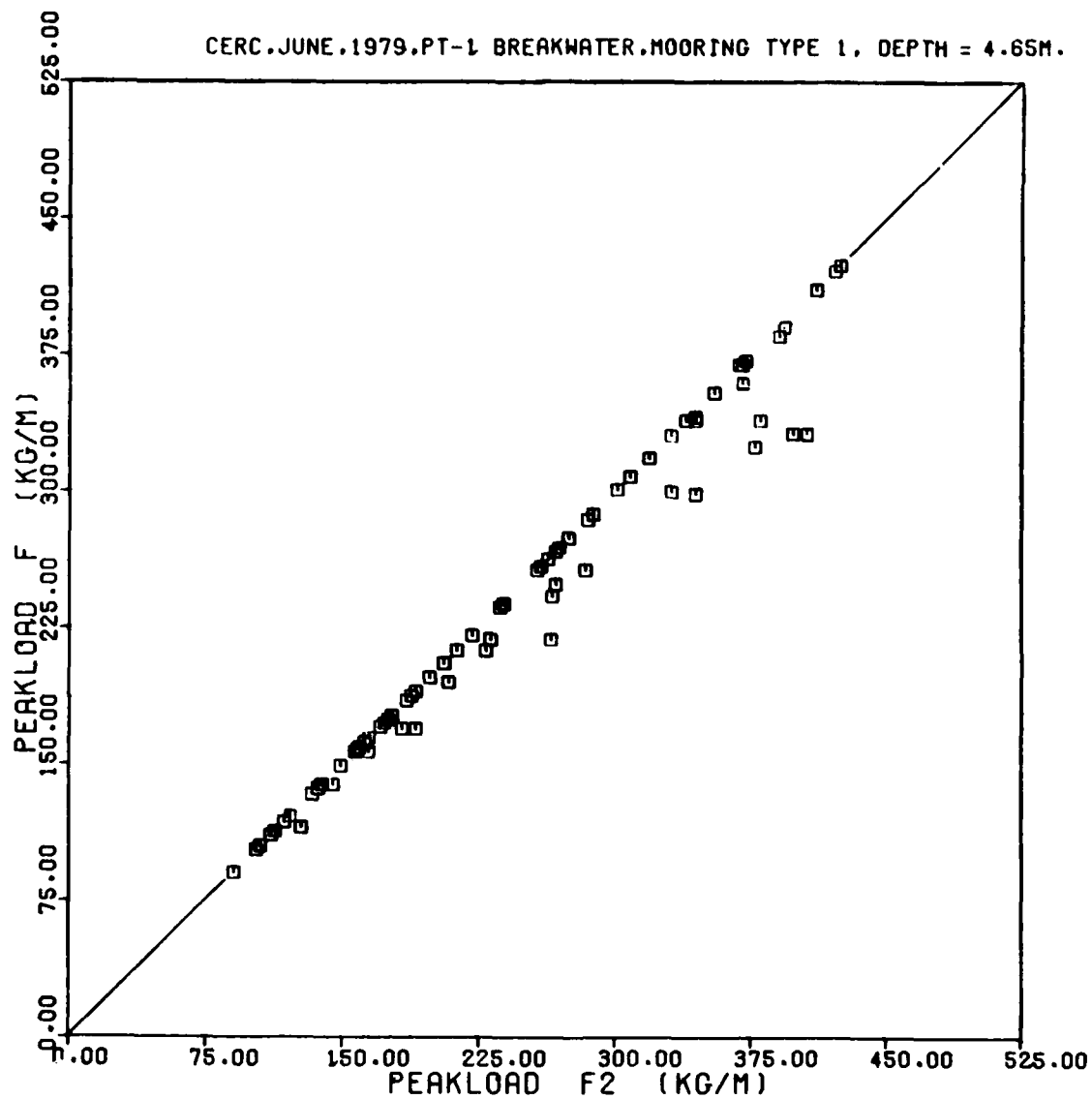


Figure B-2. Correlation of  $F$  and  $F_2$  (MS-1,  $d = 4.7$  m).

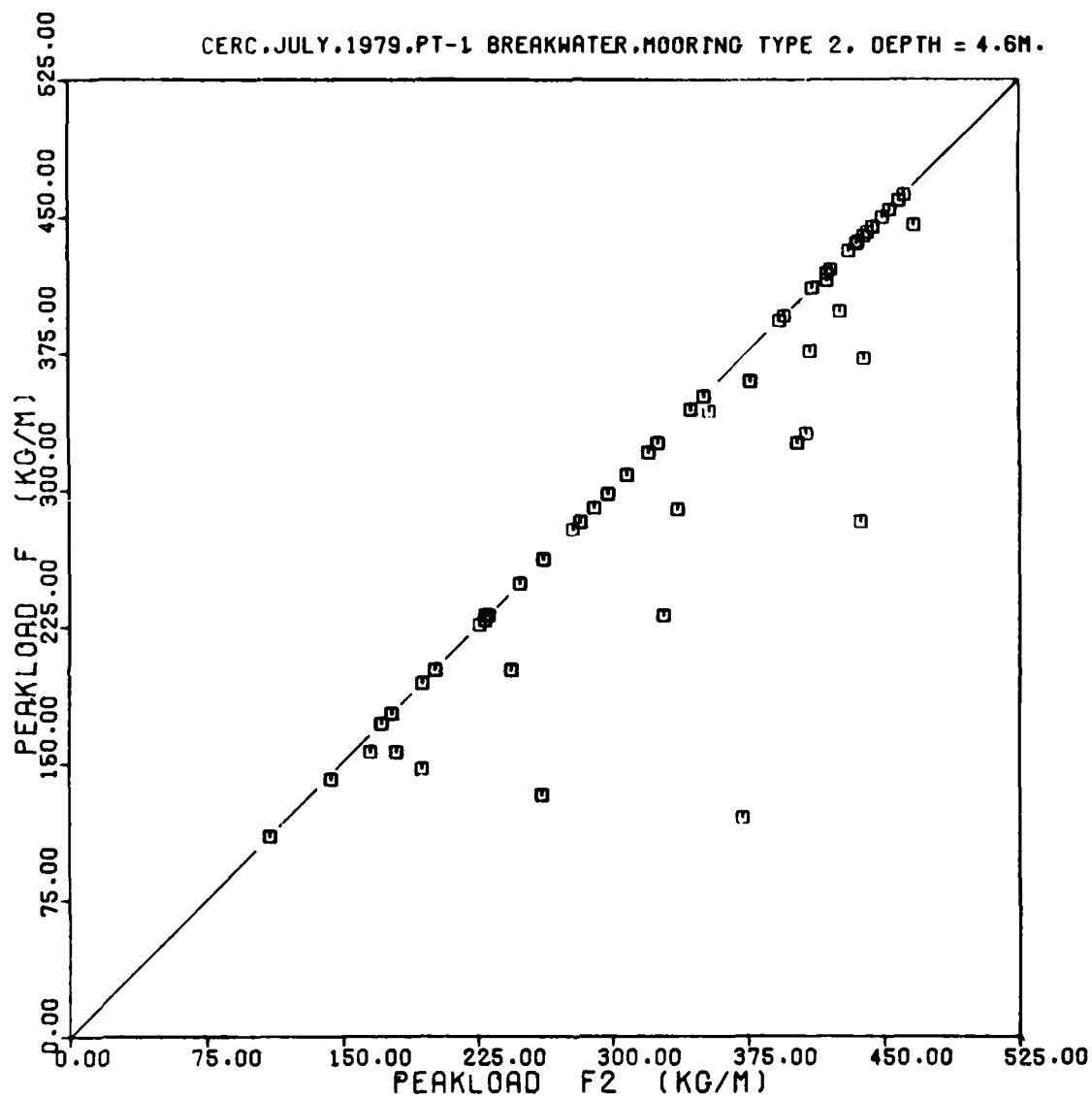


Figure B-3. Correlation of  $F$  and  $F_2$  (MS-2,  $d = 4.7$  m).

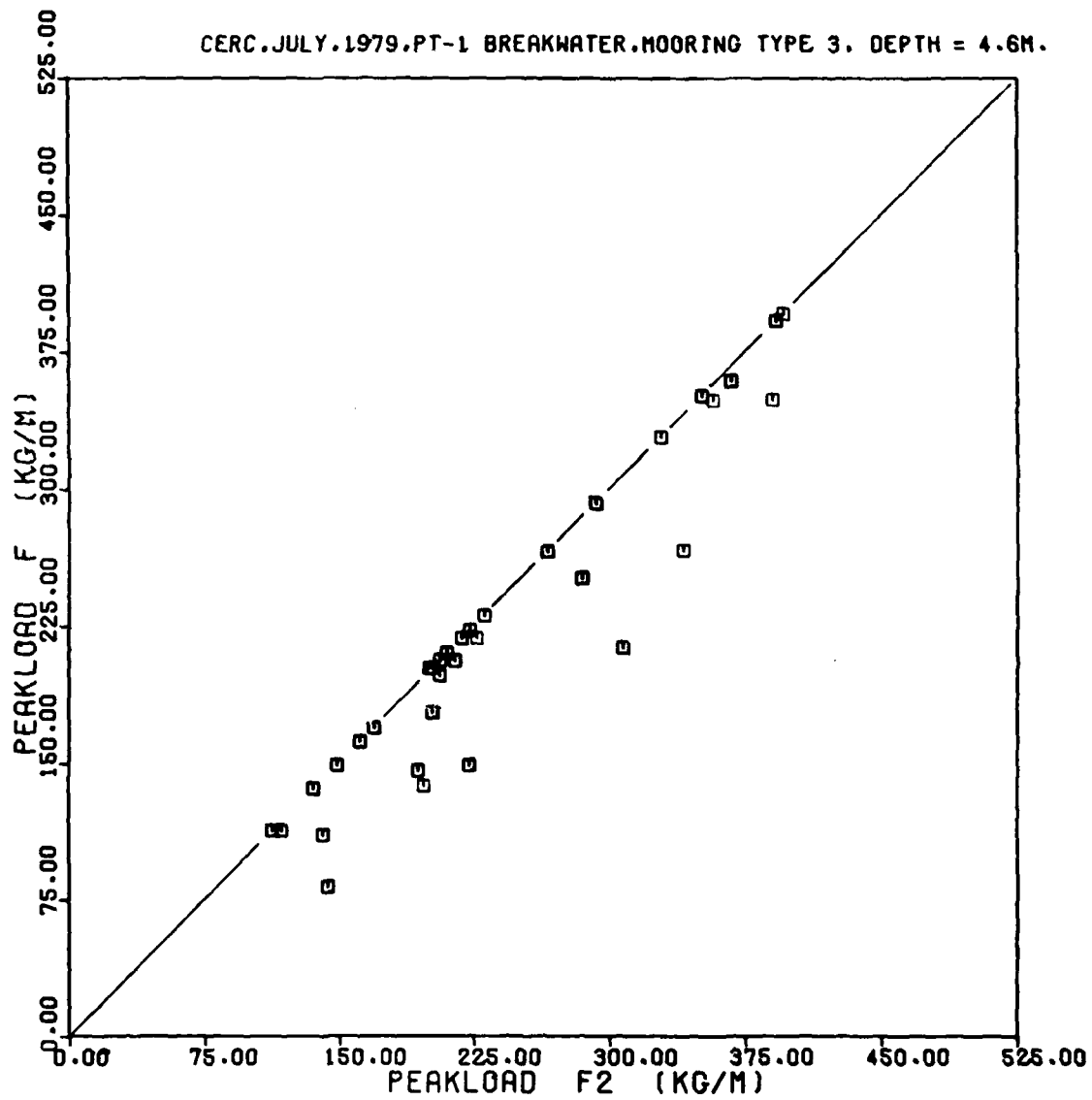


Figure B-4. Correlation of F and F<sub>2</sub> (MS-3, d = 4.7 m).



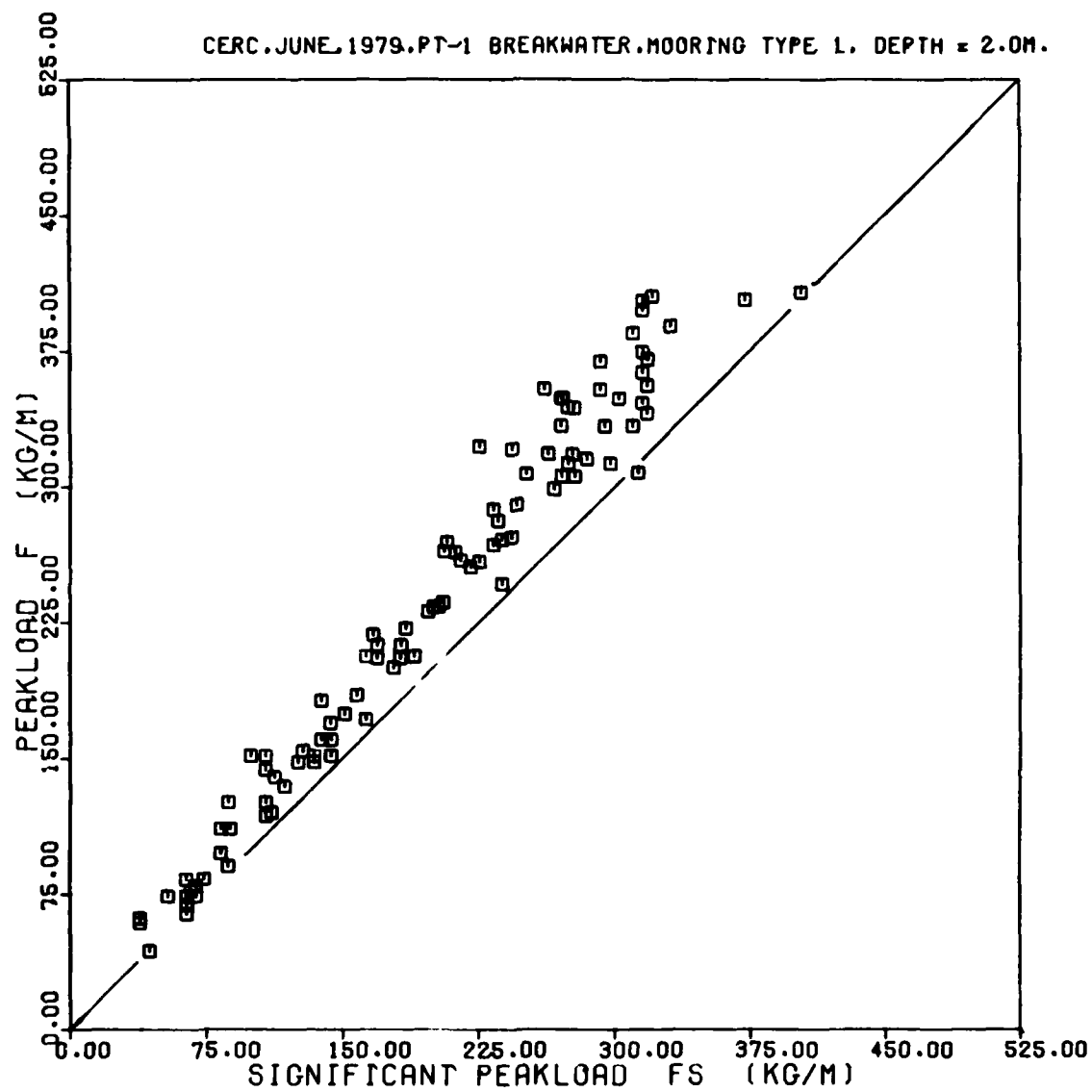


Figure B-5. Correlation of F and  $F_s$  (MS-1, d = 2.0 m).

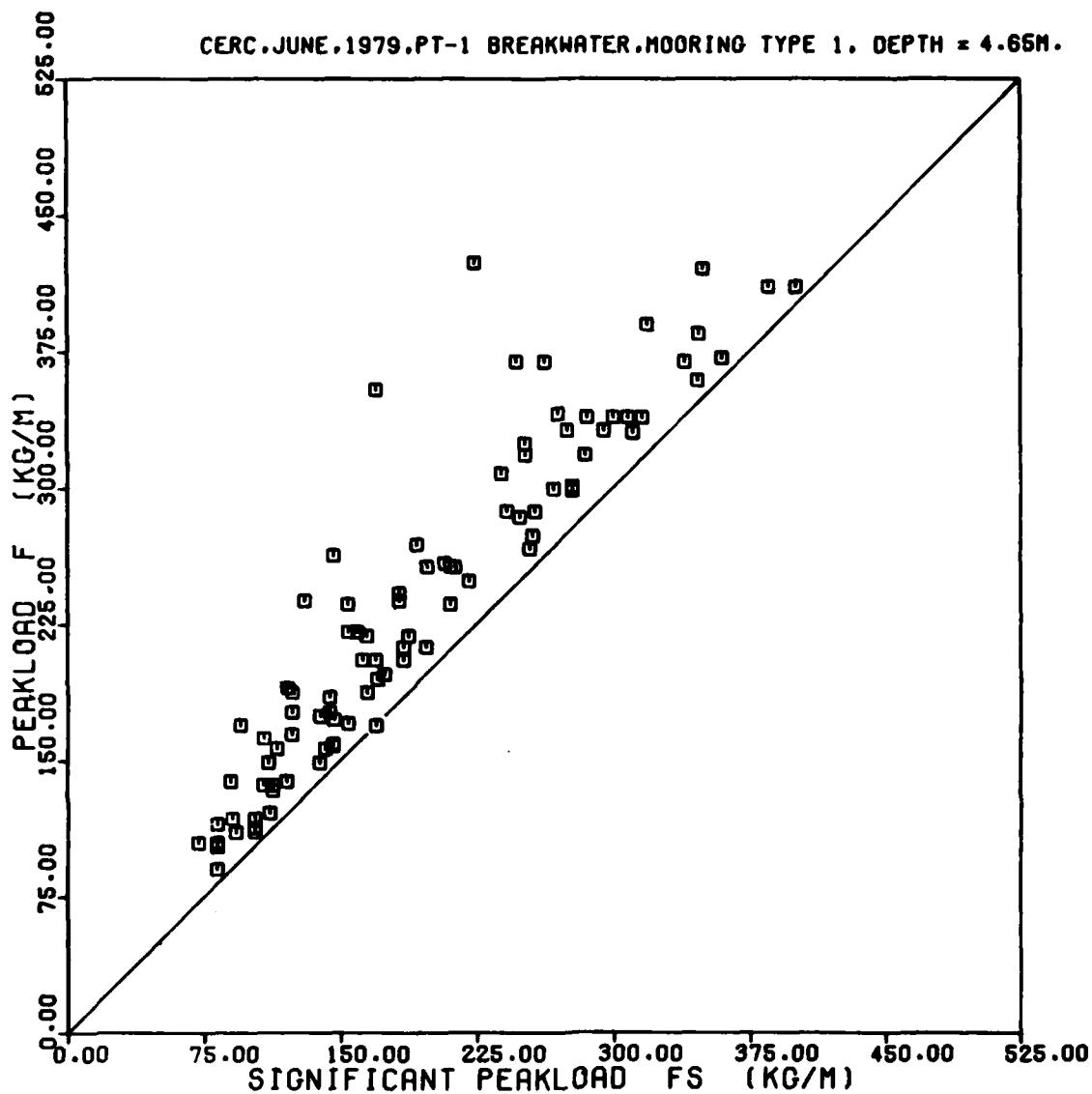


Figure B-6. Correlation of  $F$  and  $F_s$  (MS-1,  $d = 4.7$  m).

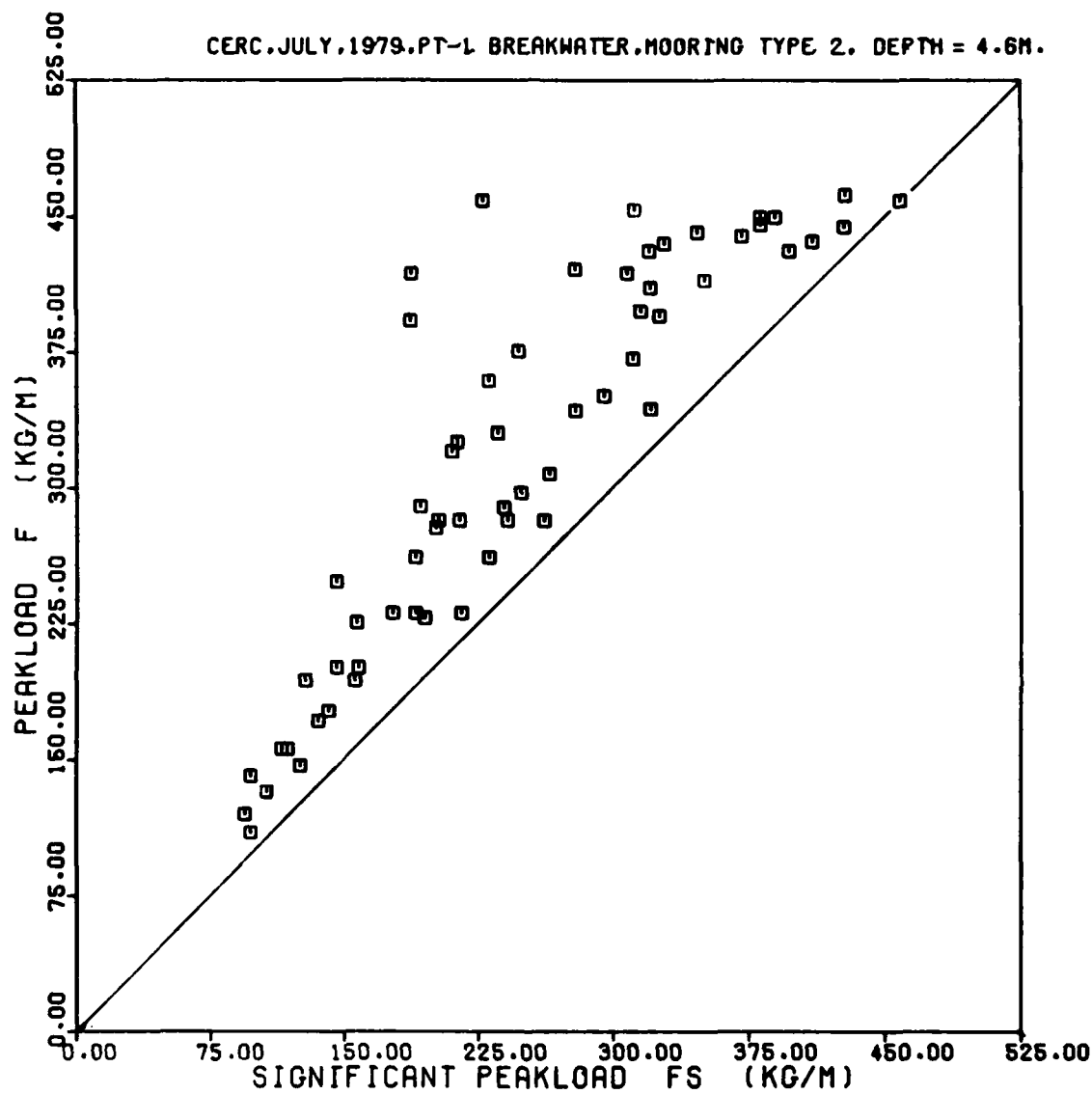


Figure B-7. Correlation of  $F$  and  $F_s$  (MS-2,  $d = 4.7$  m).

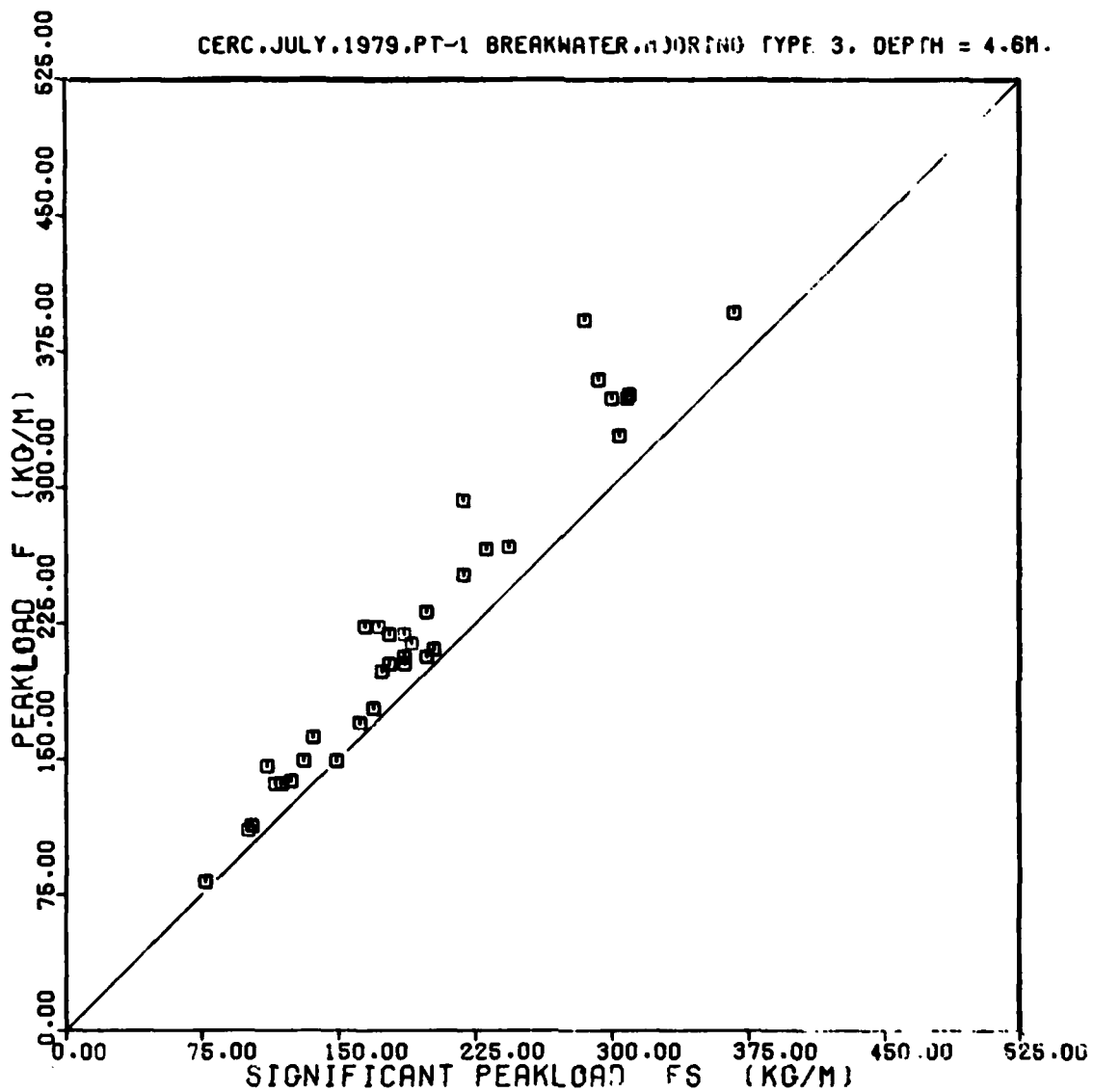


Figure B-8. Correlation of  $F$  and  $F_s$  (MS-3,  $d = 4.7$  m).

APPENDIX C

DETAILED WAVE TRANSMISSION DIAGRAM

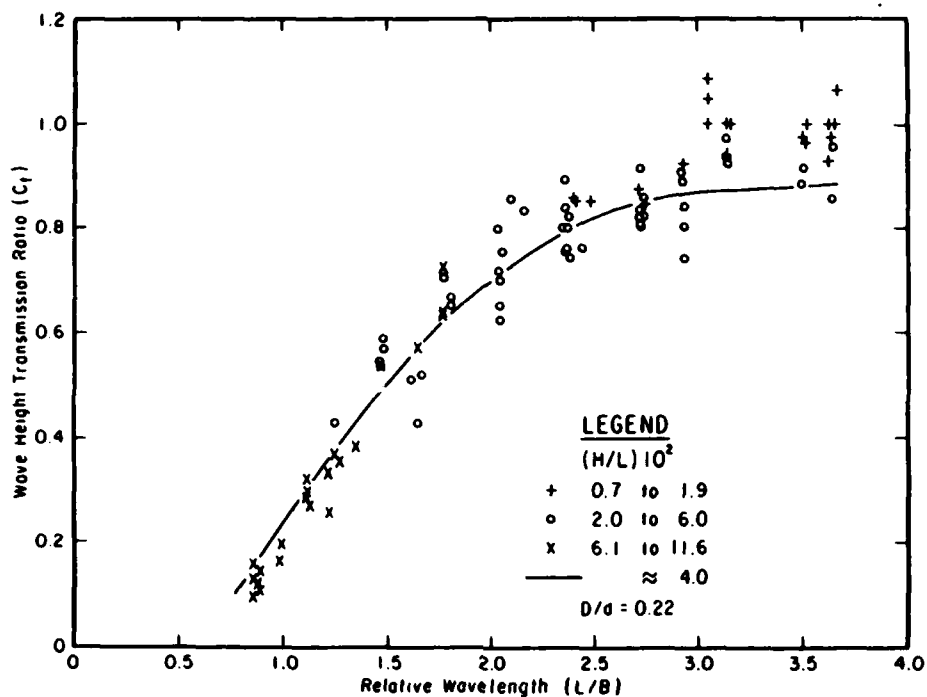


Figure C-1. PT-1 wave transmission data for MS-1.

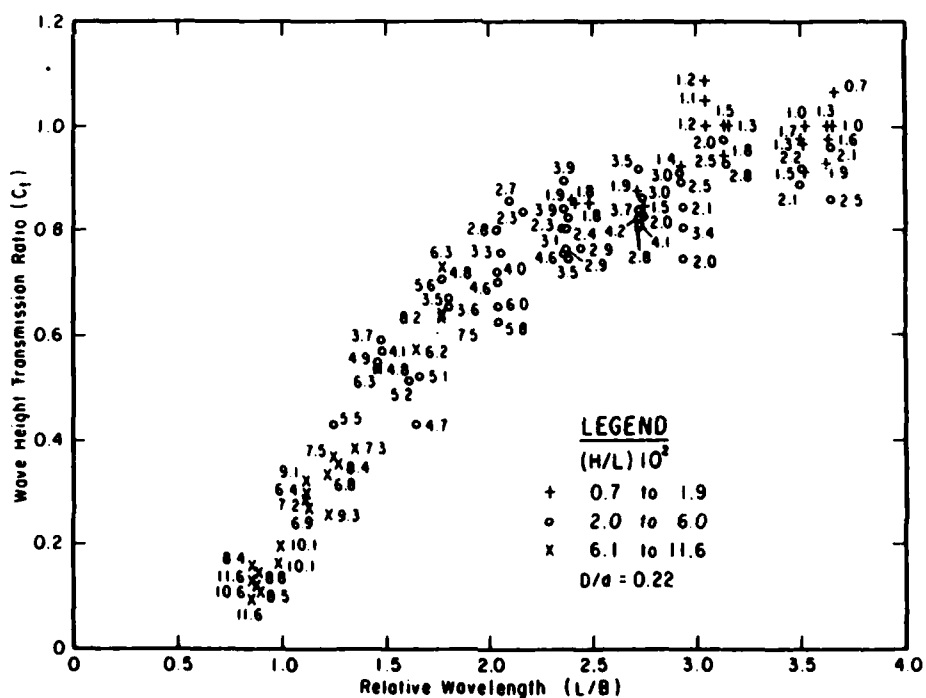


Figure C-2. PT-1 wave transmission data for MS-1 (discrete  $H/L$ ).

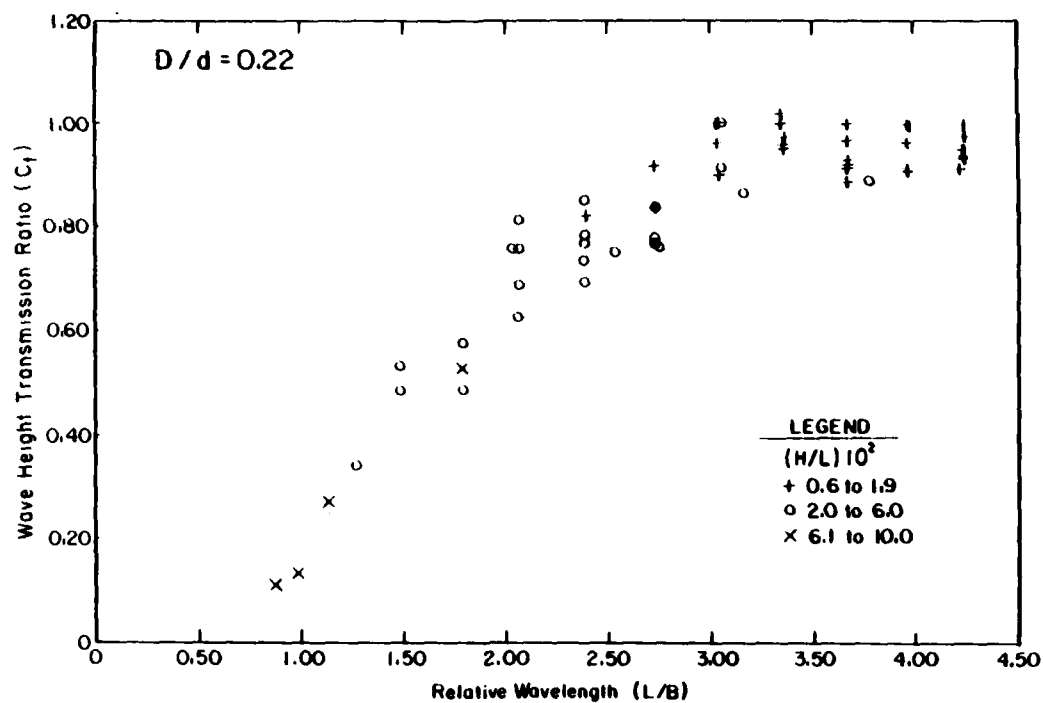


Figure C-3. PT-1 wave transmission data for MS-2.

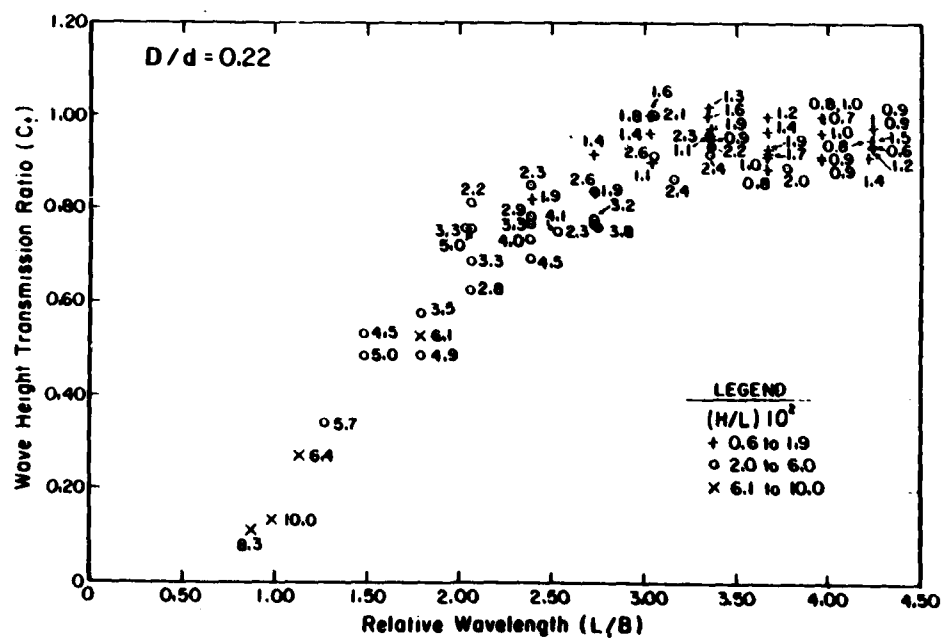


Figure C-4. PT-1 wave transmission data for MS-2 (discrete  $H/L$ ).

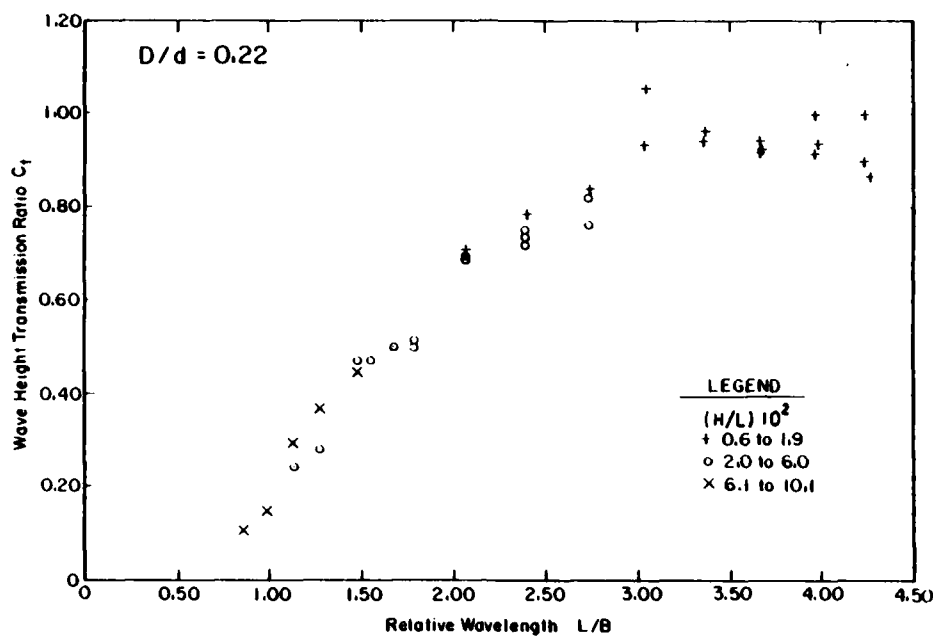


Figure C-5. PT-1 wave transmission data for MS-3.

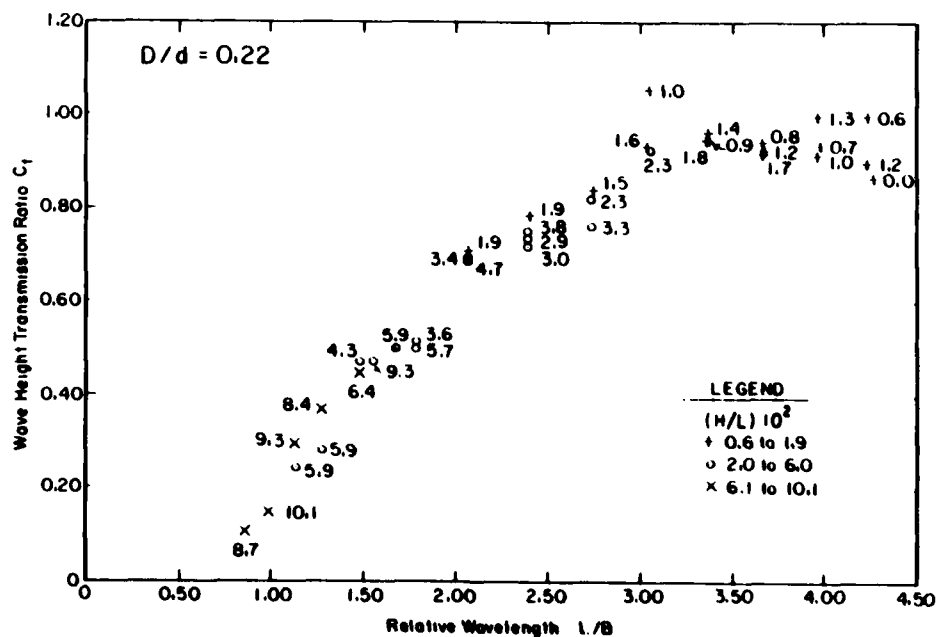


Figure C-6. PT-1 wave transmission data for MS-3 (discrete  $H/L$ ).



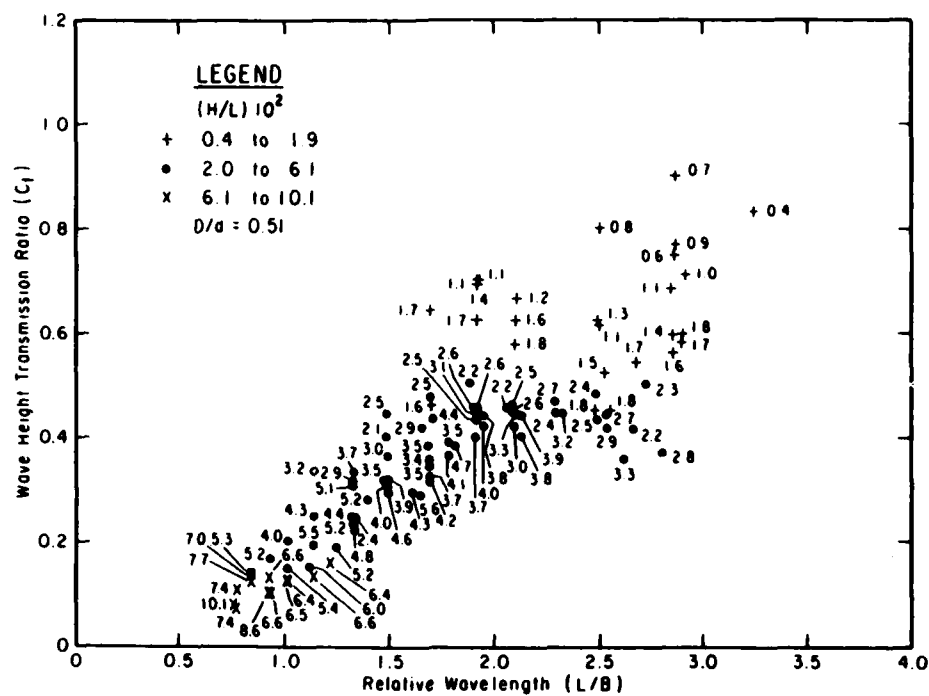


Figure C-7. PT-1 wave transmission data for MS-3  
 ( $d = 2.0$  m, discrete  $H/L$ ).

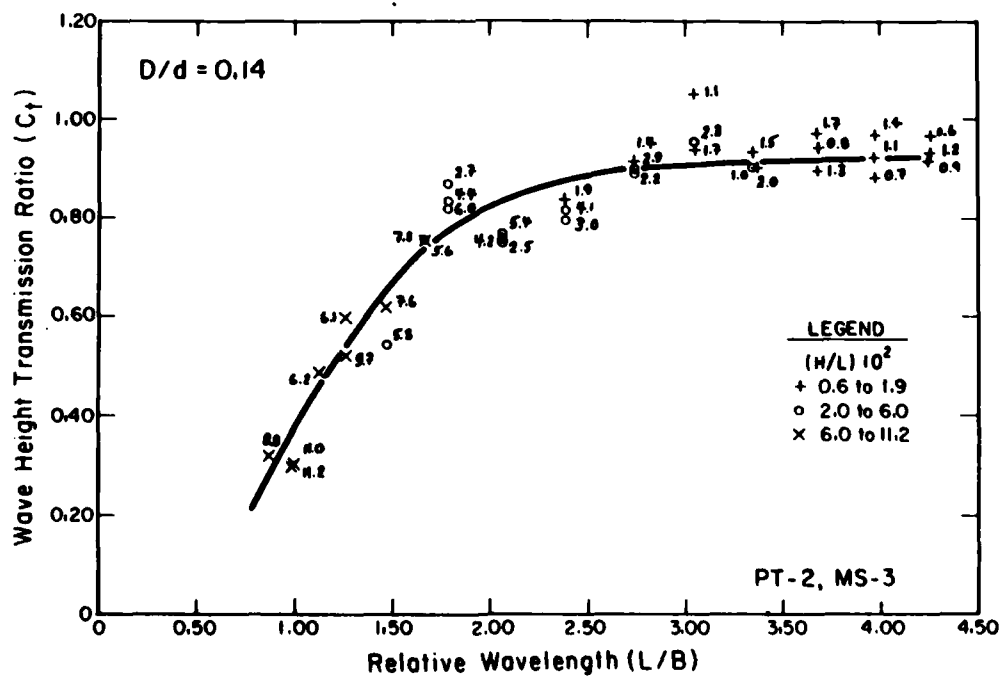


Figure C-8. PT-2 wave transmission data for MS-3  
 (discrete  $H/L$ ).

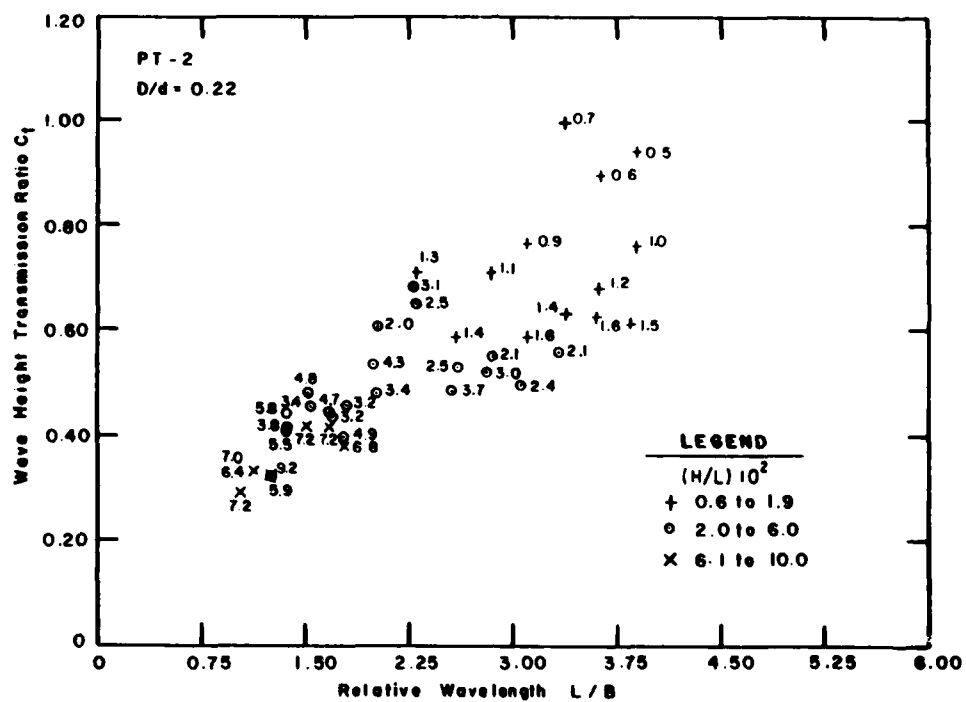


Figure C-9. PT-2 wave transmission data for MS-3  
( $d = 2.0$  m, discrete  $H/L$ ).

Harms, Volker W.

Wave transmission and mooring-force characteristics of pipe-tire floating breakwaters / by Volker W. Harms, Joannes J. Westerink, and Robert M. Sorensen--Fort Belvoir, Va. : U.S. Army, Corps of Engineers, Coastal Engineering Research Center, Springfield, Va. : available from NTIS, 1982.

[79] p. : ill. ; 28 cm.--(Technical paper / Coastal Engineering Research Center ; no. 82-4). Cover title.

"October 1982."

Report provides results of prototype-scale tests of the Pipe-Tire Breakwater (PT-Breakwater) built of scrap truck or automobile tires and incorporating massive cylindrical members such as steel or concrete pipes, telephone poles, etc.

1. Floating breakwaters. 2. Waves. 3. Mooring. 4. Tires. 5. Wave propagation. I. Title. II. Westerink, Joannes J.

III. Sorensen, Robert M. IV. Coastal Engineering Research Center (U.S.). V. Series: Technical Paper (Coastal Engineering Research Center (U.S.)); no. 82-4.

TC203 .U581tp

no. 82-4

627

Harms, Volker W.

Wave transmission and mooring-force characteristics of pipe-tire floating breakwaters / by Volker W. Harms, Joannes J. Westerink, and Robert M. Sorensen--Fort Belvoir, Va. : U.S. Army, Corps of Engineers, Coastal Engineering Research Center, Springfield, Va. : available from NTIS, 1982.

[79] p. : ill. ; 28 cm.--(Technical paper / Coastal Engineering Research Center ; no. 82-4). Cover title.

"October 1982."

Report provides results of prototype-scale tests of the Pipe-Tire Breakwater (PT-Breakwater) built of scrap truck or automobile tires and incorporating massive cylindrical members such as steel or concrete pipes, telephone poles, etc.

1. Floating breakwaters. 2. Waves. 3. Mooring. 4. Tires. 5. Wave propagation. I. Title. II. Westerink, Joannes J.

III. Sorensen, Robert M. IV. Coastal Engineering Research Center (U.S.). V. Series: Technical Paper (Coastal Engineering Research Center (U.S.)); no. 82-4.

TC203 .U581tp

no. 82-4

627

Harms, Volker W.

Wave transmission and mooring-force characteristics of pipe-tire floating breakwaters / by Volker W. Harms, Joannes J. Westerink, and Robert M. Sorensen--Fort Belvoir, Va. : U.S. Army, Corps of Engineers, Coastal Engineering Research Center, Springfield, Va. : available from NTIS, 1982.

[79] p. : ill. ; 28 cm.--(Technical paper / Coastal Engineering Research Center ; no. 82-4). Cover title.

"October 1982."

Report provides results of prototype-scale tests of the Pipe-Tire Breakwater (PT-Breakwater) built of scrap truck or automobile tires and incorporating massive cylindrical members such as steel or concrete pipes, telephone poles, etc.

1. Floating breakwaters. 2. Waves. 3. Mooring. 4. Tires. 5. Wave propagation. I. Title. II. Westerink, Joannes J.

III. Sorensen, Robert M. IV. Coastal Engineering Research Center (U.S.). V. Series: Technical Paper (Coastal Engineering Research Center (U.S.)); no. 82-4.

TC203 .U581tp

no. 82-4

627

Harms, Volker W.

Wave transmission and mooring-force characteristics of pipe-tire floating breakwaters / by Volker W. Harms, Joannes J. Westerink, and Robert M. Sorensen--Fort Belvoir, Va. : U.S. Army, Corps of Engineers, Coastal Engineering Research Center, Springfield, Va. : available from NTIS, 1982.

[79] p. : ill. ; 28 cm.--(Technical paper / Coastal Engineering Research Center ; no. 82-4). Cover title.

"October 1982."

Report provides results of prototype-scale tests of the Pipe-Tire Breakwater (PT-Breakwater) built of scrap truck or automobile tires and incorporating massive cylindrical members such as steel or concrete pipes, telephone poles, etc.

1. Floating breakwaters. 2. Waves. 3. Mooring. 4. Tires. 5. Wave propagation. I. Title. II. Westerink, Joannes J.

III. Sorensen, Robert M. IV. Coastal Engineering Research Center (U.S.). V. Series: Technical Paper (Coastal Engineering Research Center (U.S.)); no. 82-4.

TC203 .U581tp

no. 82-4

627

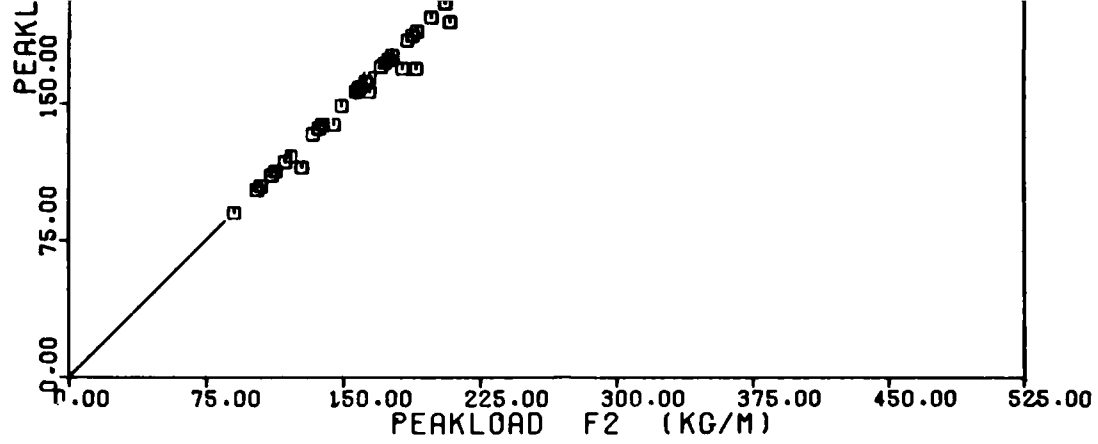


Figure B-2. Correlation of  $F$  and  $F_2$  (MS-1,  $d = 4.7$  m).

END

FILMED